The influence of human activities and soil properties on soil carbon dynamics in a diversity of soils

By

Elliot Vaughan

A dissertation submitted in partial fulfillment of
the requirements for the degree of

Doctor of Philosophy
(Geography)

At the
UNIVERSITY OF WISCONSIN-MADISON
2020

Date of final oral examination: 06/04/2020

The dissertation is approved by the following members of the Final Oral Committee:

Erika Marín-Spiotta, Professor, Geography
Joseph Mason, Professor, Geography
Alfred Hartemink, Professor, Soil Science
Thea Whitman, Assistant Professor, Soil Science

ACKNOWLEDGEMENTS

There are many people who contributed to this work, both directly and indirectly. First, thanks to everyone who helped collect data in the field and in the lab. This includes: Megs Seeley, Sanober Mirza, Catherine Kirwin, Liam Patton, Tim Whitby, Ann Olsson, Diana Tapía, Olivia Lopez, Alexander Roman, Lily Weglarek, Clarissa Perez Gomez, Emily Diaz Vallejo, Ricardo Rivera, Jesús Espinosa, José Pérez, and Brian Yudkin.

The organization Para La Naturaleza was very kind to let me collect samples on their properties, stay in their guest house, and provide help throughout. Thanks in particular to Ricardo Rodríguez and Glorimar Toledo Soto. Manuel Matos and Samuel Ríos in the Mayagüez NRCS office shared their samples, field equipment and advice. Thanks to Delvín Fernández Robles at the UPR Agricultural Extension office in Ciales for showing us around to field sites. Many other landowners graciously allowed access to their forests and fields and provided valuable land-use histories. Also, much needed moral support and cookies when our rental car broke down.

Many friends and family members supported me during my six years in grad school, and made it fun, rewarding, and manageable. My committee members, Joseph Mason, Thea Whitman, and Alfred Hartemink provided thoughtful and useful feedback. And last but certainly not least, many, many thanks to my advisor Erika Marín-Spiotta, who has been a wonderful mentor to my science, my teaching and my own mentoring throughout the last six years. I've learned so much, and this work and my professional development owe much to her.

Funding for research in Puerto Rico was provided by a Vilas Research Award from University of Wisconsin-Madison, U.S. National Science Foundation Behavioral and Cognitive Sciences CAREER Award #1349952, a UW-Madison University Fellowship, and cooperative agreement #68-7482-12-525 from the U.S. Department of Agricultural Natural Resources Conservation Service National Soil Survey Center, and several UW-Madison Geography Department Trewartha Grants. My travel to Germany and subsequent analyses was made possible through the TU München PREP program, as well as US NSF Award # 1623814 and support from Deutsche Forschungsgemeinschaft (MU 3021/4-2) in the frame of the DFG research unit FOR1806 The forgotten part of carbon cycling: Soil organic matter storage and turnover in subsoils (SUBSOM).

TABLE OF CONTENTS

Acknowledgements i

Table of Contents iii

Abstract iv

Introduction 1

Chapter 1: Radiocarbon modeling indicates dynamic soil carbon cycling and vertical transport in two tropical forests but no long-term effects of nitrogen fertilization 8

Chapter 2: Effects of soil properties and land cover on organic matter fractions and soil carbon turnover across diverse Puerto Rican soils 44

Chapter 3: Soil carbon dynamics following forest succession along a weathering gradient in a tropical karst area 83

Chapter 4: Micro-scale patterns of organic matter decomposition and storage within a burial paleosol 113

Conclusions 142

ABSTRACT

Soils represent one of the largest terrestrial reservoirs of carbon (C) and understanding the controls on soil C cycling has important implications for climate change and soil fertility. Large uncertainties remain regarding the relative importance of environmental and edaphic factors, and the role of human activities on soil C dynamics. This is especially true in soils of the tropics, which are diverse and often less studied relative to temperate soils. This dissertation sought to address these uncertainties by looking at the effect of several different anthropogenic global change drivers on soil C across a diversity of soils in Puerto Rico. The effect of long-term experimental nitrogen enrichment on soil C content weakened over time and differed within lowland and montane forests, highlighting heterogeneity in responses at the landscape level. Natural abundance radiocarbon (^{14}C) measurements indicated the dynamic nature of soil C in these forests, as the majority of C cycled on decadal time scales, even in mineral-associated fractions that are thought to be quite stable. In a regional study comparing controls on soil carbon turnover under different land covers across the island, soil properties related to parent material and soil weathering, including iron and aluminum concentrations and pH, had a greater influence on the distribution of C among soil fractions and their turnover rate than land cover and land use. Soil C and nitrogen (N) did not differ within a secondary forest chronosequence along a soil-weathering gradient, but C increased with soil pH. Spectroscopic and microscopic analyses of soil organic matter revealed differences in chemistry in buried soils depending on their exposure to the modern soil surface. This work emphasizes the importance of soil physical and chemical properties in influencing soil C dynamics and highlights the complex nature of interactions among human activities, natural disturbances, and soils in heterogenous landscapes.

INTRODUCTION

Soils contain more carbon (C) than the atmosphere and vegetation combined, much of it in forms that are sensitive to human activity (Jobbagy and Jackson 2000, Lal 2004, Trumbore 2009). Understanding controls on soil C storage is important due to the role of soils in the global C cycle and implications for climate change. Soil C is also a major component of soil organic matter (SOM) which is critical for maintaining soil fertility and food security (Lal 2004). Although many studies have attempted to elucidate the influence of human activities on soil C, many uncertainties remain. For example, human land use in the form of clearing forests and conversion to pasture, a primary anthropogenic land cover globally and in the tropics, has been shown to increase (Fisher et al. 1994, Desjardins et al. 2004, Eclesia et al. 2012), decrease (Desjardins et al. 1994, Don et al. 2011), or have no effect (Marín-Spiotta et al. 2009) on soil C stocks. While there are numerous explanations for these conflicting responses, one possibility is that differences in soil properties mediate the response of soil C to changes in land use. Soil mineralogy, texture, pH, and other properties influence the rates of accumulation and loss of SOM in soils, and thus can affect how susceptible SOM is to disturbance (Torn et al. 1997, Six et al. 2002, López-Ulloa et al. 2005, John et al. 2005, von Lützow et al. 2006). Similarly, human alteration of the global N cycle has the potential to affect soil C cycling, but responses vary between studies and may differ substantially between temperate and tropical regions (Janssens et al. 2010). Inherent soil conditions, including ambient nutrient status, are likely important for determining the response of soil C to N enrichment (Janssens et al. 2010, Cusack et al. 2011).

Because soil properties help determine the direction and magnitude of changes in soil C in response to human activity, it is important to study soil C dynamics across a range of soil environments. To date however, soils of the tropics are understudied relative to the temperate zone, especially with regards to effects of global change (Janssens et al. 2010, Cusack et al. 2016). Additionally, within the tropics, the diversity of soils is not well represented in the research literature. Wet, highly-weathered soils are overrepresented relative to their global coverage while soils in drier climates are underrepresented in studies of soil C responses to land-use change and forest succession (Powers et al. 2011, Marín-Spiotta and Sharma 2013). These biases prevent extrapolation of trends and reduce our ability to accurately understand and model patterns and processes in different soils.

My research addresses uncertainties in controls on soil responses to global change with a focus on soils from the island of Puerto Rico. Puerto Rico represents an ideal study system due to the diversity of soils (10 of 12 USDA soil orders) present in a small area (9105 km^2) and a well-chronicled history of land-use change. By the 1940s, only 6% forest cover remained on the island as land was converted to agriculture and pasture (Franco et al. 1997). Beginning in the 1940s, economic and demographic changes led to the abandonment of much agricultural land, resulting in the growth of secondary forests across the island. Today, approximately 55 % of the island is forested (Brandeis et al. 2007, Parés-Ramos et al. 2008, Marcano-Vega 2017). The extensive changes in forest cover that occurred across the island offer a unique opportunity to study the changes in ecosystem properties that accompanied these land-use and land-cover changes across a wide variety of ecosystems and soil types. These secondary forests are also affected by ongoing human activity, including increasing atmospheric nitrogen deposition. The

Puerto Rican landscape presents a useful context within which to study the influence of human activities in interaction with background soil and ecosystem heterogeneity.

My first chapter explores the effects of long-term experimental nitrogen additions on soil C cycling in lower elevation and upper elevation montane tropical forests in the Luquillo Experimental Forest. Study plots received annual N additions for 15 years and archived soil samples were used to study changes in bulk soils and organic matter fractions isolated via physical density fractionation. Whereas previous studies had observed an effect of fertilization on bulk soil and fraction C and N, we found no consistent effect after 15 years, representing a weakened effect over time. The availability of archived soils collected 9 years before my sampling allowed us to constrain modeled estimates of mean transit time using radiocarbon (^{14}C) measurements. The model estimates confirmed that there were no significant differences in C cycling between fertilized and unfertilized plots, however C cycling rates differed between the two forest types at different elevations. Our models highlight the dynamic nature of C in these soils, as the majority of C in the mineral-associated fraction was found to cycle on decadal time scales. Our models also indicate the importance of including vertical transport of C through the soil profile, as models without this term were unable to accurately represent increases in deeper soil $\Delta^{14}C$ between sampling dates.

My second chapter explores controls on soil C storage at a regional scale, expanding on my previous work done on soil samples collected across the islands of Puerto Rico, St. John, St. Thomas, and St. Croix (Vaughan et al. 2019). In this chapter we used density fractionation to separate SOM fractions from five soil orders (Entisols, Mollisols, Oxisols, Vertisols, and

Ultisols) and three land covers (forest, pasture, cropland) to look at the effects of land cover and soil properties on soil C dynamics within different fractions. We also measured extractable iron and aluminum and natural abundance ^{14}C for the mineral-associated OM fraction. We found that there were more significant differences among OM fractions due to soil order than due to land cover. Mineral fraction C concentrations and ^{14}C-derived mean transit times increased with extractable iron and aluminum concentration, suggesting that iron and aluminum help to stabilize SOM in mineral-organic associations across a diversity of soil environments. These findings contribute to an increasing body of research suggesting the importance of soil physicochemical properties and not just the more commonly measured texture in determining C storage dynamics (e.g., Rasmussen et al. 2018, Vaughan et al. 2019).

My third chapter presents results from a study of soil C storage across a chronosequence of secondary forest succession along a soil-weathering gradient in the karst region of Puerto Rico. Samples were collected from secondary forests from two age classes as well as active pastures on Mollisols and Alfisols derived from the same limestone parent material. Soil total C and N stocks were measured along with soil pH to assess the relative importance of land cover and soil properties on controlling soil C. Mollisols contained greater total C stocks than Alfisols in surface soils (0-30 cm), reflecting the contribution of parent material inorganic carbon in more shallow horizons. Despite expected increases in aboveground biomass with forest growth on pastures, there was no difference in total C or N stocks among pasture soils or forest successional stage at any depth. Soil pH was positively correlated with both total C and N stocks, indicating the role of calcium carbonate in contributing to inorganic C stocks, as well as suggesting stabilization of OM by exchangeable calcium in soils.

I also include a chapter that addresses micro-scale controls on C dynamics stemming from a fellowship I received to travel to the Technical University of Munich in Freising, Germany to conduct Nano-scale Secondary Ion Mass Spectrometry (NanoSIMS) and ^{13}C Nuclear Magnetic Resonance (NMR) spectroscopy on a buried soil from Nebraska. This project addresses similar questions regarding the fundamental environmental controls on decomposition and persistence of soil C. Specifically, I used NMR to look at changes in OM chemical composition within two OM fractions along a gradient of exposure of the Brady soil to modern surface conditions. My work shows that OM in the Brady soil is fundamentally different than modern surface soil but becomes more similar to the modern soil as it is exposed to enhanced decomposition rates as well as inputs of modern plant material. Additionally, NanoSIMS imaging of Brady soil samples from different depths after a laboratory incubation with isotopically enriched organic carbon indicates decomposition of fresh plant material at all depths, particularly by bacteria as opposed to fungi. Both of these approaches suggest that there are implications of landscape disturbance on the persistence of ancient soil C in buried soils.

Literature Cited

Brandeis, T. J., E. H. Helmer, and S. N. Oswalt. 2007. The status of Puerto Rico's forests, 2003. USDA Forest Service - Southern Research Station.

Cusack, D. F., J. Karpman, D. Ashdown, Q. Cao, M. Ciochina, S. Halterman, S. Lydon, and A. Neupane. 2016. Global change effects on humid tropical forests: Evidence for biogeochemical and biodiversity shifts at an ecosystem scale: Tropical Forests and Global Change. Reviews of Geophysics 54:523–610.

Cusack, D. F., W. L. Silver, M. S. Torn, and W. H. McDowell. 2011. Effects of nitrogen additions on above- and belowground carbon dynamics in two tropical forests. Biogeochemistry 104:203–225.

Desjardins, T., F. Andreux, B. Volkoff, and C. C. Cerri. 1994. Organic carbon and 13C contents in soils and soil size-fractions, and their changes due to deforestation and pasture installation in eastern Amazonia. Geoderma 61:103–118.

Desjardins, T., E. Barros, M. Sarrazin, C. Girardin, and A. Mariotti. 2004. Effects of forest conversion to pasture on soil carbon content and dynamics in Brazilian Amazonia. Agriculture, Ecosystems & Environment 103:365–373.

Don, A., J. Schumacher, and A. Freibauer. 2011. Impact of tropical land-use change on soil organic carbon stocks - a meta-analysis. Global Change Biology 17:1658–1670.

Eclesia, R. P., E. G. Jobbagy, R. B. Jackson, F. Biganzoli, and G. Piñeiro. 2012. Shifts in soil organic carbon for plantation and pasture establishment in native forests and grasslands of South America. Global Change Biology 18:3237–3251.

Fisher, M., I. Rao, M. Ayarza, C. Lascano, J. Sanz, R. Thomas, and R. Vera. 1994. Carbon storage by introduced deep-rooted grasses in the South American savannas. Nature 371:236–238.

Franco, P. A., P. L. Weaver, and S. Eggen-McIntosh. 1997. Forest Resources of Puerto Rico, 1990. Page 54. USDA Forest Service - Southern Research Station.

Janssens, I. A., W. Dieleman, S. Luyssaert, J.-A. Subke, M. Reichstein, R. Ceulemans, P. Ciais, A. J. Dolman, J. Grace, G. Matteucci, D. Papale, S. L. Piao, E.-D. Schulze, J. Tang, and B. E. Law. 2010. Reduction of forest soil respiration in response to nitrogen deposition. Nature Geoscience 3:315–322.

Jobbagy, E., and R. Jackson. 2000. The vertical distribution of soil organic carbon and its relation to climate and vegetation. Ecological Applications 10:14.

John, B., T. Yamashita, B. Ludwig, and H. Flessa. 2005. Storage of organic carbon in aggregate and density fractions of silty soils under different types of land use. Geoderma 128:63–79.

Lal, R. 2004. Soil Carbon Sequestration Impacts on Global Climate Change and Food Security. Science 304:1623–1627.

López-Ulloa, M., E. Veldkamp, and G. H. J. de Koning. 2005. Soil carbon stabilization in converted tropical pastures and forests depends on soil type. Soil Science Society of America Journal 69:1110.

von Lützow, M., I. Kogel-Knabner, K. Ekschmitt, E. Matzner, G. Guggenberger, B. Marschner, and H. Flessa. 2006. Stabilization of organic matter in temperate soils: mechanisms and their relevance under different soil conditions - a review. European Journal of Soil Science 57:426–445.

Marcano-Vega, H. 2017. Forest of Puerto Rico, 2014. Page 4. U.S. Department of Agriculture, Forest Service, Southern Forest Experiment Station, Asheville, NC.

Marín-Spiotta, E., and S. Sharma. 2013. Carbon storage in successional and plantation forest soils: a tropical analysis: Carbon in reforested and plantation soils. Global Ecology and Biogeography 22:105–117.

Marín-Spiotta, E., W. L. Silver, C. W. Swanston, and R. Ostertag. 2009. Soil organic matter dynamics during 80 years of reforestation of tropical pastures. Global Change Biology 15:1584–1597.

Parés-Ramos, I. K., W. A. Gould, and T. M. Aide. 2008. Agricultural Abandonment, Suburban Growth, and Forest Expansion in Puerto Rico between 1991 and 2000. Ecology and Society 13.

Powers, J. S., M. D. Corre, T. E. Twine, and E. Veldkamp. 2011. Geographic bias of field observations of soil carbon stocks with tropical land-use changes precludes spatial extrapolation. Proceedings of the National Academy of Sciences 108:6318–6322.

Rasmussen, C., K. Heckman, W. R. Wieder, M. Keiluweit, C. R. Lawrence, A. A. Berhe, J. C. Blankinship, S. E. Crow, J. L. Druhan, C. E. Hicks Pries, E. Marín-Spiotta, A. F. Plante, C. Schädel, J. P. Schimel, C. A. Sierra, A. Thompson, and R. Wagai. 2018. Beyond clay: towards an improved set of variables for predicting soil organic matter content. Biogeochemistry 137:297–306.

Six, J., C. Feller, K. Denef, S. M. Ogle, J. C. de Moraes, and A. Albrecht. 2002. Soil organic matter, biota and aggregation in temperate and tropical soils - Effects of no-tillage. Agronomie 22:755–775.

Torn, M. S., S. E. Trumbore, O. A. Chadwick, P. M. Vitousek, and D. M. Hendricks. 1997. Mineral control of soil organic carbon storage and turnover. Nature 389:170–173.

Trumbore, S. 2009. Radiocarbon and soil carbon dynamics. Annual Review of Earth and Planetary Sciences 37:47–66.

Vaughan, E., M. Matos, S. Ríos, C. Santiago, and E. Marín-Spiotta. 2019. Clay and climate are poor predictors of regional-scale soil carbon storage in the US Caribbean. Geoderma 354:113841.

CHAPTER 1

Radiocarbon modeling indicates dynamic soil carbon cycling and vertical transport in two tropical forests but no long-term effects of nitrogen fertilization

Co-authors: Erika Marín-Spiotta[1], Daniela F. Cusack[2], William H. McDowell[3], and Steven Hall[4]

[1]Department of Geography, University of Wisconsin-Madison

[2]Colorado State University

[3]University of New Hampshire

[4]Iowa State University

Abstract

Humans have substantially altered global nitrogen (N) cycling, with implications for many ecosystem processes, including soil carbon (C) cycling. Although highly-weathered tropical soils are not expected to be limited by N, a short-term study in Puerto Rico observed effects of N fertilization on bulk soil and fraction C and N within the first five years. We explore the effects of long-term experimental nitrogen additions on soil C cycling in lower elevation and upper elevation montane tropical forests in the Luquillo Experimental Forest. Study plots received annual N additions for 15 years and archived soil samples were used to study changes in bulk soils and organic matter fractions isolated via physical density fractionation. We found no consistent effect of fertilization on bulk soil or C fractions after 15 years, representing a weakened effect over time. The availability of archived soils collected 9 years before sampling allowed us to constrain modeled estimates of mean transit time using radiocarbon (^{14}C) measurements. The modelled estimates confirmed that there were no significant differences in C cycling between fertilized and unfertilized plots, however C cycling rates differed between the two forest types at different elevations. Our models highlight the dynamic nature of C in these soils, as the majority of C in the mineral-associated fraction was found to cycle on decadal time scales. Our models also indicate the importance of including vertical transport of C through the soil profile, as models without this term were unable to accurately represent increases in deeper soil $\Delta^{14}C$ between sampling dates. These findings contribute important data on long-term effects of N enrichment in tropical forests, as well as fundamental understanding of dynamic movement of C within the soil profile.

Introduction

Human activities have substantially altered the global nitrogen (N) cycle, increasing the amount of reactive N available to plants and microbes on land through direct fertilization and atmospheric deposition due to fossil fuel combustion (Vitousek et al. 1997, Galloway et al. 2004, 2008, Hietz et al. 2011). N enrichment alters multiple ecosystem processes, including plant growth, microbial decomposition rates, plant and microbial community composition, and soil pH. Due to these changes, soil organic carbon (SOC) cycling can also respond to N enrichment. SOC represents one of the largest terrestrial C reservoirs, accounting for about 2300 Pg of C (Jobbagy and Jackson 2000, Carvalhais et al. 2014), and changes in the SOC pool can have implications for climate change. Many studies have found changes in SOC cycling following N enrichment, yet the direction and magnitude of changes are not consistent and may change with time (Gärdenäs et al. 2011).

Global syntheses tend to show an increase in soil C content following N fertilization (Pregitzer et al. 2007, Janssens et al. 2010) although individual studies have observed increased SOC storage (Cusack et al. 2011b), decreased SOC storage (Khan et al. 2007), or no change in overall stocks but changes in different pools of SOC (Neff et al. 2002, Giardina et al. 2004). The divergent responses of SOC to N enrichment can occur because SOC storage is a balance between plant inputs of OM, and physical and microbial losses of SOM. Plants and soil microbes may respond differently to nutrient enrichment, resulting in decoupling between above and belowground ecosystem processes (Cusack et al. 2011b). The influence of N enrichment on plant inputs and microbial decomposition are mediated by ambient soil N status, soil pH, litter C:N, and other

parameters, which could explain some of the observed variability from site to site (Janssens et al. 2010, Gärdenäs et al. 2011, Camenzind et al. 2018).

The response of tropical forest soils to N addition is especially uncertain, given fewer experiments in these latitudes and the fact that tropical forests may exhibit different patterns of nutrient limitation than temperate systems, where the majority of N addition experiments have occurred (Janssens et al. 2010). Although plant growth in tropical forests on strongly weathered soils can be limited by N (Vitousek 1984, Vitousek and Howarth 1991, LeBauer and Treseder 2008), there is evidence that N limitation of NPP and microbial activity may be less common in tropical regions compared to temperate regions (Reich and Oleksyn 2004, Janssens et al. 2010, Camenzind et al. 2018). Classical nutrient limitation theory predicts older tropical soils to be relatively N-rich and limited more by phosphorus (P) (Walker and Syers 1976). Nonetheless, soils of the tropics are diverse (Townsend et al. 2008) and global syntheses of the effects of N additions may not accurately capture or predict regional trends. For example, a recent meta-analysis of tropical N addition experiments found that microbial activity responded positively to N addition in montane forests, and negatively in lower elevation forests, suggesting that nutrient limitation may vary with climate and degree of soil weathering, both of which vary with elevation (Camenzind et al. 2018).

Anthropogenic perturbations to the N cycle tend to be ongoing and chronic, and ecosystem responses to elevated N may change through time. Most field N enrichment studies report results from just a few years of fertilization. Long-term studies are needed to understand the full implications of N additions. Additional methods, including physical SOC fractionation combined

with ^{14}C measurements, can allow for a more detailed understanding of soil C dynamics within operationally defined C pools, even if bulk soil C responses are difficult to detect.

Our research builds on a long-term field N fertilization experiment to investigate changes in bulk soil C and soil organic matter pools (SOM) isolated by density fractionation following 15 years of continuous N additions in an upper- and lower-elevation montane forest in the Luquillo Experimental Forest in Puerto Rico. The two forests differ in elevation, precipitation, and ambient soil N concentration, with smaller soil N stocks in the upper elevation forest (Table 1). Previous work at these two sites revealed changes in bulk SOC, SOC pools, and microbial communities and enzyme activities following 3 years of N fertilization (Cusack et al. 2011a, 2011b), but no change in aboveground C storage or litter production. The increase in bulk SOC was attributed to an increase in the mineral-associated fraction, which offset decreases in free and aggregate-associated particulate C pools.

This study extends measurements an additional 11 years for a longer view of SOC dynamics. The availability of archived soils, coupled with natural abundance radiocarbon (^{14}C) measurements and modeling of the mineral-associated SOC fraction, provide the opportunity to explore temporal changes in how different pools of SOM respond to N fertilization. We asked: (1) How have C and N stocks in mineral-associated and particulate SOM pools changed following 15 years of nitrogen fertilization?; (2) How does nitrogen addition influence the rate of soil C cycling in the mineral-associated SOM pool?; and (3) Does N addition affect soil C cycling differently in forests with different environmental conditions?

Methods

Site Selection

Soils were collected from two different forest types within the Luquillo Experimental Forest in Puerto Rico as described by McDowell et al. (1992). The forests occur at different elevations and represent different soil, bedrock, and vegetation types. The lower elevation forest, classified as a wet tropical rainforest, is in the Bisley watershed and is located 260 meters above sea level (m.a.s.l.) with mean annual precipitation (MAP) of 3500 mm yr^{-1} (Heartsill-Scalley et al. 2007) and mean annual temperature (MAT) of 23 °C. Vegetation in the lower elevation site is dominated by tabonuco trees (*Dacryodes excelsa*). The upper elevation site, classified as a lower montane forest, is in the Icacos watershed and is located at 640 m.a.s.l with a MAP of 4300-4500 mm yr^{-1} (Murphy et al. 2017) and MAT of 21 °C. The forest at this site is considered Colorado-type after the dominant palo colorado tree species (*Cyrilla racemiflora*). Atmospheric nitrogen deposition in the Luquillo Mountains averaged 2.7 kg N ha^{-1} yr^{-1} over the last 10 years, which represents a significant increase from pre-industrial levels, but no change during the course of the experiment (*National Atmospheric Deposition Program* 2020).

Soils at both sites are comprised primarily of clay-rich Oxisols, with Inceptisols on more rapidly eroding slopes (McDowell et al. 1992, Johnson et al. 2015, Porder et al. 2015). Soils at the upper elevation site contain greater soil P and lower soil N compared to the lower elevation forest (Table 1). Underlying bedrock at the lower elevation forest is comprised of andesitic to basaltic

volcanic sedimentary rocks while the upper elevation forest is underlain by quartz diorite (McDowell et al. 1992).

Nitrogen addition plots were established by W.H. McDowell in 2000 in a paired design, with 3 pairs of plots at each site, for a total of 6 plots per site. Within each pair of plots, one plot was assigned to receive fertilization and one was designated as a control. Fertilized plots were separated from the paired control plot by at least 10 m. Fertilized plots received 50 kg N ha^{-1} yr^{-1} NH_4NO_3 in two annual applications with a hand-held broadcaster from 2002 to 2017.

Soil Sampling

Soils initially were sampled before fertilization began in 2002, and following fertilization in 2005, 2008, 2011, and 2017. We report data from all sampling dates for bulk soil C and N concentrations and from 2008 and 2017 for SOM fractionation. For soils collected in 2005, 2008, 2011, and 2017, soils in each plot were collected using a 2-cm diameter corer at five random points along three 10-m transects. At each point, soils were collected from 0 to 10 cm, 10 to 20 cm, 20 to 30 cm, and 30 to 40 cm depth intervals. Samples were composited by depth within each transect, for a total of 3 samples per depth per plot. Soils were shipped overnight and refrigerated at 4 °C until processing. The samples that were collected in 2002 were collected differently, with soil collected from 0 to 10 cm and 0 to 30 cm. Soils were collected for bulk density measurements in 2005 following the procedure outlined in Cusack et al. (Cusack et al. 2011b). We assume no change in bulk density over the course of the experiment.

Soils were sieved while moist through a 4.75 mm sieve to homogenize the soil and remove rocks and roots while minimizing aggregate disturbance. A subsample was air-dried and ground to a fine powder using a SpexMill 8000D and analyzed for bulk soil organic C and total N concentrations. A subsample of 20 g of field moist soil was used for SOM fractionation as described below.

SOM Fractionation

We performed SOM fractionation for soils collected in 2017 from the 0 to 10 cm and 10 to 20 cm depths from two transects. SOM was separated into three fractions by density following the general method proposed by Swanston et al. (2005). We followed the exact method described by Cusack et al. (2011b). In short, sodium polytungstate (NaPT) with a density of 1.85 g/ml was used to float a free light fraction (fLF), representing free particulate organic matter (POM), after centrifugation. After removing the fLF, the remaining soil was mixed using a Polymix blender and sonicated using a Branson Sonifier at an energy of 200 J mL^{-1} to break apart aggregates. The light fraction was again floated and removed after centrifugation, yielding the occluded light fraction (oLF), which represents POM released from the disruption of aggregates. The remaining OM in the pellet is considered the dense or heavy fraction (HF) which represents mineral-associated OM. All three fractions were rinsed multiple times to remove residual NaPT. The oLF and fLF were dried at 60 °C and the HF was dried at 105° C. All samples were weighed and ground to a fine powder using a SpexMill. We report C and N data for fractions two ways. First, we calculated the content of C and N in each fraction per gram of soil recovered in each fraction

(mg C g bulk soil^{-1} or mg N g bulk soil^{-1}). We also report the proportion of recovered C and N in each fraction (the three fractions together add to 1.0). We refer to these as C content per fraction, and fraction proportion respectively.

Soil C, N, and pH Analyses

Soil C and N concentrations for bulk soil and all fractions were measured using a Flash 2000 elemental analyzer (Thermo Fisher Scientific, Cambridge, UK). All samples were run in duplicate with replicate error of < 10% and aspartic acid as a standard and both aspartic acid and soil reference material as a check standard. As these soils contain no carbonates, all C was assumed to be organic. Soil pH was measured using a glass electrode in a 2:1 slurry of 1.0 M KCl to soil after allowing the mixture to equilibrate for 30 minutes.

^{14}C Analyses and Modeling

Natural abundance ^{14}C was measured for the heavy fraction of one transect of samples per site for soils collected from 0 to 10 cm and 10 to 20 cm in 2008 and 2017. A subsample of heavy fraction was graphitized at the Houghton Carbon, Water, and Soils Lab (USDA-FS Northern Research Station). Radiocarbon measurements were conducted at the Keck Carbon Cycle AMS Facility at the University of California-Irvine. We report radiocarbon values as Δ ^{14}C (‰):

$$\Delta\ ^{14}C = (A_{SN}/A_{ABS} - 1) \times 1000$$

where A_{SN} is the activity of ^{14}C in the sample normalized for isotopic fractionation and decay-corrected to 1950 and A_{ABS} is the absolute international standard activity of oxalic acid (Stuiver and Polach 1977). The A_{SN} values were normalized for isotopic fractionation using measured $\delta^{13}C$ values.

""

Soil ^{14}C dynamics were modeled using a four-pool model to represent a slow-cycling and passive pool within the heavy fraction for each depth (Baisden et al. 2013, Hall et al. 2015). In the model formulation below, the subscript 'slow10' refers to the slow-cycling pool for 0 to 10 cm, 'pass10' is the passive pool for 0 to 10 cm, 'slow20' is the slow-cycling pool for 10 to 20 cm, and 'pass20' is the passive pool for 10 to 20 cm. We used the "GeneralModel_14" function in *SoilR* v. 1.1 (Sierra and Mueller 2014) to fit a steady-state model as follows:

$$\frac{dC(t)}{dt} = I \begin{pmatrix} ß_{slow10} \\ ß_{pass10} \\ ß_{slow20} \\ ß_{pass20} \end{pmatrix} + \begin{pmatrix} -k_{slow10} & 0 & 0 & 0 \\ 0 & -k_{pass10} & 0 & 0 \\ a & 0 & -k_{slow20} & 0 \\ 0 & 0 & 0 & -k_{pass20} \end{pmatrix} \begin{pmatrix} C_{slow10} \\ C_{pass10} \\ C_{slow20} \\ C_{pass20} \end{pmatrix}.$$

In the equation above, I represents the input fluxes to the system, $ß_i$ represents the proportion of inputs to pool i, k_i represents the decomposition coefficient for pool i, and C_i represents the amount of carbon in pool i, and a represents a transfer coefficient of C from pool *slow10* to *slow20*. ^{14}C content of input fluxes and pools are accounted for in the model.

For our model, we assumed that inputs to all pools equaled losses to decomposition such that C stocks remained constant, as we found no consistent evidence of changing C stocks through time in our study. We assumed a passive pool turnover time of 1000 years, thus fixing k_{pass10} *and*

k_{pass20} at 0.00,1 following Baisden et al. (2013), and within the range assumed by other ^{14}C modeling studies in the tropics (Trumbore et al. 1995, Hall et al. 2015). In order to estimate C_{slow10} and C_{slow20}, we defined the total amount of C in the heavy fraction (C_{HF}) as:

$$C_{HF} = C_{pass} + C_{slow}$$

$$C_{HF} = P_{slow} C_{HF} + (1 - P_{slow}) C_{HF}$$

where P_{slow} is the proportion of C in the slow pool and C_{HF} is the measured amount of C in the heavy fraction.

We also assumed a transfer of carbon from the 0 to 10 cm slow-cycling pool to the 10 to 20 cm slow cycling pool. This was implemented after attempts to fit models to each depth independently were unable to match observed data in many of the 10 to 20 cm samples, especially in samples that showed an increase in $\Delta^{14}C$ through time. Including this transfer coefficient improved the model fit to the data in most cases and can be taken to represent the downward transfer of C possibly in the form of dissolved organic carbon (DOC), colloidal C, or through bioturbation.

Thus, our model contains five free parameters (k_{slow10}, P_{slow10}, k_{slow20}, P_{slow20}, and a) and can be simplified as:

$$\frac{dC(t)}{dt} = \begin{pmatrix} k_{slow10}\, C_{slow10} \\ k_{pass10}\, C_{pass10} \\ k_{slow20}\, C_{slow20} \\ k_{slow10}\, C_{slow10} \end{pmatrix} + \begin{pmatrix} -k_{slow10} & 0 & 0 & 0 \\ 0 & -0.001 & 0 & 0 \\ a & 0 & -k_{slow20} & 0 \\ 0 & 0 & 0 & -0.001 \end{pmatrix} \begin{pmatrix} P_{slow10} C_{HF} \\ (1 - P_{slow10}) C_{HF} \\ P_{slow20} C_{HF} \\ (1 - P_{slow20}) C_{HF} \end{pmatrix}.$$

We ran the model between the years 1700 to 2018. We included a lag time of 3 years for C from the atmosphere to reside in plant biomass before entering the mineral-associated pool, as in Hall et al. (2015). For atmospheric ^{14}C inputs, we used the ^{14}C radiocarbon data for zone 2, provided by Hua et al. (2013) through the year 2009, and then used forecasted $\Delta^{14}C$ values for 2009 to 2017 which have been found to closely match northern hemisphere values during that time period (Sierra 2018). We assumed a starting $\Delta^{14}C$ value of -109 ‰ for the passive pool based on expected ^{14}C decay rates for pools with 1000 year turnover. To determine a starting value for the slow pool we first calculated a one-pool steady state turnover time for the slow pool using a starting $\Delta^{14}C$ value of 0 ‰. We then used this turnover time to back-calculate a starting $\Delta^{14}C$ value for the slow pools, or we used the 2008 $\Delta^{14}C$ value, whichever was lesser.

We estimated the values of the free parameters using the *FME* package in R (Soetaert and Petzoldt 2010) similar to the example provided in Sierra et al. (2014). First, we created a cost function with the "modCost" function and then fit a model to our observations using the "modFit" function using the "Nelder-Mead" method. Mean transit time, mean age of the system, and mean age of each pool were defined as in (Sierra et al. 2017) and calculated using the functions "systemAge" and "transitTime" from *SoilR*.

Statistical Analyses

All statistical analyses were conducted using R version 3.6 (R Core Team 2018). The response variables we tested for the most recent sampling date (2017) were bulk soil C and N

concentrations, bulk soil C/N ratio, density fraction C and N concentrations, and density fraction contribution to bulk soil C and N. We included forest type, fertilization treatment, depth, and all interactions between these factors as predictor variables in all analyses. We pooled all variables by plot, using the average of the three transects. We analyzed bulk soil C and N variables using a linear mixed model with nested design (equivalent to a split-split plot design) with the *lme* function in the *nlme* package (Pinheiro et al. 2019). We considered each pair of plots as a block, with the forest type applied at this level. The fertilizer treatment was nested within the forest type, and depth was nested within the fertilizer treatment. Thus, forest, depth, and treatment were fixed effects and the plot pair was considered a random effect. This allowed us to control for spatial heterogeneity and account for possible correlation between depth increments within a plot. We also calculated a fertilization response effect for each response variable by calculating the difference between paired fertilized plots and control plots. A value > 0 indicates a positive response to fertilization, and a value < 0 indicates a negative response to fertilization. We conducted two-sided t-tests to test for differences from 0.

Results

Bulk soil carbon and nitrogen

Soil C and N concentrations in 2017 were not different between forests, although there was greater variability in the upper elevation forest (Fig. 1). Soil C and N concentrations decreased with depth for both forests (Fig. 1, $p < 0.0001$). Soil C stocks to 40 cm were marginally greater in the upper elevation forest (98.0 ± 7.5 Mg C ha^{-1}) than the lower elevation forest (79.3 ± 4.1

Mg C ha^{-1}) ($p = 0.07$). Soil N stocks were marginally greater in the lower elevation forest (6.2 ± 0.3 Mg C ha^{-1}) than in the upper elevation forest (4.7 ± 0.2 Mg C ha^{-1}) ($p = 0.07$, data not shown).

Fifteen years of N fertilization had variable effects on bulk soil C and N. There was no significant effect of fertilization on bulk soil C concentrations or stocks in either forest (Fig. 1, 2). There was a trend toward increased soil C concentrations with fertilization at all depths in the upper elevation forest with two of the three pairs showing substantially greater C concentrations in fertilized plots compared to control plots and one pair showing no difference (Fig. 2). Soil C concentrations in the upper elevation forest were more variable. Bulk soil N also showed variable, but generally positive responses to fertilization in both forests (Fig. 1, 2). There was a significant increase in N for the deepest soils in the lower forest ($p = 0.005$). There was no change in bulk soil C/N ratio with fertilization at any depth in either forest. Although bulk soil C and N concentrations fluctuated during the course of the 15-year experiment, the 2011 and 2017 measurements showed no significant difference from the 2008 data (Figure 3).

Soil carbon fractions

There was no effect of fertilization on SOM fraction C or N concentrations or their contributions to bulk soil C and N stocks. SOM fraction data did differ by forest type and soil depth. For all sites, a majority of C (66-87 %) and N (79-94 %) was found in the mineral-associated heavy fraction (HF) (Fig. 4). HF contributed a greater proportion of C and N in the lower elevation forest than in the upper elevation forest ($p < 0.001$ for both C and N) and there was a marginally

greater contribution to total C and N in the 10 to 20 cm depth ($p = 0.08$ for C, $p = 0.07$ for N). In the lower elevation forest, HF contributed an average of 81 % of C and 90 % of N for 0 to 10 cm, and 86 % of C and 93 % N for 10 to 20 cm. In the upper elevation forest, HF contributed 71 % of C and 82 % of N for 0 to 10 cm, and 75 % of C and 86 % of N for 10 to 20 cm. HF C concentrations did not differ by forest and were marginally greater for deeper soils ($p = 0.08$). HF N concentrations were greater in the lower elevation forest ($p =0.003$) and for deeper soils ($p = 0.03$).

The occluded light fraction (oLF) comprised 9-13 % of recovered C and 4-9 % of recovered N for all sites and depths. There was no difference in oLF C contribution or concentration by treatment, depth, or forest. There was a greater proportion of oLF N in the upper elevation forest ($p = 0.008$) and greater N concentration in the 0 to 10 cm soils ($p = 0.05$).

The free light fraction (fLF) comprised 4-18 % of recovered C and 2-10 % of recovered N for all sites and depths. There was a greater proportion of fLF C in the upper elevation forest ($p < 0.0001$) and a marginally lower proportion of fLF C in the deeper soils ($p = 0.06$). There was a greater fLF C concentration in the upper elevation forest ($p = 0.01$). Patterns for fLF N contribution were similar to patterns for C.

Radiocarbon values and cycling rates

Soil $\Delta^{14}C$ values varied by forest type and soil depth, but not by fertilizer treatment (Table 2). $\Delta^{14}C$ values were greater in the lower elevation forest than in the upper elevation forest and in

the 0 to 10 cm layer than in the 10 to 20 cm layer, indicating a greater contribution of bomb carbon, although this trend was more pronounced in the 2008 samples than in the 2017 samples. Soil $\Delta^{14}C$ values in the 0 to 10 cm layer decreased between 2008 and 2017 in 11 out of 12 plots, with an average decrease of 32 ‰ in the lower elevation forest, and an average decrease of 18 ‰ in the upper elevation forest. On the other hand, in the 10 to 20 cm layer, $\Delta^{14}C$ values only decreased in 4 out of 12 plots. Instead, $\Delta^{14}C$ values increased an average of 14 ‰ in the lower elevation forest and 30 ‰ in the upper elevation forest.

Models that treated the two depths independently were not able to accurately represent increases in soil $\Delta^{14}C$ values for the 10 to 20 cm layer. To better fit the data, a term representing a downward transfer of C from the 0 to 10 cm layer to the 10 to 20 cm layer was added to the model, which significantly improved model fits for most sites. Models generally showed no effect of fertilization on C cycling rates and suggested similar cycling rates overall between forests, but with faster C cycling in surface soils of the upper elevation forest and faster C cycling in deeper soils in the lower elevation forest. Modeled pool ages for the slow pool were greater for deeper soils in both forests (Table 2). Average pool ages for the 0 to 10 cm slow pool were 30 years for the lower elevation forest and 15.7 years for the upper elevation forest. Average pool ages for the 10 to 20 cm layer were 83 years for the lower elevation forest, and 147 years for the upper elevation forest. The mean transit time, which incorporates C passing through all four pools, averaged 39.5 years in the lower elevation forest and 27.3 years in the upper elevation forest (Table 3). Mean system ages averaged 299 years for both the lower elevation forest, and upper elevation forests. The fertilization treatment had no effect on system age or transit times in either forest. The average proportion of C in the slow pool did not differ

significantly by forest, depth, or treatment. Between 64 % and 88 % of carbon was found in the slow pool for all sites (Table 2).

The downward transfer coefficient, which represents the proportion of the steady-state slow pool C flux that was transferred from the upper depth to the lower depth, ranged from 0.002 to 0.006 for plots, representing 0.2 % to 0.6 % of decomposed C transferred downward and incorporated into the 10 to 20 cm slow pool. The average proportion of decomposed C transferred between depths was 0.005 for the lower elevation forest and 0.004 for the upper elevation forest.

Discussion

Varying effect of fertilization through time

Fifteen years of fertilization did not have consistent effects on soil C cycling in two Puerto Rican forests. Earlier work at these sites that showed an effect of fertilization on numerous aspects of C cycling, including increases in bulk soil C and N concentrations and stocks, changes in SOM fractions, and differences in microbial communities (Cusack et al. 2011a, 2011b). Although several of the trends we observed were in the same direction as previously measured (e.g., increases in bulk soil C concentrations), the overall effects were weaker and more variable. Our findings agree with studies in other tropical and temperate systems that have observed no changes in bulk soil C and N with N fertilization (Neff et al. 2002, Giardina et al. 2004, Li et al. 2006). Unlike these other studies, we did not observe a change in cycling rates or fraction contributions. Generally our findings support the idea that responses to fertilization are site-

specific (Hagedorn et al. 2003, Torn et al. 2005) and can change through time (Mo et al. 2006, Fang et al. 2007).

Previously at these sites, there was no evidence of N fertilization effects on NPP, aboveground biomass, or litterfall suggesting a lack of N limitation on plant communities and that changes in microbial communities were responsible for the observed differences in soil C (Cusack et al. 2011a, 2011b). Increases in bulk soil C were hypothesized to be related to increased decomposition of particulate OM and conversion to forms of C that could be stabilized in mineral associations (Cusack et al. 2011b). It is possible this was driven by observed increases in dead root biomass with fertilization, which may have temporarily increased soil C. Our SOM fractionation data did not support that this is still happening as there were no significant differences between SOM fractions by treatment.

The reduced effect of N fertilization on soil C cycling in these forests over time suggests the importance of long-term studies to fully understand the effects of chronic N enrichment. N fertilization has been shown to decrease microbial biomass on average (Treseder 2008), influence microbial community structure (Cusack et al. 2011a) and/or microbial enzyme activity (Waldrop et al. 2004, Waldrop and Zak 2006, Cusack 2013), with attendant changes in decomposition rates, particularly of certain forms of SOM (Janssens et al. 2010). However, most of these studies are conducted after just a few years of fertilization. Longer-term studies of N fertilization often show less significant responses. For example, there is evidence for diminishing effects of N fertilization on microbial communities in a humid temperate forest where changes in microbial biomass and enzyme activity were less pronounced following five years of fertilization

than after one year (Guo et al. 2017). Another long-term fertilization study in Panama found no effect of 10 years of fertilization on microbial biomass or enzyme activities (Turner and Wright 2014). Soil microbial communities facing long-term N enrichment may adapt physiologically or undergo community restructuring over the course of several years and reach a new equilibrium, at which point ongoing effects of fertilization may be minimized.

Another possibility is that soil microbial communities at our sites have responded to changing soil conditions, which have also equilibrated following extended fertilization. A small change in pH due to fertilization was observed following three and five years of fertilization (Cusack et al. 2011b), however we did not measure any significant difference in pH between control and fertilized plots (data not shown). Microbial communities are especially sensitive to changes in pH and it is possible that the short-term changes in decomposition and microbial communities reported by Cusack et al. (2011a) were driven in part by microbial responses to early pH change, which is no longer a factor.

We hypothesized that SOC dynamics in the higher elevation forest would change more strongly with N fertilization, due to lower ambient soil N concentrations and previous findings at these sites and in the tropics more broadly (Cusack et al. 2011b, Camenzind et al. 2018). We did not find consistent evidence of this as neither forest showed a consistent response to fertilization, although generally there was a larger average difference between paired fertilized and control plots in the upper elevation forest.

Active cycling of mineral-associated carbon

Our radiocarbon modeling confirmed that there was no strong effect of fertilization on soil C dynamics. However, models and our fractionation data indicated different SOC dynamics between the two forests and by depth, contributing more broadly to our understanding of C cycling dynamics at these sites. In all sites, the majority of C and N was in the mineral-associated pool. This is consistent with other studies in highly-weathered tropical soils that have found between 70 % and 90 % of C in the mineral-associated fraction (Marín-Spiotta et al. 2009, Cusack et al. 2011b, Hall et al. 2015). The two forests differed in the proportion of mineral-associated C, with greater proportions of mineral-associated C and N in the lower elevation forest and greater proportions of free- and occluded-light fraction in the upper elevation. This is likely driven by the difference in climate between the two forests, with cooler temperatures, and greater precipitation at the upper elevation forest potentially slowing rates of decomposition and allowing for greater buildup of particulate OM (fLF and oLF). Previous work within the Luquillo Experimental Forest has shown lower soil oxygen concentrations and greater clay content with increasing elevation and precipitation in the Luquillo Experimental Forest (Silver et al. 1999, Liptzin et al. 2011), which would suggest lower rates of decomposition of litter and particulate SOM in shallow soils.

In general, our models suggest that SOC in the mineral-associated pool at these sites is quite dynamic, with the majority of C in the top 20 cm depth (~60 to 80 % for most sites) found in the "slow" pool with decadal turnover (30 to 80 years for the lower elevation forest, 15 to 150 years for the upper elevation forest). Mineral-associated C is often thought to be relatively stable, but our results support other work showing active cycling of mineral-associated C over decadal

scales (Torn et al. 2013, Hall et al. 2015). Our estimates of pool age and turnover are similar to studies from nearby forests (Hall et al. 2015) and other tropical systems (Trumbore et al. 1995). We found evidence of generally older C and slower cycling in the 10 to 20 cm soils than in the 0 to 10 cm soils.

The large proportion of decadal-cycling C indicates that the lack of a response to fertilization that we observed is likely not due to a slow response in the mineral-associated C pool, given that the duration of experimental fertilization was of a similar period as the slow-pool transit time. In fact, our findings may help justify the rapid response to fertilization observed in the mineral fraction for these sites after just three years of fertilization (Cusack et al. 2011b). These findings also indicate that mineral-associated C in these forests may be responsive on short time scales to other changes such as land-use change or hurricane disturbance.

Using radiocarbon data from archived soils allowed us to better constrain our models. Turnover times for soil C are often estimated from one sampling time and assuming one homogeneous SOC pool. This approach often leads to two different solutions for turnover (Marín-Spiotta et al. 2008) and can lead to opposing interpretations as compared with the two-pool approach we adopted here (Hall et al. 2015). For example, using one time-point and a single-pool model to estimate turnover times for sites in this study usually gave one solution with a turnover time of less than ten years, and one with a turnover time over 100 years. Using two time-points provided a qualitatively different answer, whereby most of the dense fraction C had a turnover time of 14 to 40 years, with a few sites over 100 years.

Our models for sites were generally able to accurately fit the measured radiocarbon data, in agreement with findings from similar forests (Hall et al. 2015). Some studies have suggested that more complex model structures may better represent soil C dynamics, and it's possible that this would have improved model performance in the cases where we were not able to perfectly fit the data. Given the number of parameters we estimated from limited data points, there was some flexibility in the model parameters that produced good fits for our data. However, the parameters of interest generally converged on similar values and our models seem to accurately represent general patterns of soil C dynamics.

Dynamic transport of soil C

Our models also highlighted the dynamic nature of C transport with depth in these soils. Our first attempts to model the two soil depths independently were not able to successfully capture enrichment of radiocarbon in the deeper soil between the two sampling dates. This indicated that bomb C is still being incorporated into deeper soil horizons. Our explanation for this is that this C resides in the upper soil and then is eventually released downward, causing the deeper soils to lag behind surface soils in the accumulation and eventual depletion of this enriched signal. There are a number of different mechanisms by which C could be transported downward. Both forests receive high levels of precipitation and transport of dissolved organic carbon (DOC) down through the soil profile is likely responsible for significant C fluxes (Cusack et al. 2011b, Hall et al. 2015). Colloidal transport of C has also been shown to be an important mechanism of C transfer under high rainfall conditions (Marin-Spiotta et al. 2011), especially in soils high in iron oxides undergoing redox reactions (Buettner et al. 2014). These highly weathered and sometimes

saturated soils would facilitate colloidal transfer. Bioturbation, especially due to earthworm activity, could also contribute significantly to C transfer between depths at these sites (González et al. 2006).

Despite the importance of this transfer term for fitting our models to the observed ^{14}C data, the rate of downward C transfer was less than 1 % of the slow pool C flux from soil layer above. Some plots were not able to be modeled accurately, which could be due to the fact that our model only accounted for mineral-associated C, whereas DOC produced from roots, POM and litter in the overlying soil layers could contribute additional C to the 10 to 20 cm mineral-associated pool.

Although levels of atmospheric N deposition did not change appreciably during this experiment, it is possible that decades of low-level N enrichment have masked differences between control plots and fertilized plots. Landscape evolution and disturbance may have also confounded some of the effects of fertilization and/or changes in ^{14}C between sampling dates. These sites are on slopes and subject to small and large disturbances. In both forests, two pairs of plots showed similar responses to fertilization, and one pair of plots showed markedly different responses between the treatments. For at least one of these pairs in the upper elevation forest, significant erosion and soil movement has occurred, which may obscure any effects of fertilization, and contribute to the observed variability in soil ^{14}C. In addition, large spatial variability in these heterogeneous landscapes, even at the within plot scale, also could have masked temporal trends.

Conclusions

Our work showed that 15-year N enrichment of two forests in the Luquillo Mountains Puerto Rico had no consistent effect on soil C dynamics, despite strong effects earlier in the experiment. The use of natural abundance ^{14}C samples collected from two time points allowed us to more accurately constrain models of soil C dynamics, which indicate that soil C in these forests is dynamically cycling, with the majority of C in the mineral-associated pool cycling on decadal time scales. Our models also indicate the importance of transport of C from surface to underlying soils to accurately capture C dynamics, further highlighting the dynamic nature of C cycling in these soils.

Our results have implications for global C cycling studies and modeling efforts, as well as forest soil and nutrient management. They also provide additional evidence that C cycling in topographically-diverse, highly-weathered soils is spatially and temporally dynamic. Mineral-associated C is often thought to be stable, but we show that it contains a significant portion cycling on decadal scales, which increases its susceptibility to disturbance. Ecosystem enrichment with N is projected to continue growing into the future, especially in tropical regions, and has the potential to influence many different ecosystem responses at a variety of timescales. There is growing understanding of the need to couple models of soil C cycling with nutrients, to better understand soil responses to a variety of global changes, including climate change, and nutrient enrichment (Gärdenäs et al. 2011, Abramoff et al. 2017). However, accurate representation and testing of long-term patterns requires long-term data, and our results show that short-term patterns may not hold indefinitely.

Tables

Table 1. Site characteristics for two Puerto Rican forests. Data are from Cusack et al. (2011b).

Forest	Watershed	Elevation (m.a.s.l)	MAT (°C)	MAP (mm yr^{-1})	Lithology	Ambient Soil N %	Aboveground C (Mg Ha^{-1})
Lower elevation	Bisley	260	23°	3500	Andesitic to basaltic volcanic sedimentary rock	0.37	81.5
Upper elevation	Icacos	640	21°	4400	Quartz diorite	0.24	91

Table 2. Summary data from model outputs by treatment, depth, and forest. Each line represents the mean (SE) for the number of plots given by *n*. The change in $\Delta^{14}C$ represents the difference between a plot's $\Delta^{14}C$ as measured in 2017 and 2008, with negative numbers representing a decrease in $\Delta^{14}C$ with time.

Forest	Depth	Treatment	n	$\Delta^{14}C$ 2008 (‰)	$\Delta^{14}C$ 2017 (‰)	Change $\Delta^{14}C$ (‰)	Slow Pool Age (yrs)	Proportion in Slow Pool
Lower	0 to 10 cm	Control	3	85.5 (15.4)	56.2 (9.9)	-29.3 (6.3)	30.2 (18.7)	0.81 (0.03)
		Fertilized	3	98.1 (12.7)	64.2 (3.3)	-33.9 (9.5)	29.8 (13.4)	0.79 (0.05)
		All Plots	*6*	91.8 (9.4)	60.2 (5)	-31.6 (5.2)	30.0 (10.3)	0.80 (0.02)
	10 to 20 cm	Control	3	26.9 (43.3)	31.7 (32.5)	4.8 (14.4)	108.6 (73.6)	0.65 (0.13)
		Fertilized	3	28.8 (43.1)	51.5 (10.6)	22.7 (33.8)	57.9 (30.4)	0.64 (0.16)
		All Plots	*6*	27.9 (27.3)	41.6 (15.9)	13.7 (16.9)	83.3 (37.4)	0.65 (0.09)
Upper	0 to 10 cm	Control	3	62.9 (24.3)	34.7 (7.3)	-28.2 (17.6)	11.1 (3.0)	0.70 (0.02)
		Fertilized	3	55.8 (12.4)	48.3 (8.6)	-7.5 (4.5)	20.3 (15.1)	0.79 (0.03)
		All Plots	*6*	59.4 (12.3)	41.5 (5.9)	-17.8 (9.4)	15.7 (7.2)	0.75 (0.02)
	10 to 20 cm	Control	3	6.6 (35.1)	34 (9.5)	27.4 (25.9)	119.3 (75.6)	0.64 (0.08)
		Fertilized	3	10 (3.1)	43.3 (10.8)	33.3 (10.8)	175.1 (8.0)	0.88 (0.03)
		All Plots	*6*	8.3 (15.8)	38.7 (6.8)	30.4 (12.6)	147.2 (36.2)	0.76 (0.07)

Table 3. Summary of model outputs. Mean transit time (MTT) and mean system age (MSA) are given for the entire four pool model, consisting of the slow and passive pools for both 0 - 10 cm and 10 – 20 cm.

Forest	Treatment	n	Mean Transit Time (yrs)	Mean System Age (yrs)	Transfer Coefficient
Lower	Control	3	37.8 (16.9)	298.3 (64.3)	0.005 (0.0001)
	Fertilized	3	41.2 (15.4)	299.2 (82.2)	0.005 (0.0004)
	All Plots	6	39.5 (10.3)	298.7 (46.7)	0.005 (0.002)
Upper	Control	3	20.7 (5.4)	354.0 (34.4)	0.005 (0.0002)
	Fertilized	3	34.0 (24.7)	244.1 (24.2)	0.004 (0.0007)
	All Plots	6	27.3 (11.7)	299.1 (30.9)	0.004 (0.0004)

Figures

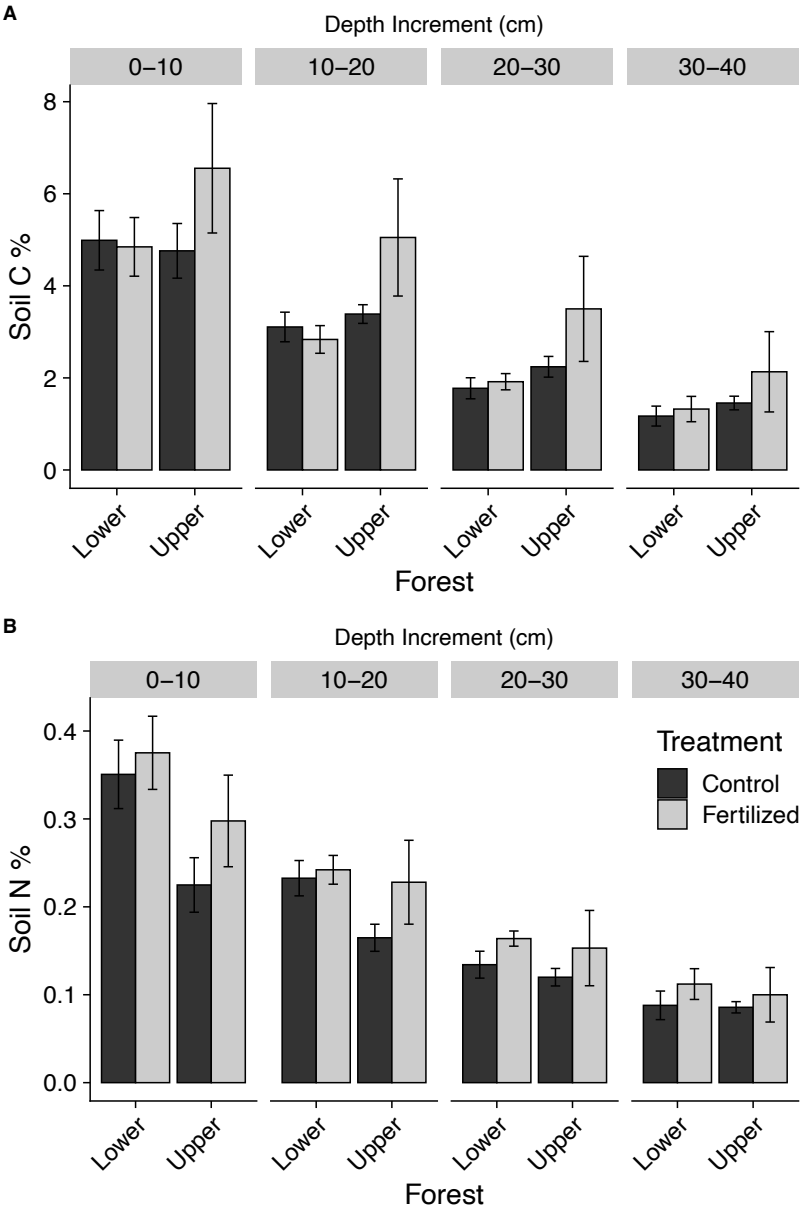

Figure 1. Soil carbon (a) and nitrogen (b) concentrations by forest, depth for two Puerto Rican forests as measured in 2017. Data are means from 3 plots per treatment for forest. The error bar represents the standard error. Note the difference in scale of the y-axis.

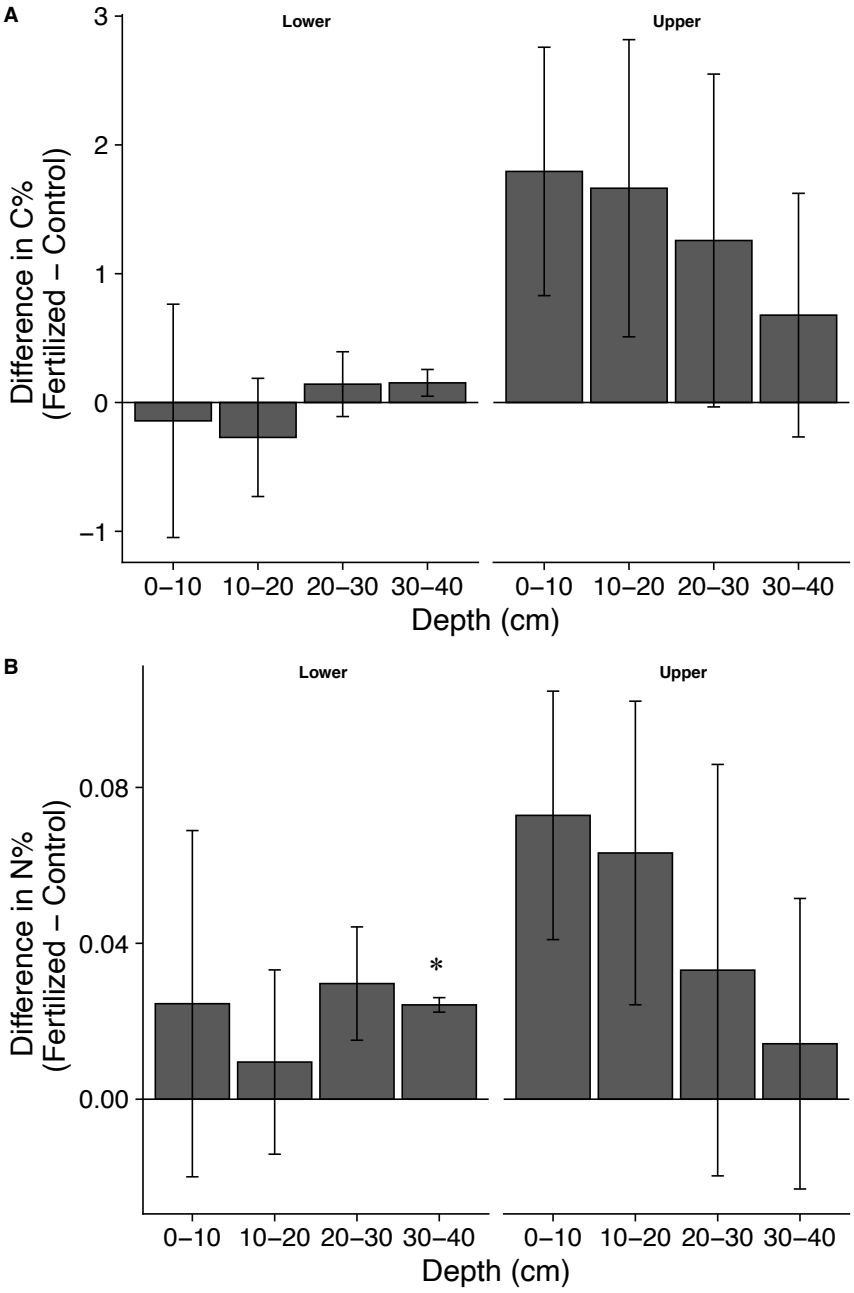

Figure 2. Differences in soil carbon (a) and nitrogen (b) between paired plots in 2017. Bar heights represent the average difference between three pairs of plots. A positive value indicates the fertilized plot had higher C or N, and a negative value indicates that the control plot had higher C or N. Error bars indicate the standard error. Asterisks denote a difference that was significantly different from 0 ($p < 0.05$). Note the difference in scale of the y-axis.

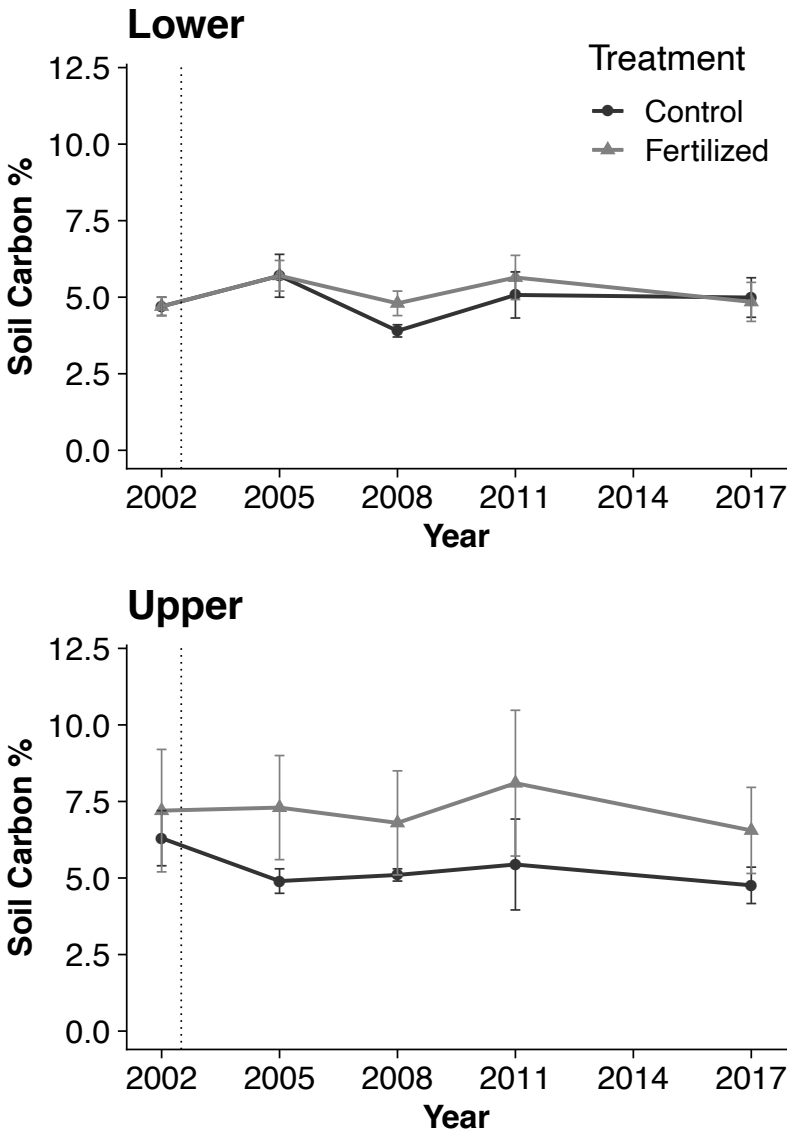

Figure 3. Bulk soil carbon through time for each treatment for 0 to 10 cm. The vertical dashed line represents when the fertilization treatment was started.

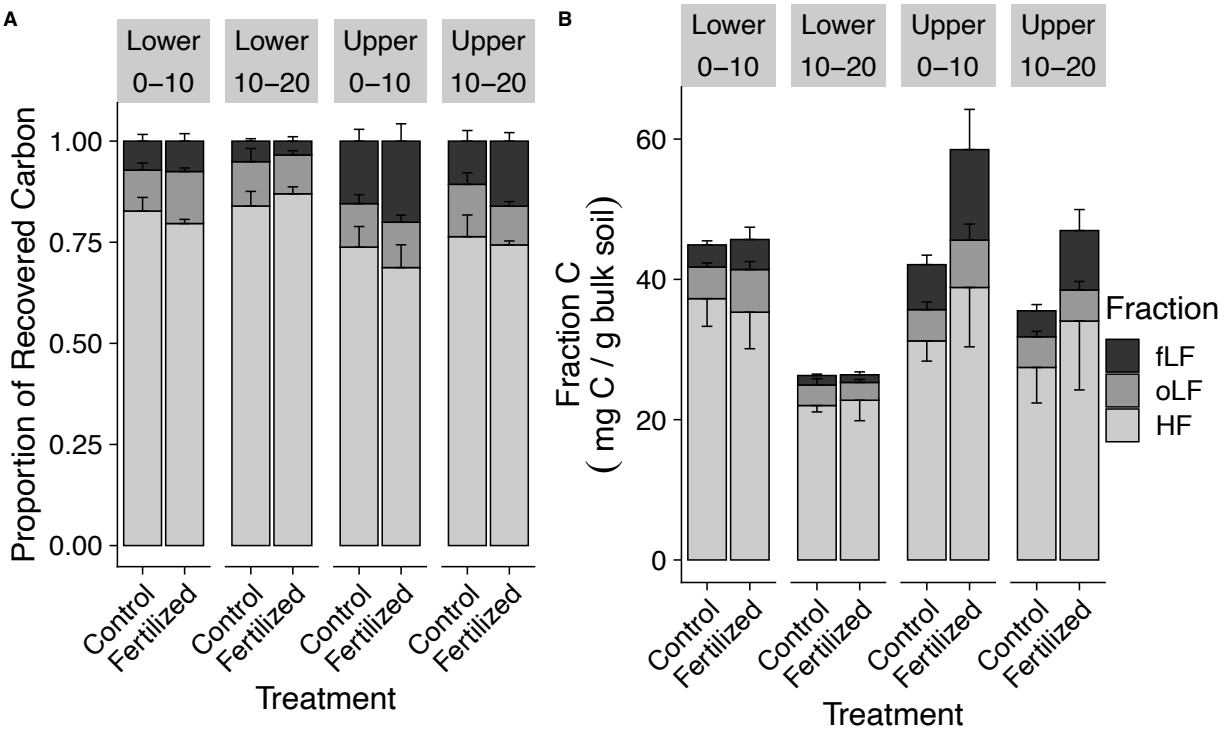

Figure 4. Distribution of soil organic carbon in three density fractions; a free light fraction (fLF), an occluded light fraction (oLF), and a heavy fraction (HF). Figure A shows the relative proportion of recovered carbon in each fraction. Figure B shows the carbon content per gram bulk soil for each fraction.

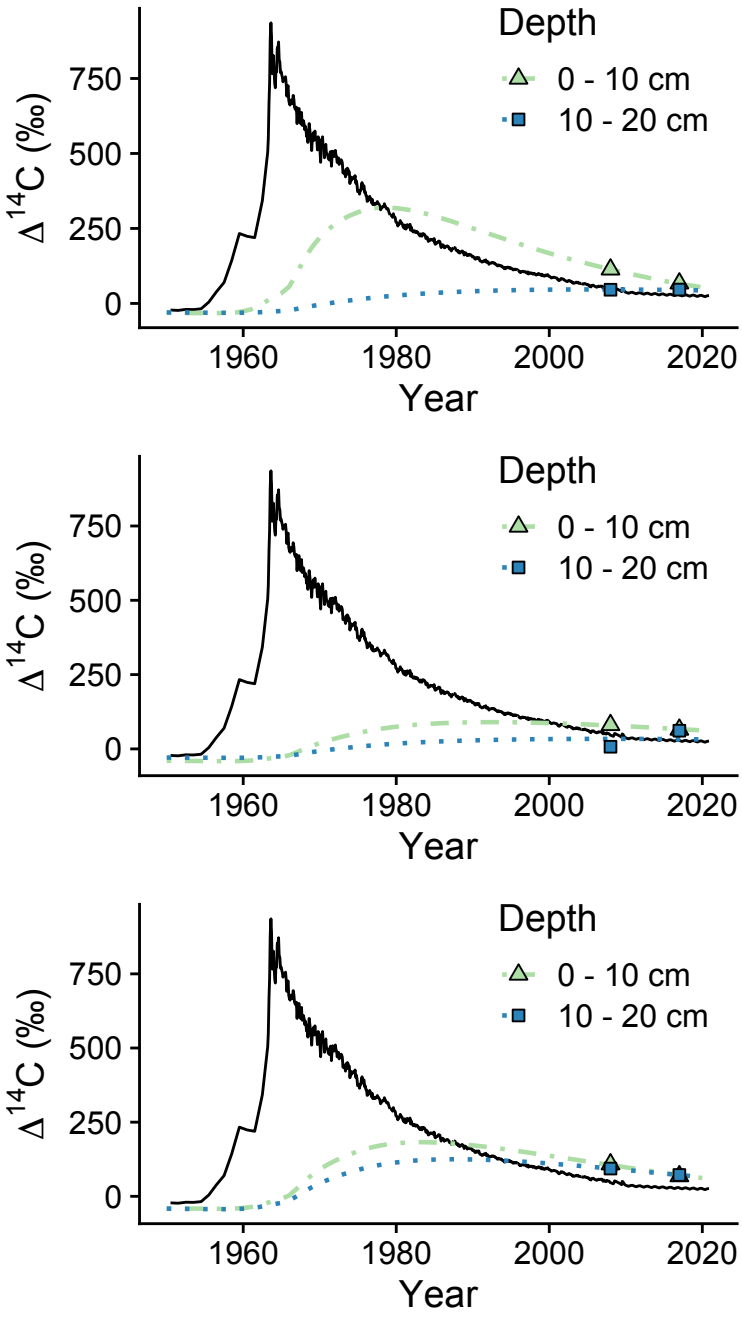

Figure 5. Modeled heavy fraction ^{14}C values for two soil depths of three representative plots. The solid black represents atmospheric radiocarbon, while the colored dashed lines represent the weighted $\Delta^{14}C$ given by models with parameters optimized to fit the two data points for each depth. The green dashed line and triangles represent the 0 to 10 cm depth, and the blue dotted line and squares represent the 10 to 20 cm depth. The top panel shows a plot with a modest increase in 10 to 20 cm $\Delta^{14}C$ between 2008 and 2017, which the model captured well. The middle panel shows a plot with a larger increase in 10 to 20 cm $\Delta^{14}C$, which was not as accurately modeled. The bottom panel shows a plot with a decrease in $\Delta^{14}C$ for in both the 0 to 10 and 10 to 20 cm layers.

Literature Cited

Abramoff, R. Z., E. A. Davidson, and A. C. Finzi. 2017. A parsimonious modular approach to building a mechanistic belowground carbon and nitrogen model: Parsimonious, Modular Model of Belowground C and N Cycling. Journal of Geophysical Research: Biogeosciences 122:2418–2434.

Baisden, W. T., R. L. Parfitt, C. Ross, L. A. Schipper, and S. Canessa. 2013. Evaluating 50 years of time-series soil radiocarbon data Towards routine calculation of robust C residence times. Biogeochemistry 112:129–137.

Buettner, S. W., M. G. Kramer, O. A. Chadwick, and A. Thompson. 2014. Mobilization of colloidal carbon during iron reduction in basaltic soils. Geoderma 221–222:139–145.

Camenzind, T., S. Hättenschwiler, K. K. Treseder, A. Lehmann, and M. C. Rillig. 2018. Nutrient limitation of soil microbial processes in tropical forests. Ecological Monographs 88:4–21.

Carvalhais, N., M. Forkel, M. Khomik, J. Bellarby, M. Jung, M. Migliavacca, M. Mu, S. Saatchi, M. Santoro, M. Thurner, U. Weber, B. Ahrens, C. Beer, A. Cescatti, J. T. Randerson, and M. Reichstein. 2014. Global covariation of carbon turnover times with climate in terrestrial ecosystems. Nature 514:213–217.

Cusack, D. F. 2013. Soil nitrogen levels are linked to decomposition enzyme activities along an urban-remote tropical forest gradient. Soil Biology and Biochemistry 57:192–203.

Cusack, D. F., W. L. Silver, M. S. Torn, S. D. Burton, and M. K. Firestone. 2011a. Changes in microbial community characteristics and soil organic matter with nitrogen additions in two tropical forests. Ecology 92:621–632.

Cusack, D. F., W. L. Silver, M. S. Torn, and W. H. McDowell. 2011b. Effects of nitrogen additions on above- and belowground carbon dynamics in two tropical forests. Biogeochemistry 104:203–225.

Fang, H., J. Mo, S. Peng, Z. Li, and H. Wang. 2007. Cumulative effects of nitrogen additions on litter decomposition in three tropical forests in southern China. Plant and Soil 297:233–242.

Galloway, J. N., F. J. Dentener, D. G. Capone, E. W. Boyer, R. W. Howarth, S. P. Seitzinger, G. P. Asner, C. C. Cleveland, P. a Green, E. a Holland, D. M. Karl, a F. Michaels, J. H. Porter, a R. Townsend, and C. J. Vöosmarty. 2004. Nitrogen Cycles: Past, Present, and Future. Biogeochemistry 70:153–226.

Galloway, J. N., A. R. Townsend, J. W. Erisman, M. Bekunda, Z. Cai, J. R. Freney, L. A. Martinelli, S. P. Seitzinger, and M. A. Sutton. 2008. Transformation of the Nitrogen Cycle: Recent Trends, Questions, and Potential Solutions. Science 320:889–892.

Gärdenäs, A. I., G. I. Ågren, J. A. Bird, M. Clarholm, S. Hallin, P. Ineson, T. Kätterer, H. Knicker, S. I. Nilsson, T. Näsholm, S. Ogle, K. Paustian, T. Persson, and J. Stendahl. 2011. Knowledge gaps in soil carbon and nitrogen interactions – From molecular to global scale. Soil Biology and Biochemistry 43:702–717.

Giardina, C. P., D. Binkley, M. G. Ryan, J. H. Fownes, and R. S. Senock. 2004. Belowground carbon cycling in a humid tropical forest decreases with fertilization. Oecologia 139:545–550.

González, G., C. Y. Huang, X. Zou, and C. Rodríguez. 2006. Earthworm invasions in the tropics. Biological Invasions 8:1247–1256.

Guo, P., J. Jia, T. Han, J. Xie, P. Wu, Y. Du, and K. Qu. 2017. Nonlinear responses of forest soil microbial communities and activities after short- and long-term gradient nitrogen additions. Applied Soil Ecology 121:60–64.

Hagedorn, F., D. Spinnler, and R. Siegwolf. 2003. Increased N deposition retards mineralization of old soil organic matter. Soil Biology and Biochemistry 35:1683–1692.

Hall, S. J., G. McNicol, T. Natake, and W. L. Silver. 2015. Large fluxes and rapid turnover of mineral-associated carbon across topographic gradients in a humid tropical forest: insights from paired 14C analysis. Biogeosciences 12:2471–2487.

Heartsill-Scalley, T., F. N. Scatena, C. Estrada, W. H. McDowell, and A. E. Lugo. 2007. Disturbance and long-term patterns of rainfall and throughfall nutrient fluxes in a subtropical wet forest in Puerto Rico. Journal of Hydrology 333:472–485.

Hietz, P., B. L. Turner, W. Wanek, A. Richter, C. A. Nock, and S. J. Wright. 2011. Long-term change in the nitrogen cycle of tropical forests. Science 334:664–666.

Hua, Q., M. Barbetti, and A. Z. Rakowski. 2013. Atmospheric Radiocarbon for the Period 1950–2010. Radiocarbon 55:2059–2072.

Janssens, I. A., W. Dieleman, S. Luyssaert, J.-A. Subke, M. Reichstein, R. Ceulemans, P. Ciais, A. J. Dolman, J. Grace, G. Matteucci, D. Papale, S. L. Piao, E.-D. Schulze, J. Tang, and B. E. Law. 2010. Reduction of forest soil respiration in response to nitrogen deposition. Nature Geoscience 3:315–322.

Jobbagy, E., and R. Jackson. 2000. The vertical distribution of soil organic carbon and its relation to climate and vegetation. Ecological Applications 10:14.

Johnson, A. H., H. X. Xing, and F. N. Scatena. 2015. Controls on Soil Carbon Stocks in El Yunque National Forest, Puerto Rico. Soil Science Society of America Journal 79:294–304.

Khan, S. A., R. L. Mulvaney, T. R. Ellsworth, and C. W. Boast. 2007. The Myth of nitrogen fertilization for soil carbon sequestration. Journal of Environment Quality 36:1821.

LeBauer, D. S., and K. K. Treseder. 2008. Nitrogen limitation of net primary productivity in terrestrial ecosystems is globally distributed. Ecology 89:371–379.

Li, Y., M. Xu, and X. Zou. 2006. Effects of nutrient additions on ecosystem carbon cycle in a Puerto Rican tropical wet forest. Global Change Biology 12:284–293.

Liptzin, D., W. L. Silver, and M. Detto. 2011. Temporal dynamics in soil oxygen and greenhouse gases in two humid tropical forests. Ecosystems 14:171–182.

Marín-Spiotta, E., W. L. Silver, C. W. Swanston, and R. Ostertag. 2009. Soil organic matter dynamics during 80 years of reforestation of tropical pastures. Global Change Biology 15:1584–1597.

Marín-Spiotta, E., C. W. Swanston, M. S. Torn, W. L. Silver, and S. D. Burton. 2008. Chemical and mineral control of soil carbon turnover in abandoned tropical pastures. Geoderma 143:49–62.

McDowell, W. H., W. B. Bowden, and C. E. Asbury. 1992. Riparian nitrogen dynamics in two geomorphologically distinct tropical rain forest watersheds: subsurface solute patterns. Biogeochemistry 18:53–75.

Mo, J., S. Brown, J. Xue, Y. Fang, and Z. Li. 2006. Response of litter decomposition to simulated N deposition in disturbed, rehabilitated and mature forests in subtropical China. Plant and Soil 282:135–151.

Murphy, S. F., R. F. Stallard, M. A. Scholl, G. González, and A. J. Torres-Sánchez. 2017. Reassessing rainfall in the Luquillo Mountains, Puerto Rico: Local and global ecohydrological implications. PLOS ONE 12:e0180987.

National Atmospheric Deposition Program. 2020. . National Atmospheric Deposition Program.

Neff, J. C., A. R. Townsend, G. Gleixner, S. J. Lehman, J. Turnbull, and W. D. Bowman. 2002. Variable effects of nitrogen additions on the stability and turnover of soil carbon. Nature 419:915–917.

Pinheiro, J., D. Bates, S. DebRoy, D. Sarkar, and R Core Team. 2019. nlme: Linear and Nonlinear Mixed Effects Models.

Porder, S., Arthur. H. Johnson, H. X. Xing, G. Brocard, S. Goldsmith, and J. Pett-Ridge. 2015. Linking geomorphology, weathering and cation availability in the Luquillo Mountains of Puerto Rico. Geoderma 249–250:100–110.

Pregitzer, K. S., A. J. Burton, D. R. Zak, and A. F. Talhelm. 2007. Simulated chronic nitrogen deposition increases carbon storage in Northern Temperate forests. Global Change Biology 0:071121035853002-???

R Core Team. 2018. R: A language and environment for statistical computing. R Foundation for Statistical Computing.

Reich, P. B., and J. Oleksyn. 2004. Global patterns of plant leaf N and P in relation to temperature and latitude. Proceedings of the National Academy of Sciences 101:11001–11006.

Sierra, C. A. 2018. Forecasting atmospheric radiocarbon decline to pre-bomb values. Radiocarbon 60:1055–1066.

Sierra, C. A., and M. Mueller. 2014. SoilR.

Sierra, C. A., M. Müller, H. Metzler, S. Manzoni, and S. E. Trumbore. 2017. The muddle of ages, turnover, transit, and residence times in the carbon cycle. Global Change Biology 23:1763–1773.

Sierra, C. A., M. Müller, and S. E. Trumbore. 2014. Modeling radiocarbon dynamics in soils: SoilR version 1.1. Geoscientific Model Development 7:1919–1931.

Silver, W. L., A. E. Lugo, and M. Keller. 1999. Soil oxygen availability and biogeochemistry along rainfall and topographic gradients in upland wet tropical forest soils. Biogeochemistry 44:301–328.

Soetaert, K., and T. Petzoldt. 2010. FME.

Stuiver, M., and H. A. Polach. 1977. Reporting of 14C Data. Radiocarbon 19:355–363.

Swanston, C. W., M. S. Torn, P. J. Hanson, J. R. Southon, C. T. Garten, E. M. Hanlon, and L. Ganio. 2005. Initial characterization of processes of soil carbon stabilization using forest stand-level radiocarbon enrichment. Geoderma 128:52–62.

Torn, M. S., M. Kleber, E. S. Zavaleta, B. Zhu, C. B. Field, and S. E. Trumbore. 2013. A dual isotope approach to isolate soil carbon pools of different turnover times. Biogeosciences 10:8067–8081.

Torn, M. S., P. M. Vitousek, and S. E. Trumbore. 2005. The influence of nutrient availability on soil organic matter turnover estimated by incubations and radiocarbon modeling. Ecosystems 8:352–372.

Townsend, A., G. Asner, and C. Cleveland. 2008. The biogeochemical heterogeneity of tropical forests. Trends in Ecology & Evolution 23:424–431.

Treseder, K. K. 2008. Nitrogen additions and microbial biomass: a meta-analysis of ecosystem studies. Ecology Letters 11:1111–1120.

Trumbore, S. E., E. A. Davidson, P. Barbosa de Camargo, D. C. Nepstad, and L. A. Martinelli. 1995. Belowground cycling of carbon in forests and pastures of eastern Amazonia. Global Biogeochemical Cycles 9:515–528.

Turner, B. L., and S. J. Wright. 2014. The response of microbial biomass and hydrolytic enzymes to a decade of nitrogen, phosphorus, and potassium addition in a lowland tropical rain forest. Biogeochemistry 117:115–130.

Vitousek, M. V., D. A. John, W. H. Robert, E. L. Gene, A. M. Pamela, W. S. David, and G. T. David. 1997. Human alteration of the global nitrogen cycle: sources and consequences. Ecological Applications 7:737–750.

Vitousek, P. M. 1984. Litterfall, nutrient cycling, and nutrient limitation in tropical forests. Ecology 65:285–298.

Vitousek, P. M., and R. W. Howarth. 1991. Nitrogen Limitation on Land and in the Sea - How Can It Occur. Biogeochemistry 13:87–115.

Waldrop, M. P., and D. R. Zak. 2006. Response of oxidative enzyme activities to nitrogen deposition affects soil concentrations of dissolved organic carbon. Ecosystems 9:921–933.

Waldrop, M. P., D. R. Zak, R. L. Sinsabaugh, M. Gallo, and C. Lauber. 2004. Nitrogen deposition modifies soil carbon storage through changes in microbnial enzymatic activity. Ecological Applications 14:1172–1177.

Walker, T. W., and J. K. Syers. 1976. The fate of phosphorus during pedogenesis. Geoderma 15:1–19.

CHAPTER 2

Effects of soil properties and land cover on organic matter fractions and soil carbon turnover across diverse Puerto Rican soils

Co-authors: Erika Marín-Spiotta[1]

[1]Department of Geography, University of Wisconsin-Madison

Abstract

Tropical soils contain a significant portion of the global carbon (C) stocks, with important implications for climate change and soil fertility. Despite the importance of understanding controls on soil C at the landscape scale, uncertainties remain which hamper our ability to predict patterns of soil C storage as well as responses of soil C to human land use. The amount of C in soil is affected by soil properties, including soil texture, pH, clay mineralogy, and landscape level variables such as vegetation, climate, and land management. Interactions between these variables at different spatial scales remains challenging to predict. This study seeks to improve our understanding of controls on soil C dynamics across a diverse range of five soil orders from Puerto Rico and the US Virgin Islands. Previous work at these sites found that traditional predictors of soil C, such as clay and climate, did not accurately predict C stocks (Vaughan et al. 2019). We conducted physical density fractionation on soil organic matter (OM) pools, and measured radiocarbon (^{14}C) and sodium pyrophosphate-extractable iron (Fe) and aluminum (Al). There were more significant differences in OM fractions associated with soil order than with land cover. Mineral fraction C concentrations and ^{14}C-derived mean transit times increased with extractable iron and aluminum concentration, suggesting that iron and aluminum help to stabilize SOM in mineral-organic associations across a diversity of soil environments. These findings contribute to an increasing body of research suggesting the importance of soil physicochemical properties and not just the more commonly measured texture in determining C storage dynamics (e.g., Rasmussen et al. 2018).

Introduction

Soils of the tropics are an important component of the global carbon (C) budget, containing between 30 % and 40 % of global soil C (Carvalhais et al., 2014; Jobbágy and Jackson, 2000). Understanding the factors controlling soil C cycling in the tropics could have important implications for global climate change as well as nutrient availability and soil fertility. Numerous factors control soil organic carbon (SOC) accumulation and loss, including human land use, climate, vegetation, soil biological activity, texture, and soil mineralogy (Brown and Lugo, 1990; Jobbágy and Jackson, 2000; Li et al., 2012; Marín-Spiotta and Sharma, 2013). These factors interact to determine SOC dynamics at a variety of scales, and there is substantial interest in better understanding the importance of these different factors and at which scales each is important (Rasmussen et al. 2018, Wiesmeier et al. 2019). Despite this interest, there remains uncertainty in using these factors to predict SOC dynamics across scales. This may be particularly true in tropical systems, which are under-studied relative to temperate systems, and show geographic bias of studies (Powers et al. 2011).

Although climate exerts powerful control on processes that influence soil C dynamics at continental scales, it becomes less predictive at finer scales (Wiesmeier et al. 2019), especially in places with diverse geologic histories (Vaughan et al. 2019). Land cover and land use change (hereafter combined as "land change") have been shown to influence soil C stocks in a number of tropical studies (Fisher et al. 1994, Beinroth et al. 1996, Neumann-Cosel et al. 2011, Li et al. 2012) but some studies have observed changes only in individual C pools (Marín-Spiotta et al.

2009). There is also evidence that soil properties can interact with land change to influence SOC dynamics (López-Ulloa et al. 2005).

Clay content, or the fine fraction including fine silt of soil is believed to be positively related to the potential of soil to stabilize and store C long-term and, as it varies at smaller scales than climate, is expected to provide additional predictive power at the sub-regional scale and below (Wiesmeier et al. 2019) . However, clay content does not always correlate strongly with soil C content (Rasmussen et al. 2018, Vaughan et al. 2019), and studies have shown the importance of not just clay and silt content, but particularly clay mineralogy and chemical composition in determining how effective clay is at stabilizing SOC (Torn et al. 1997, Rasmussen et al. 2018). For example, surface area of clay-sized particles (1:1 vs. 2:1 clays vs. metal (hydr)oxides) helps control the reactivity of clay with organic matter (OM) (Kaiser and Guggenberger 2003, Wiesmeier et al. 2019).

Among measures of soil mineralogy, concentrations of different phases of iron (Fe) and aluminum (Al), especially oxides and (oxy)hydroxides, consistently show a positive relationship with SOM content (Torn et al. 1997, Kaiser and Guggenberger 2000, Schneider et al. 2010, Mikutta and Kaiser 2011, Beare et al. 2014, Heckman et al. 2018). Metal oxides are reactive and contribute greatly to the surface area of soils, allowing for sorption of OM. Thus, iron and aluminum may be some of the most important determinants of SOM accumulation and persistence, especially in certain soils (Bruun et al. 2010, Wiesmeier et al. 2019). The inclusion of iron and aluminum fractions has been shown to improve predictions of local to global scale SOC stocks (Bruun et al. 2010, Beare et al. 2014, Rasmussen et al. 2018). Extraction of soils

using sodium pyrophosphate specifically targets iron and aluminum associated with OM in organo-metal complexes (Loveland and Digby 1984, Coward et al. 2017). These extractions can be combined with radiocarbon measurements of transit time and system age of SOM to further inform our understanding of important mechanisms of SOM stabilization in soils.

This research aims to better understand SOC dynamics across a range of tropical soils for which texture alone was not a strong predictor of soil C and parent material appeared to be more important in explaining patterns of soil C storage (Vaughan et al. 2019). I used soil samples collected by the Natural Resource Conservation Service (NRCS) as part of the Rapid Carbon Assessment (RaCA) in Puerto Rico and the US Virgin Islands (Vaughan et al. 2019). These samples include seven soil orders, as well as a diversity of parent materials and environmental conditions. We combine SOM fractionation, radiocarbon measurements, and iron and aluminum extractions to ask the following questions:

1. How do SOC fractions vary across land covers and soil orders?
2. How do SOC cycling rates vary across land covers and soil orders?
3. How do sodium pyrophosphate-extractable iron and aluminum fractions correlate with SOC stocks and cycling rates across a wide range of soils?

We hypothesized that there would be difference in SOC fraction proportions and C contents across difference soil orders and land covers. Specifically, we predicted that croplands would have less contribution from the free and occluded light fraction than forests and pastures. We hypothesized that SOC cycling would be slower in forests and in soil orders with higher activity

clays, such as Vertisols. Finally, we hypothesized that iron and aluminum concentrations would be positively related to soil C content, as well as associated with slower soil C cycling rates.

Methods

Sample Selection

Soil samples were collected from the islands of Puerto Rico and the US Virgin Islands in collaboration with the USDA NRCS following the protocols of the Rapid Carbon Assessment (RaCA) (Soil Survey Staff and Locke 2016). Sampling sites were selected to be representative of the diversity of soils across the islands under five main land covers: forest, pasture, cropland, wetland, and rangeland. Seven soil orders are represented in the dataset (Oxisol, Ultisol, Mollisol, Entisol, Inceptisol, Vertisol, and Histosol). For each soil order and land use combination, a number of regionally important soil series were selected proportionate to the geographic extent of that soil order and land use. Sampling sites within each soil series were chosen randomly from a subset of accessible locations for a total of 30 sites (Fig. 1). Soils were sampled by horizon down to 1 m from five pits at each site.

A subsample of 11 sites representative of the diversity of soil orders and land covers was selected for soil organic matter fractionation, radiocarbon (^{14}C) analysis, and iron and aluminum extraction (Table 1). We include forest, pasture, and crop sites from Entisols, Mollisols, Oxisols, Vertisols, and Ultisols. For each site, one or two pits were selected for OM fractionation using the 0-5 cm sample (hereafter the A horizon) and the uppermost B horizon sample. Values

reported for all measurements are the mean values for all analytical and pit replicates within a site along with one standard error (SE).

Site mean annual precipitation (MAP) and temperature data were extracted from the dataset in Daly et al. (2003) for each site across the island of Puerto Rico. Both average minimum January temperature and average maximum July temperature were used in analyses instead of mean annual temperature because they were available at a finer spatial scale (15″ or approximately 450m grid size). Climate data for the US Virgin Islands came from the nearest available weather station (US National Oceanic and Atmospheric Administration).

SOM Fractionation

Soil organic matter was separated into three pools following the density fractionation procedure described by Swanston et al. (2005). We used sodium polytungstate (NaPT) with a density of 1.65 g mL^{-1} after determining that this density accurately separated particulate organic matter (POM) and mineral-associated organic matter (MAOM) across the range of soils used in this study.

Specifically, 20 g of air-dried soil was gently mixed with 75 mL NaPT and centrifuged to float the free light fraction (fLF) representing free POM. The fLF was removed and the remaining soil was mixed using a Polymix blender and sonicated using a Branson Sonifier with an energy of 200 J mL^{-1} to break apart aggregates. The samples were centrifuged and the light fraction was floated and removed, representing the occluded light fraction (oLF), or POM contained inside

aggregates. The remaining OM in the soil pellet is considered the heavy fraction (HF) and represents MAOM. All fractions were rinsed at least 5 times with Academic deionized water on 0.8 µm filters to remove residual NaPT. The oLF and fLF were oven-dried at 60 °C and the HF was oven-dried at 105 °C. All fractions were weighed and then ground using a SpexMill 8000D.

C and N for each fraction were measured on a Flash 2000 elemental analyzer (Thermo Fisher Scientific, Cambridge, UK). Samples were run in duplicate with a replicate error of < 10% using aspartic acid as a standard, and both aspartic acid and soil reference material as check standards. We report soil fraction data in two ways. First, we calculated the content of C and N in each fraction per gram of soil recovered in each fraction (mg C g bulk soil^{-1} or mg N g bulk soil^{-1}). We also report the proportion of recovered C and N in each fraction (the three fractions together add to 1.0). We refer to these as C content per fraction, and fraction proportion respectively.

^{14}C Analyses and modeling

Natural abundance ^{14}C was measured on one heavy fraction sample for the A and B horizon for six sites (12 total samples), and on nine total oLF samples. A subsample of each fraction was graphitized at the Houghton Carbon, Water, and Soils Lab (USDA-FS Northern Research Station). Radiocarbon measurements were conducted at the Keck Carbon Cycle AMS Facility at the University of California-Irvine. We report radiocarbon values as $\Delta\ ^{14}C$ (‰):

$$\Delta\ ^{14}C = (A_{SN}/A_{ABS} - 1) \times 1000$$

where A_{SN} is the activity of 14C in the sample normalized for isotopic fractionation and decay-corrected to 1950 and A_{ABS} is the absolute international standard activity of oxalic acid (Stuiver and Polach 1977). The ASN values were normalized for isotopic fractionation using measured δ13C values.

We modeled C mean transit times (MTT) for each fraction using a time-dependent, steady-state model that assumes annual atmospheric inputs to a single homogenous pool within each fraction (Trumbore et al. 1995, Torn et al. 2002, Sollins et al. 2006, Khomo et al. 2017). Under these assumptions, MTT is equivalent to mean residence time, mean system age and mean turnover time, but we use mean transit time to avoid confusion (Sierra et al. 2017). For atmospheric ^{14}C inputs, we used the ^{14}C radiocarbon data for zone 2, provided by Hua et al. (2013) through the year 2009, and then used forecasted $\Delta^{14}C$ values for 2009 to 2013 which have been found to closely match northern hemisphere values during that time period (Sierra 2018). Because we did not have archived samples to constrain our models, most of our oLF samples and a few of our HF samples had two possible solutions, one representing the increasing limb of the bomb carbon curve, and one representing the decreasing limb (Marín-Spiotta et al. 2008). For the heavy fraction, we felt comfortable discarding the shorter MTT for most samples, based on estimated system inputs and the fact that it is unlikely that mineral-associated OM would have average MTTs less than 20 years, even in rapidly cycling tropical systems (Trumbore 1993, Trumbore et al. 1995, Torn et al. 1997). For the oLF, we report both potential solutions as a "faster" MTT and a "slower" MTT as both solutions were reasonable, and we lacked a way to better constrain the models.

Iron and aluminum extractions

Iron and aluminum were extracted from a subsample of 20 heavy fractions from 10 sites using sodium pyrophosphate ($Na_4P_2O_7$). Sodium pyrophosphate is thought to primarily target iron and aluminum associated with SOM in organo-metal complexes (Loveland and Digby 1984, Coward et al. 2017, Heckman et al. 2018). Specifically, we added 32 ml of 0.1M sodium pyrophosphate with pH of 10 to 0.5 g of air-dried heavy fraction soil. Samples were shaken for 16 hours. After shaking, samples were centrifuged at 18000 RPM for 20 minutes. The supernatant was poured into a syringe and filtered through 0.2 µm Whatman GD/X Sterile filters. The filtered solution was refrigerated at 4 ˚C until analysis. Just prior to analysis, samples were diluted 1:10 in Academic deionized water to minimize the matrix effect from high concentrations of sodium in the extractant. All samples were run in duplicate.

Iron and aluminum concentrations of the extractions were measured using Inductively Coupled Plasma-Optical Emission Spectroscopy (ICP-OES) in the University of Wisconsin-Madison Water Sciences Laboratory. Standard curves and check standards for iron and aluminum were prepared in a matrix of 1:10 diluted sodium pyrophosphate to account for a matrix effect from the sodium. Iron concentrations were measured at wavelengths of 238.204 nm and 239.562 nm and aluminum concentrations were measured at wavelengths of 308.215 nm and 396.215 nm. The concentrations from each wavelength were averaged, and then this aqueous concentration was used to calculate Fe and Al concentrations per gram of dried soil. Values were averaged for the two analytical replicates.

Statistical analyses

All statistical analyses were conducted using *R* version 3.6.2 (R Core Team 2019). Assumptions of homogeneity of variance and normality of residuals were checked visually using plots for each model, and variables were transformed as needed. Soil pH was the only variable that needed to be log-transformed. Because many analyses were conducted on samples from A and B horizons within the same pit, independence could not always be assumed. We addressed this in two ways. For testing the significance of categorical variables (e.g., land cover or soil order) we treated analyses as split-plot designs, with horizon nested within sites. For continuous variables, we conducted linear regressions using the full set of samples and then independently by horizon for a more conservative approach. We report both analyses.

Results

Organic matter fractions

For all sites and horizons, the majority of C (72 – 97 %) and N (83 – 99 %) was found in the heavy fraction (HF) (Fig. 2). Between 1 – 8 % of C and 0.2 – 4 % of N was found in the free light fraction (fLF), and between 1 – 23% of C and 0.2 – 14 % of N was found in the occluded light fraction (oLF). The proportion and concentration of C and N for all three fractions differed by soil horizon. There was a greater proportion of C and N in the HF and lower proportion of C and N in oLF and fLF in the B horizons than the A horizons (Fig. 2; Fig. 3). There were also

smaller concentrations of total recovered C and N and amounts of C and N in each fraction in the B horizon (Fig. 2; Fig. 3).

Land cover had no effect on the proportion or concentration of C found in any fraction, although the amount of total C recovered was greatest in forest soils (Fig 2). There were marginally significant interactions between soil order and horizon for the proportion contributed by both the HF ($p = 0.06$) and oLF ($p = 0.08$) (Fig. 2). For both fractions, there were marginally significant differences in the A horizon samples, and no differences by soil order for the B horizons. These differences were primarily driven by Mollisols, which had lower proportions of HF C and relatively more oLF C. Trends were similar for N, with no effect on fraction proportion by land cover, and with a lower proportion of N in the HF and oLF (Fig. 3).

^{14}C and mean transit time

Our samples exhibited substantial variability in $\Delta^{14}C$ values across sites. Within the HF, samples ranged from being quite depleted in $\Delta^{14}C$ (-89.12 ‰), indicating little incorporation of recent bomb C, to being enriched in $\Delta^{14}C$ (98.73 ‰), indicating substantial incorporation of modern bomb C. In all sites, HF $\Delta^{14}C$ decreased with soil depth (Fig. 4). Modeled mean transit times of HF samples ranged from 62 years to 499 years for the A horizon samples, and from 151 to 866 years for the B horizon samples (Fig. 4). The slowest transit times were associated with an Ultisol cropland, and the fastest transit times were associated with a Mollisol forest site.

There was less variability in oLF $\Delta^{14}C$ values, and all samples were enriched in ^{14}C, with a range from 27.5 ‰ to 102 ‰. Modeled mean transit times ranged from 6 to 22 years for the "fast" mean transit time, and from 55 to 187 years for the "slow" mean transit time. There was no difference in $\Delta^{14}C$ values or mean transit times between oLF samples in the A and B horizons.

Iron and aluminum extractions

Across all soil types, sodium pyrophosphate extracted greater amounts of Fe than Al ($p = 0.007$) and there was no difference in extractable Fe or Al by horizon (Fig. 5). A horizon samples contained 3.15 (± 0.55) mg Fe per gram of soil and B horizon samples contained 1.91 (± 0.53) mg Fe per gram of soil. A horizon samples contained 1.25 (± 0.19) mg Al per gram soil, and B horizon samples contained 1.04 (± 0.18) mg Al per gram soil. The greatest concentrations of extractable Fe and Al were found in two Ultisol samples, followed by an Oxisol site and then an Inceptisol site. The lowest concentrations of both Fe and Al were from Vertisol and Mollisol sites. There was a strong positive correlation between the amount of Fe extracted and the amount of Al extracted from all samples ($p < 0.0001$, $R^2 = 0.74$; Fig. 6).

There were positive relationships between extractable Fe concentrations and percent HF carbon for all samples ($p = 0.004$, $R^2 = 0.44$; Fig. 8), within just A horizon samples ($p = 0.02$, $R^2 = 0.42$) and within just B horizon samples ($p = 0.002$, $R^2 = 0.64$). There were also positive correlations between horizon bulk soil percent C and Fe concentrations ($p = 0.01$, $R^2 = 0.25$) and Al concentrations ($p = 0.04$, $R^2 = 0.18$) (Fig. 9). The amount of variability explained for bulk soil C

was lower than for just HF C values. Horizon C densities (g C cm^{-3}) were positively correlated with Fe concentrations only in the B horizon samples ($p = .024$, $R^2 = 0.41$).

There was a positive correlation between Fe concentrations and modeled HF MTTs for all samples ($p = 0.04$, $R^2 = 0.30$; Fig. 7). When separated by horizon, there was only a significant relationship between Fe concentrations and MTT for the B horizon ($p = 0.03$). There was a marginally significant relationship between Al concentrations and MTT for all samples ($p = 0.06$, $R^2 = 0.27$; Fig. 7), and for just the B horizon samples ($p = 0.08$). There were no significant relationships between $\Delta^{14}C$ values and either Fe or Al concentrations.

The amount of extractable Fe and Al was negatively correlated with horizon pH ($p < 0.0001$ for both Fe and Al; Fig. 10). There was a positive relationship between A horizon Fe and Al concentrations and mean annual precipitation (MAP) ($p = 0.04$ and $p = 0.02$ respectively). There was no relationship between soil Fe and Al concentrations and mean annual maximum temperature. Fe and Al concentrations in the A horizon decreased with increasing mean annual minimum temperature ($p = 0.02$ for both Al and Fe; Fig. 10).

Discussion

Density fractions differed by horizon and soil order, but not by land cover

The amount and proportion of C isolated in density fractions across a diversity of soil environments in Puerto Rico and the US Virgin Islands was unaffected by land cover, with no

differences among forests, pastures or croplands. These results contrast with an earlier study on Puerto Rican Oxisols that reported depletions of fLF in active pastures relative to reference forests and replenishment during early secondary forest succession (Marín-Spiotta et al. 2009). Other studies in temperate soils have reported land use effects on the distribution of C among density fractions (Mueller and Koegel-Knabner 2009) although one large scale study from Australia found that soil C fractions were more sensitive to soil and environmental condition than to land use (Rabbi et al. 2014). The lack of an observed effect of land use in our study may be due to variability in soil properties given the diversity of soil orders. Soil properties such as soil texture, clay mineralogy, and pH can influence OM fraction distribution through effects on aggregation and mineral-associations (Six et al. 2004).

There was some evidence of differing fraction proportions by soil order, primarily in the A horizon samples. In particular, Mollisols contained relatively more oLF C than the other soil orders. This can perhaps be attributed to the greater bulk soil OC contents in mollic epipedons, as well as the presence of exchangeable calcium in these limestone-derived soils, both of which can promote aggregate formation (Six et al. 2004, Rowley et al. 2018). The one Vertisol site we looked at also had a relatively higher proportion of C and N in the oLF, which is somewhat surprising given the high reactivity of clay minerals in Vertisols, and expectation that a greater portion of C would be associated with the mineral fraction, as seen in one comparative study in Germany (Don et al. 2009). However, highly reactive clays can also promote aggregation so both mechanisms are likely important in Vertisols. There was variability in OM distribution within soil orders, which is unsurprising given the broad classification of soil orders, however, these

patterns suggest the importance of different soil forming factors in determining mechanisms of OM stabilization.

The amount and proportion of C in density fractions did differ by horizon, with greater values in the HF in B horizons, as expected by general observations of the increasing importance of mineral-organo associations with depth (Spielvogel et al. 2008, Rumpel and Kögel-Knabner 2011). The majority of C and N (> 70 % of C, > 80% N) in all soils was found in the mineral-associated HF, similar to findings from a variety of tropical soils (Marín-Spiotta et al. 2009, Hall et al. 2015).

Iron and aluminum concentrations correlated with more and older carbon

Concentrations of extractable OM-associated Fe and Al were positively correlated with soil organic C concentrations. Fe and Al oxides provide extensive and effective sorptive surfaces for SOM and dissolved organic carbon (DOC), and colloidal interactions between OM and pyrophosphate-extractable Fe and Al can provide a high degree of protection from microbial decomposition and SOM persistence in the soil (Torn et al. 1997, Kaiser and Guggenberger 2000, Mikutta and Kaiser 2011, Saidy et al. 2012, Riedel et al. 2013). Thus, high concentrations of iron and aluminum oxides and hydroxides can promote C accumulation in soils. This mechanism may be even more important in highly weathered soils composed predominantly of 1:1 clays, as the dominant clay matrix provides relatively less sorptive surface area (Bruun et al. 2010, Saidy et al. 2013, Khomo et al. 2017). While we observed positive correlations across soil types in our dataset, the one Vertisol site exhibited low concentrations of Fe and Al but relatively

high concentrations of C. Vertisols are dominated by 2:1 clays with high specific surface area, which provide sorptive surfaces for OM.

There was a stronger relationship between Fe and Al concentrations and HF C content than there was with bulk soil C content. This can probably be explained by the importance of organo-metal complexes in the dense fraction, which primarily isolates mineral-associated C, and the fact that metal oxides are less involved in OM stabilization of free or occluded POM, which constitute up to 30 % of bulk soil C in these soils. While a number of studies corroborate our finding of correlations between Fe and Al and bulk soil C (Kaiser and Guggenberger 2000, Hall and Silver 2015, Rasmussen et al. 2018), one other Puerto Rican study found poor correlations with bulk soil C content (Coward et al. 2017), although that study looked at just Oxisols and Inceptisols. We also observed a stronger relationship between bulk soil C and Fe and Al concentrations in B horizon samples compared to A horizon samples, which is likely due to the greater proportion of C recovered in the HF in B horizons.

In conjunction with greater C contents, ^{14}C data indicated decreased cycling rates of C in the mineral-associated fraction of SOM with increasing concentrations of Fe and Al. This corroborates other studies which have also found older and slower cycling C in sites with greater Fe and Al oxide concentrations (Torn et al. 1997, Masiello et al. 2004). One exception to this relationship was the one Vertisol site, which had the third longest mean transit time, but low concentrations of Fe and Al. There was a stronger relationship between HF mean transit time and Fe and Al concentrations in the B horizon than in the A horizon. This can't be explained by the proportion of C in the HF, or by overall concentrations of Fe and Al, as we did not observe

significant differences by horizon. Instead, this may be due to more dynamic C cycling in A horizon soils driven primarily by difference in litter and root inputs, as well as variations in soil moisture and DOC production.

^{14}C and C cycling rates differed greatly across the sites

The MTT of HF samples varied substantially for the samples in this study, from 62 years to 866 years. There were consistent trends with depth, as $\Delta^{14}C$ values decreased with depth in all sites, following well-established ^{14}C depth patterns (Mathieu et al. 2015). Interestingly, the longest MTTs were from highly weathered, warm, and wet Ultisols, contrary to predictions based solely on climate and the presence of mostly 1:1 clays (Mathieu et al. 2015). This further suggests the importance of stabilization of OM by Fe and Al. The range of HF MTTs reported here fall within estimates from other studies, from the shorter end (Marín-Spiotta et al. 2008) to the longer end (Trumbore et al. 1995).

The problems associated with assigning one specific MTT solution for the oLF fractions speak to the importance of archived soil samples that can be used to better constrain ^{14}C models (e.g., Chapter 1). MTTs of decadal versus centennial timescales lead to very different interpretations of soil C dynamics. As C in aggregates is thought to be particularly susceptible to human land change (Six et al. 2000, Six and Paustian 2014), a better understanding of dynamics in this fraction is useful to assess changes and recovery of soil C following land conversion. This approach also assumes one homogenous C pool within each fraction, despite increasing understanding that even fractions defined by density separation contain heterogenous mixtures of

C ages (Trumbore et al. 1995, Torn et al. 1997, Sierra et al. 2012, Schrumpf and Kaiser 2015, Hall and Silver 2015). Although it is still useful to get average MTT values for a pool, not all C dynamics will be captured using this approach.

Iron and aluminum varied in relation to environmental and pedological conditions

Fe and Al concentrations were greatest in acidic soils and warmer and wetter sites, although only in the A horizon. Specifically, Fe and Al concentrations were greatest in Ultisols, Oxisols, and one Inceptisol site. Fe and Al oxides are products of weathering and stable in acidic soils. Given the strong relationship between these climate variables and soil weathering, and in turn soil pH, it is unsurprising that these environmental variables correlated with Fe and Al.

The amounts of Fe and Al extracted from our soils were in the range, although lower than those reported by another study from Puerto Rico. Coward et al. (2017) working on Oxisols and Inceptisols reported a mean pyrophosphate extractable Fe value of 5.0 mg Fe g^{-1} soil, slightly higher than ours. Of the various extractants used in that study, sodium pyrophosphate was the only one to extract similar amounts of Fe between Oxisols and Inceptisols, consistent with our findings of similar Fe concentrations in Inceptisols, Oxisols, and Ultisols. In that same study, sodium pyrophosphate extracted a small proportion of total Fe from soils, but a significant proportion of dissolved organic carbon (DOC), suggesting the importance of this Fe fraction for understanding soil C dynamics.

Most major biogeochemical soil C models (e.g., CENTURY and RothC) include information on soil texture, climate and land management, but are lacking specific mineralogical detail (Parton et al. 1988, Coleman and Jenkinson 1996, Schmidt et al. 2011). Recent research has shown that including measures of soil mineralogy, and in particular iron and aluminum concentrations can improve estimates and predictions of soil C dynamics (Torn et al. 1997, Garrido and Matus 2012, Mathieu et al. 2015, Rasmussen et al. 2018). Previous work using this dataset found that traditional predictors of SOC did not accurately model SOC stocks (Vaughan et al. 2019). Mean annual temperature, precipitation, and percent clay were not significant predictors of SOC stocks. Percent silt + clay, pH, and land cover were correlated with SOC stocks, but total predictive power was low. The reasonably strong correlations we found between Fe and Al and soil C content and cycling rates lend support to the inclusion of these measures in efforts to predict SOC stocks, and explain more variability than any single factor used previously (Vaughan et al. 2019).

Conclusion

Our study of C dynamics within different density fractions shows substantial variation in C cycling rates, soil mineralogy, and C pool distribution between tropical soils formed on different parent materials and under different environmental conditions. Specifically, these processes differed more by soil order than by forest, pasture or cropland cover types. Concentrations of Fe and Al in soils were positively correlated to soil C content, especially in the mineral-associated pools and in B horizon samples. Heavy fraction mean transit times increased with Fe and Al concentrations, suggesting OM stabilization due to organo-metal associations. This study

highlights the importance of studying these and other soil properties to improve our ability to predict C stocks in addition to more commonly studied properties like clay and climate which may not be adequate across a diversity of soils (Vaughan et al. 2019). This work also addresses the importance of studying diverse soils of the tropics. Studies of tropical soil C are known to be geographically biased, which may hinder our interpretation of the effects of land change on soil C dynamics (Powers et al. 2011). We contribute data on relationships between soil C cycling rates, mineralogy, and OM fraction distribution from soil types and environmental conditions that are under-studied globally to improve predictions of soil C stocks and dynamics.

Table 1. Site and soil information for samples used in this study.

Land Cover	Soil Series	Soil Order	Soil Subgroup	Parent Material	Lat.	Long.	MAP (mm)	Mean Min. Temp. (C)	SOC Stock (Mg ha^{-1})	A horizon fine silt + clay (%)	A horizon pH
Forest	Pandura	Inceptisol	Dystric Eutrudepts	plutonic rocks	18.12	-65.95	2385	18.7	124	36	4.77
	Fredricksdal	Mollisol	Lithic Haplustolls	igneous bedrock	18.36	-65.01	999	24.2	150	74	6.75
	Los Guineos	Oxisol	Humic Hapludox	sandstone	18.12	-66.08	2042	17.0	181	74	4.70
	Humatas	Ultisol	Typic Haplohumults	basic igneous	18.23	-67.05	2163	17.9	172	76	5.30
Pasture	Coloso	Inceptisol	Vertic Dystrudepts	alluvial sediments	18.27	-66.03	1597	18.8	145	81	5.07
	Descalabrado	Mollisol	Typic Haplustolls	mixed basic volcanic rock	18.01	-66.24	1046	20.8	94	75	6.93
	Coto	Oxisol	Typic Eutrustox	limestone	18.47	-67.12	1418	20.9	203	67	5.23
Crop	Talante	Entisol	Aeric Fluvaquents	floodplain, granitic regolith	18.07	-65.88	2025	21.4	64	37	4.71
	Caguabo	Inceptisol	Typic Eutrudepts	basalt	18.25	-66.90	1888	18.4	61	58	7.04
	Espinosa	Ultisol	Typic Kandiudults	mixed origin	18.41	-66.36	1703	20.3	211	89	4.96
	Fraternidad	Vertisol	Typic Haplusterts	volcanic rock and limestone	18.03	-66.52	924	21.0	139	70	7.70

Table 2. SOM density fraction C, N, Fe, Al, and ^{14}C data.

Series	Soil Order	Land Cover	Horizon	Bulk Soil C %	Bulk Soil N %	Fraction	Fraction % C	Fraction % N	C:N	Fraction C concentration (mg C g bulk soil^{-1})	Proportion of C	Al (mg g soil^{-1})	Fe (mg g soil^{-1})	$\Delta^{14}C$ (‰)
Espinosa	Ultisol	Crop	A	3.76	0.31	fLF	28.49	1.04	27.84	1.99	0.06			
						oLF	40.95	2.12	19.35	2.62	0.07			34.1
						HF	3.10	0.27	11.40	30.55	0.87	1.95	3.44	-35.01
			B	2.41	0.22	fLF	29.94	0.85	35.14	1.15	0.05			
						oLF	43.51	1.66	26.63	1.73	0.07			27.48
						HF	2.09	0.21	10.12	20.78	0.88	2.16	5.46	-89.12
Fraternidad	Vertisol	Crop	A	2.55	0.26	fLF	27.63	1.43	19.31	1.31	0.06			
						oLF	32.73	2.12	15.47	5.01	0.22			33.86
						HF	1.29	0.16	7.99	12.64	0.72	0.18	0.05	19.11
			B	1.48	0.16	fLF	43.37	0.95	45.66	0.52	0.04			
						oLF	36.33	1.62	22.46	3.17	0.23			
						HF	1.00	0.14	7.15	9.89	0.73	0.29	0.15	-56.01
Fredricksdal	Mollisol	Forest	A	4.70	0.47	fLF	28.01	1.43	19.76	1.80	0.05			
						oLF	32.00	1.71	19.02	6.72	0.17			102.19
						HF	2.95	0.35	8.49	28.71	0.78	0.32	0.57	98.73
			B	1.96	0.24	fLF	31.70	1.21	26.31	1.12	0.06			
						oLF	35.97	1.43	25.20	1.55	0.09			
						HF	1.50	0.21	7.05	14.87	0.85	0.41	0.35	-0.03
Los Guineos	Oxisol	Forest	A	6.62	0.61	fLF	31.98	1.45	22.45	4.26	0.08			
						oLF	42.91	1.67	26.74	6.33	0.11			
						HF	4.22	0.41	10.56	40.76	0.81	1.81	5.55	
			B	1.16	0.11	fLF	38.76	1.33	29.05	0.14	0.01			
						oLF	37.94	1.92	19.73	0.17	0.02			
						HF	0.99	0.10	10.37	9.92	0.97	0.91	0.42	

Humatas	Ultisol	Forest	A	5.53	0.50	fLF	26.36	1.25	21.17	1.61	0.04			
						oLF	32.84	1.50	22.28	2.82	0.07			85.38
						HF	3.40	0.30	11.36	33.51	0.88	1.87	3.55	91.85
			B	1.62	0.14	fLF	34.56	0.94	36.83	0.51	0.03			
						oLF	42.03	0.96	45.03	1.61	0.09			
						HF	1.21	0.12	9.89	12.00	0.88	1.69	1.24	-19.46
Coto	Oxisol	Pasture	A	3.47	0.38	fLF	23.07	1.13	20.46	1.52	0.05			
						oLF	28.89	1.83	16.11	1.43	0.05			38.81
						HF	2.57	0.27	9.44	25.36	0.90	0.64	1.59	25.41
			B	1.38	0.17	fLF	27.71	0.81	34.70	0.13	0.01			
						oLF	17.62	0.45	39.08	0.18	0.02			
						HF	1.14	0.16	7.27	11.39	0.97	0.65	1.61	-39.34
Caguabo	Inceptisol	Crop	A	2.07	0.22	fLF	32.37	1.57	20.70	0.91	0.06			
						oLF	33.67	1.99	16.95	1.45	0.09			
						HF	1.36	0.16	8.38	13.51	0.86			
			B	1.03	0.11	fLF	28.45	1.14	24.97	0.07	0.01			
						oLF	37.32	1.58	23.58	1.11	0.12			
						HF	0.79	0.10	8.19	7.85	0.87			
Pandura	Inceptisol	Forest	A	4.77	0.42	fLF	26.42	1.11	23.72	2.49	0.05			
						oLF	36.86	1.60	23.06	3.89	0.08			81.16
						HF	3.32	0.30	10.84	32.39	0.87	0.97	2.39	88.6
			B	2.41	0.23	fLF	29.08	1.12	26.00	0.52	0.04			
						oLF	40.99	1.27	32.23	0.55	0.04			
						HF	1.75	0.18	9.24	17.47	0.92	0.47	0.98	41.3
Descalabrado	Mollisol	Pasture	A	2.87	0.27	fLF	22.86	1.10	20.79	2.09	0.08			
						oLF	29.71	1.64	18.21	3.13	0.13			
						HF	2.04	0.22	9.41	20.03	0.79	0.57	0.55	
			B	1.30	0.12	fLF	23.22	0.94	24.77	0.33	0.03			
						oLF	30.27	1.11	27.18	0.52	0.04			

						HF	1.15	0.10	11.84	11.51	0.93	0.66	0.41
Talante	Entisol	Crop	A	0.90	0.08	fLF	21.93	1.11	19.77	0.48	0.06		
						oLF	41.72	2.42	17.45	0.50	0.06		
						HF	0.74	0.07	10.20	7.40	0.88	0.78	1.82
			B	0.90	0.09	fLF	20.74	0.98	21.21	0.31	0.04		
						oLF	37.99	1.78	21.49	0.32	0.04		
						HF	0.78	0.07	11.99	7.78	0.93	0.93	2.12
Coloso	Inceptisol	Pasture	A	2.64	0.25	fLF	25.88	1.07	24.30	1.12	0.05		
						oLF	37.29	2.30	16.24	1.54	0.07		
						HF	2.02	0.20	10.10	20.05	0.88	1.03	4.55
			B	1.92	0.19	fLF	27.24	1.01	27.09	0.31	0.02		
						oLF	40.19	1.86	21.60	0.99	0.06		
						HF	1.50	0.14	10.43	14.97	0.92	0.75	3.04

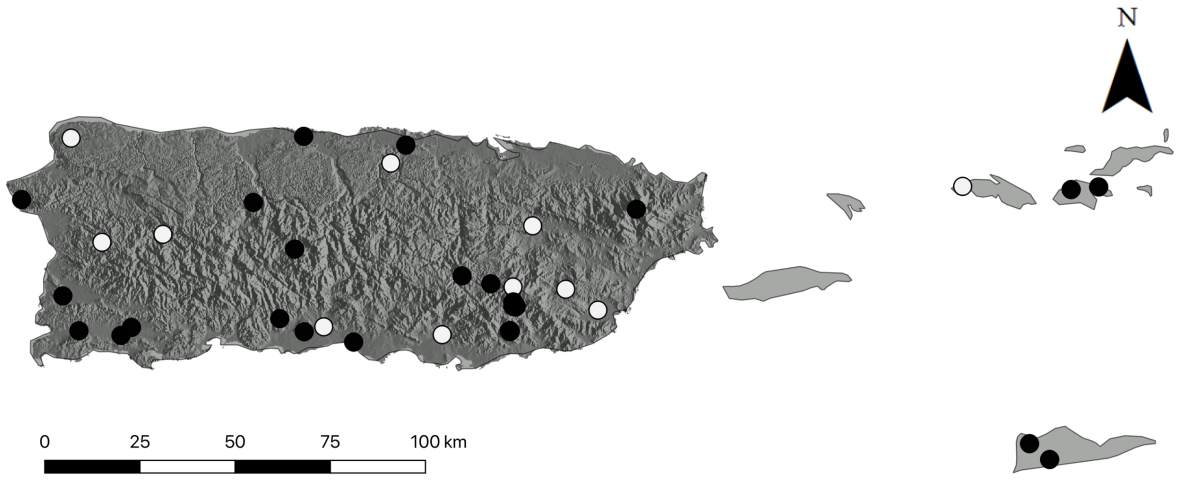

Figure 1. Location of all 30 study sites in Puerto Rico and the US Virgin Islands used in the broader RaCA dataset as reported in Vaughan (2019). Sites that were selected for density fractionation are indicated by white circles.

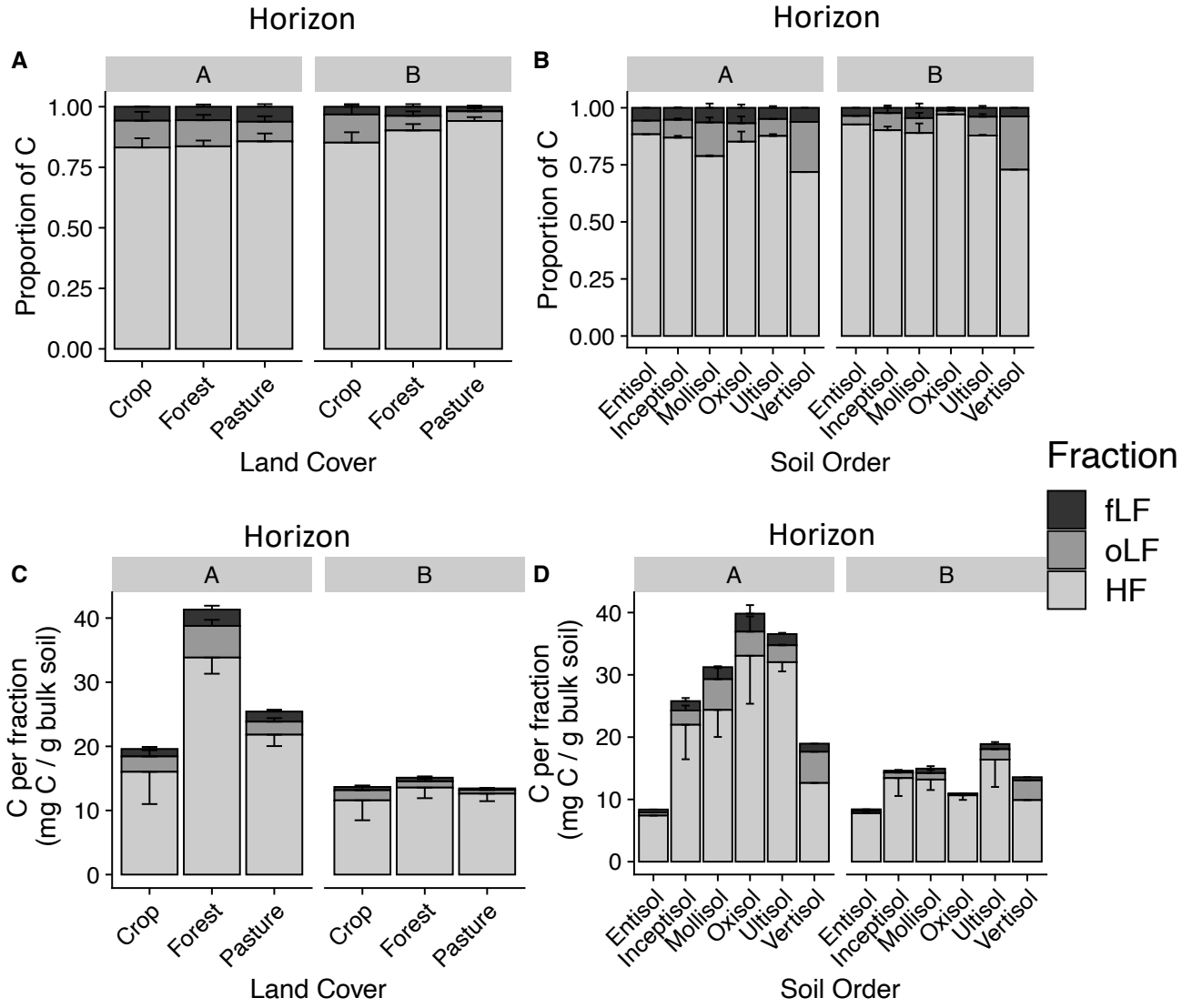

Figure 2. Density fractionation data by land cover (A, C) and soil order (B, D). C per fraction is defined as mg C g^{-1} bulk soil. Within each plot, data are shown for the A horizon and B horizon. Plots A and B show the fraction C as a proportion of all C recovered through density fractionation. Plots C and D show the C concentration in each fraction in relation to the bulk soil. For all plots, the black shaded bar is the free light fraction (fLF), the intermediate gray bar is the occluded light fraction (oLF), and the light gray bar is the heavy fraction (HF). Error bars represent one standard error (shown in one direction to avoid overlap). Soil orders without error bars only had one replicate.

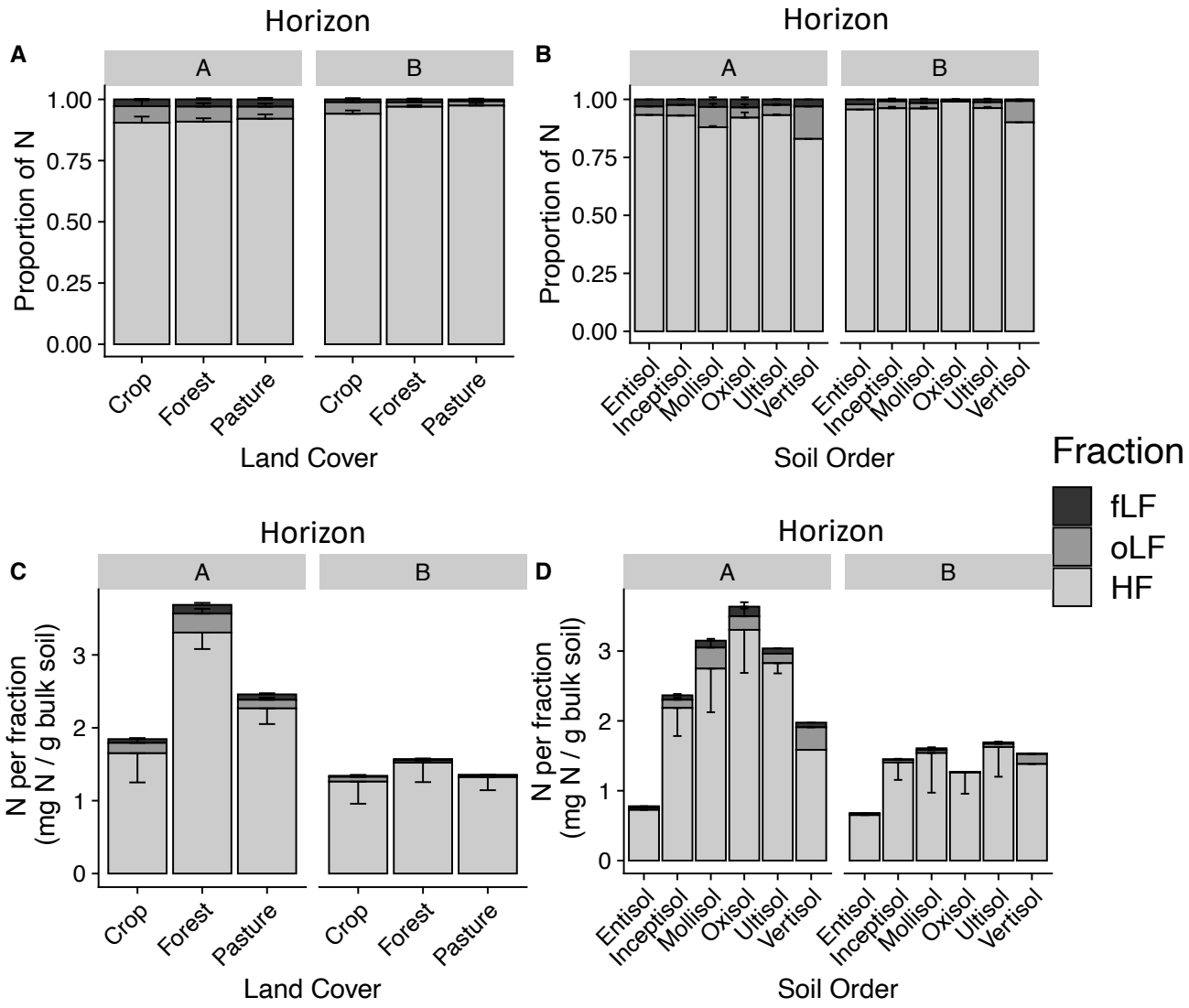

Figure 3. Density fractionation nitrogen (N) data by land cover (A, C) and soil order (B, D). N per fraction is defined as mg N g^{-1} bulk soil. Within each plot, data are shown for the A horizon and B horizon. Plots A and B show the fraction N as a proportion of all N recovered through density fractionation. Plots C and D show the N concentration in each fraction in relation to the bulk soil. For all plots, the black shaded bar is the free light fraction (fLF), the intermediate gray bar is the occluded light fraction (oLF), and the light gray bar is the heavy fraction (HF). Error bars represent one standard error. Soil orders without error bars only had one replicate.

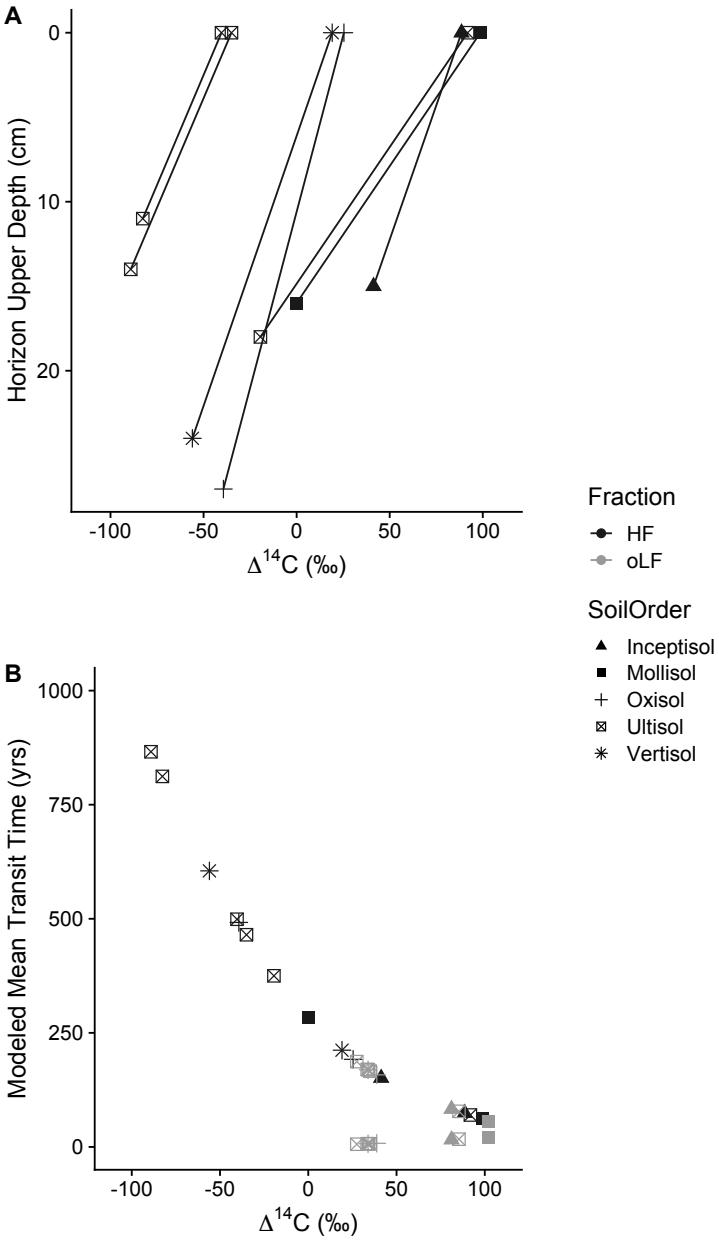

Figure 4. $\Delta^{14}C$ data across fractions and soil orders. Panel A shows HF $\Delta^{14}C$ values within a pit for the A and B horizons. Only one pit is represented per site, except for the Ultisol samples on the far left, which represent two separate pits from the same site. Panel B shows the modeled mean transit times for different samples. The curve going from the top left to the bottom right represents the 'slower' transit time for all HF and oLF samples, and the points below that represent the 'faster' transit time for oLF samples (see Methods for more detail).

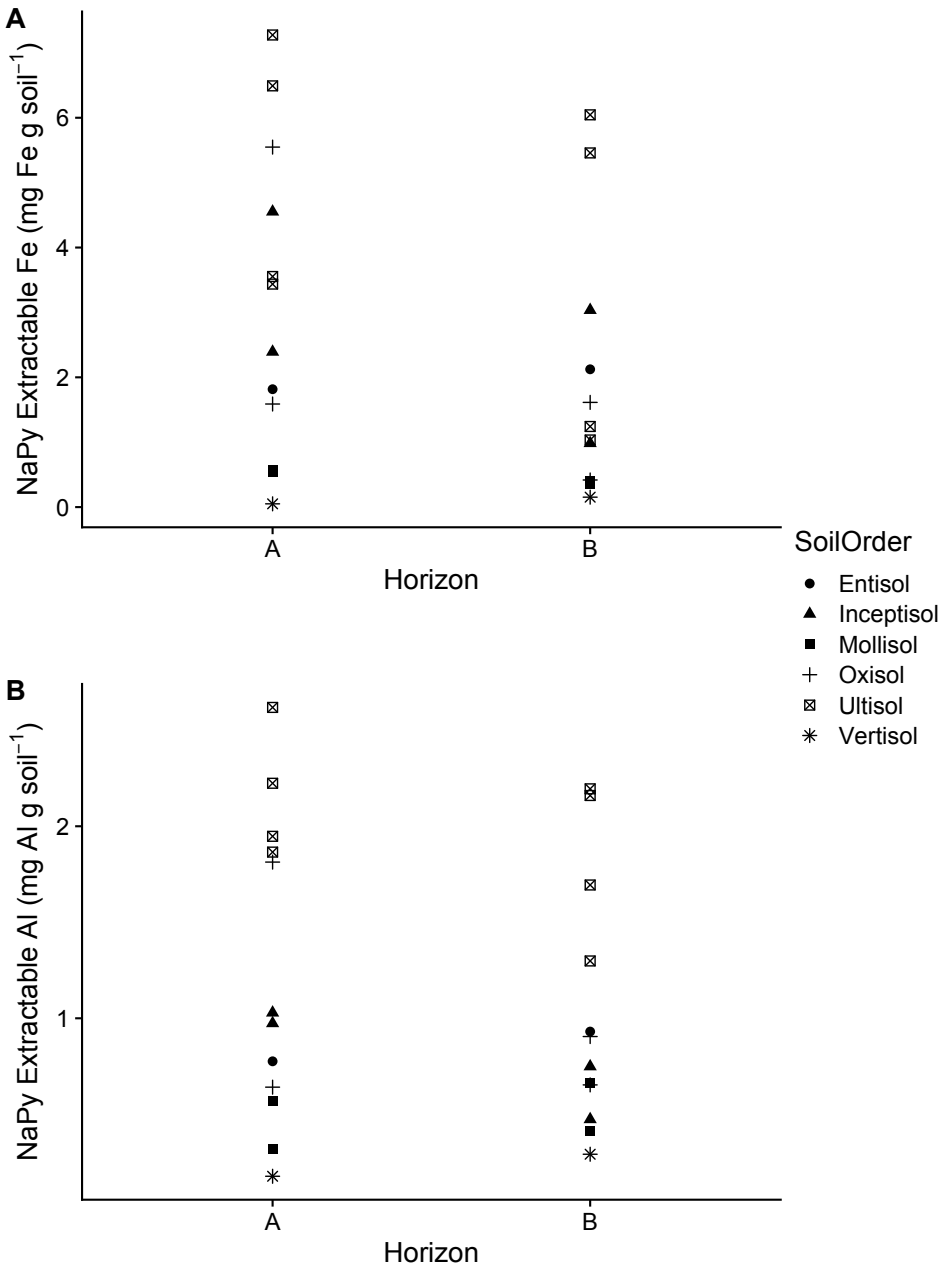

Figure 5. Sodium pyrophosphate extractable iron (Fe) and aluminum (Al) from A and B horizons across six soil orders. Note the different scale of the y-axes.

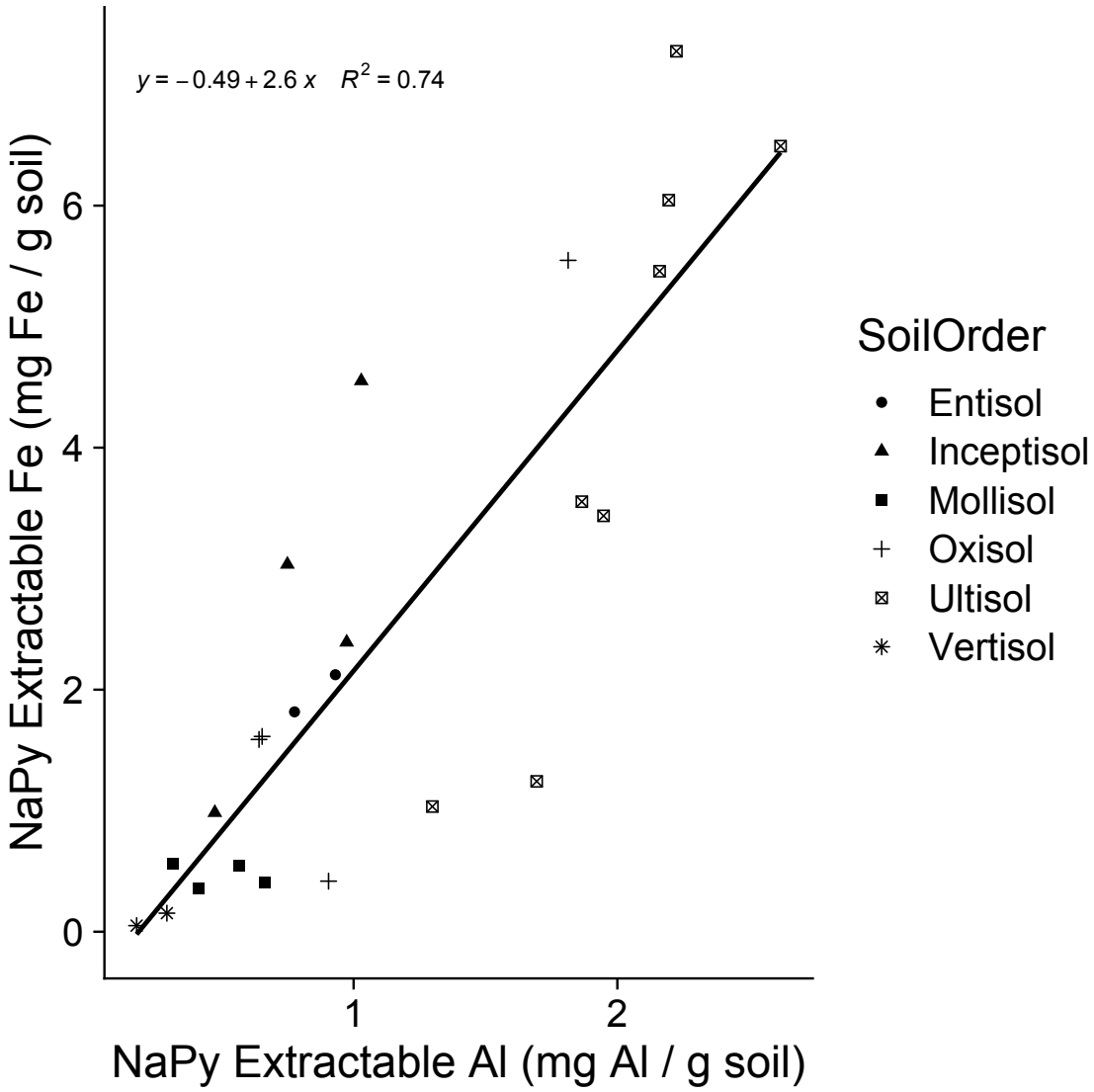

Figure 6. Extractable iron (Fe) in relation to extractable aluminum (Al).

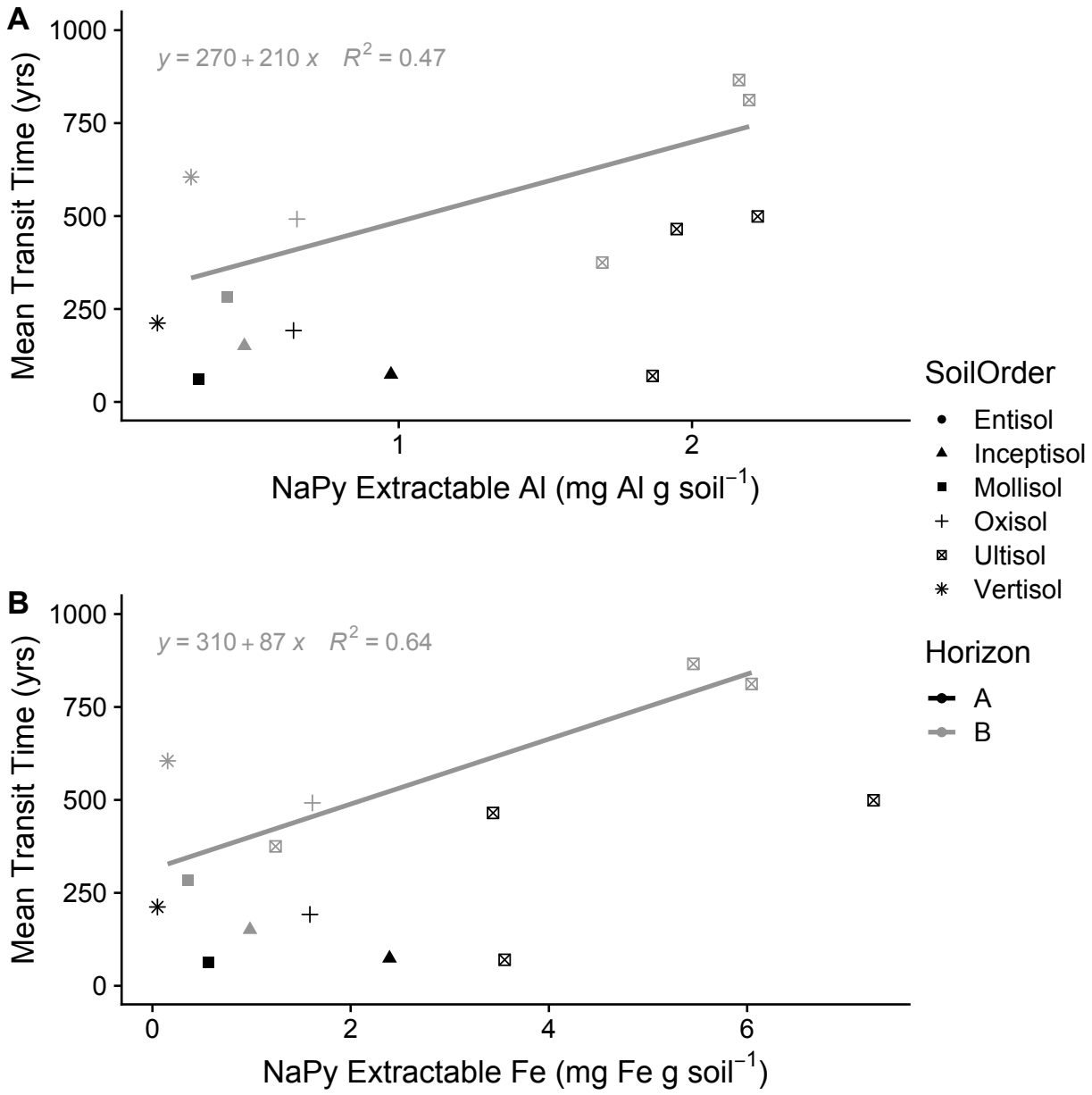

Figure 7. Relationships between sodium pyrophosphate extractable Al and Fe and modeled mean transit times (MTT). There was a significant relationship between Fe and MTT and a marginally significant relationship between Al and MTT for both horizons combined. The regression lines shown are just for the relationships in the B horizon, which were significant for Fe ($p = 0.03$), and marginally significant for Al ($p = 0.08$).

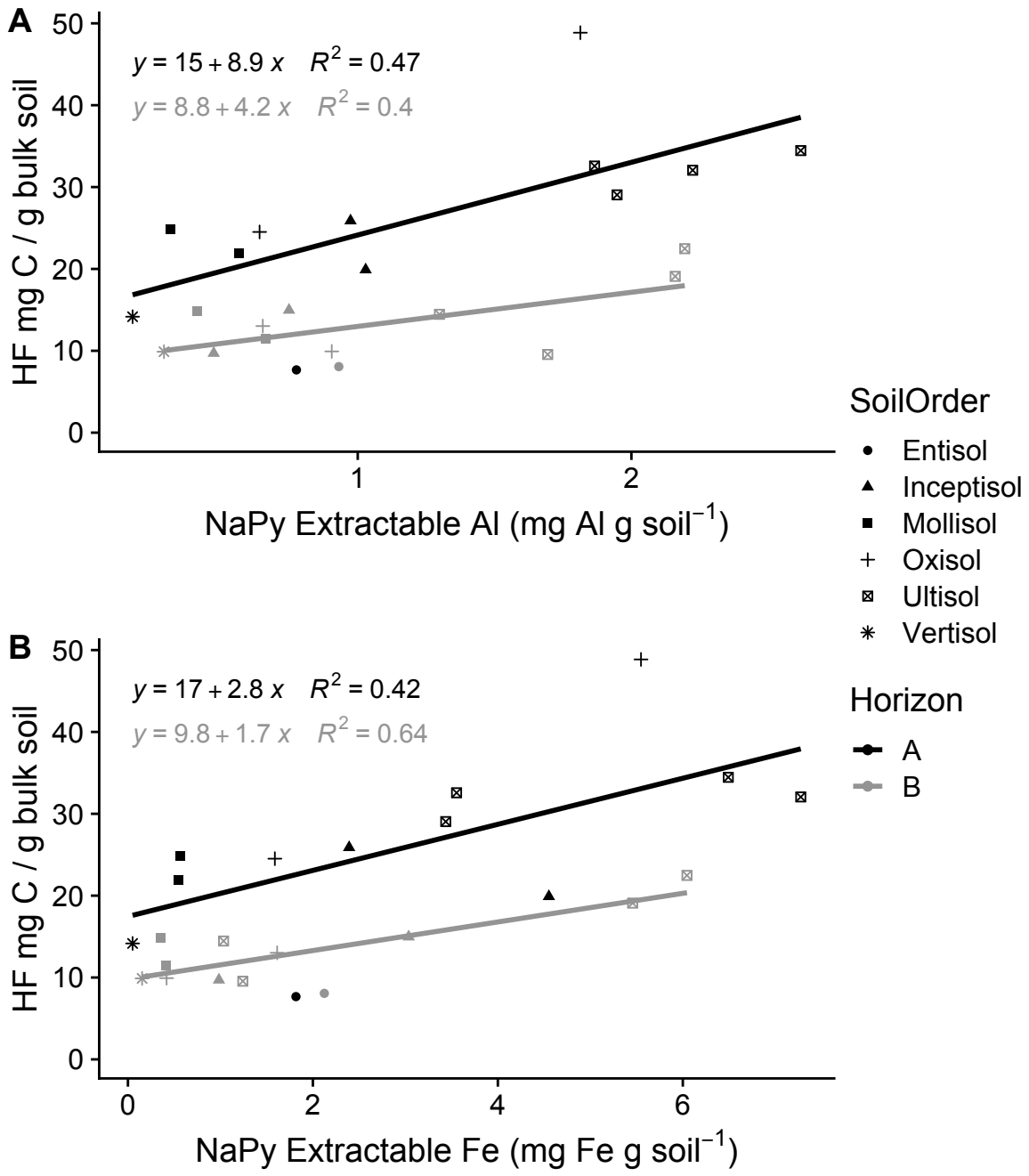

Figure 8. Heavy fraction (HF) carbon concentrations related to extractable Fe and Al. Relationships are significant within each horizon for both Fe and Al ($p < 0.05$). Note the difference in the x axis between plots. HF C concentration is defined as the amount of C recovered in the HF per gram of air-dried bulk soil.

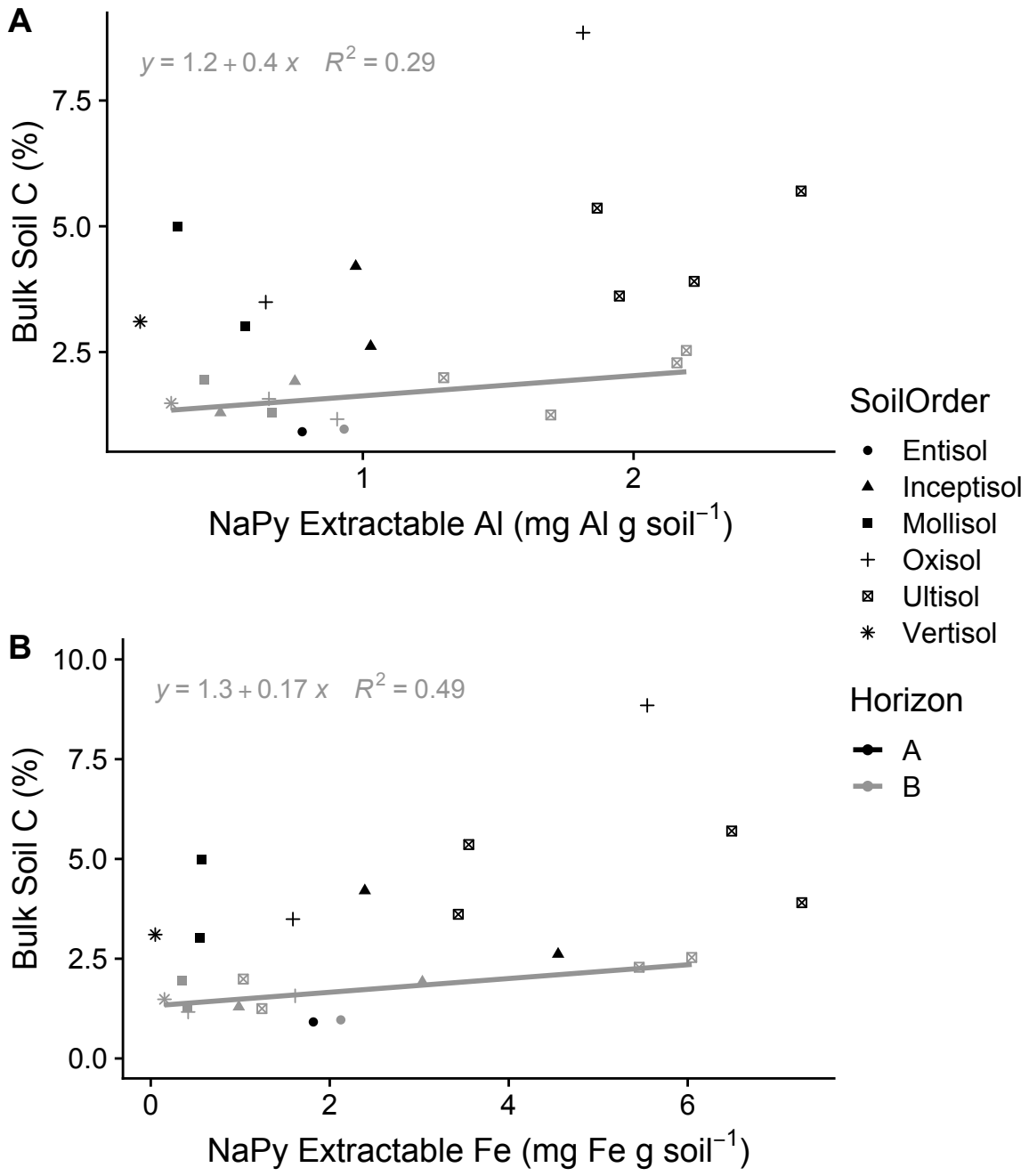

Figure 9. Relationship between horizon bulk soil C percent and extractable Al (A) and Fe (B) concentrations. Regression lines are shown just for the B horizons, where the relationship was marginally significant for Al ($p = 0.06$) and significant for Fe ($p = 0.02$).

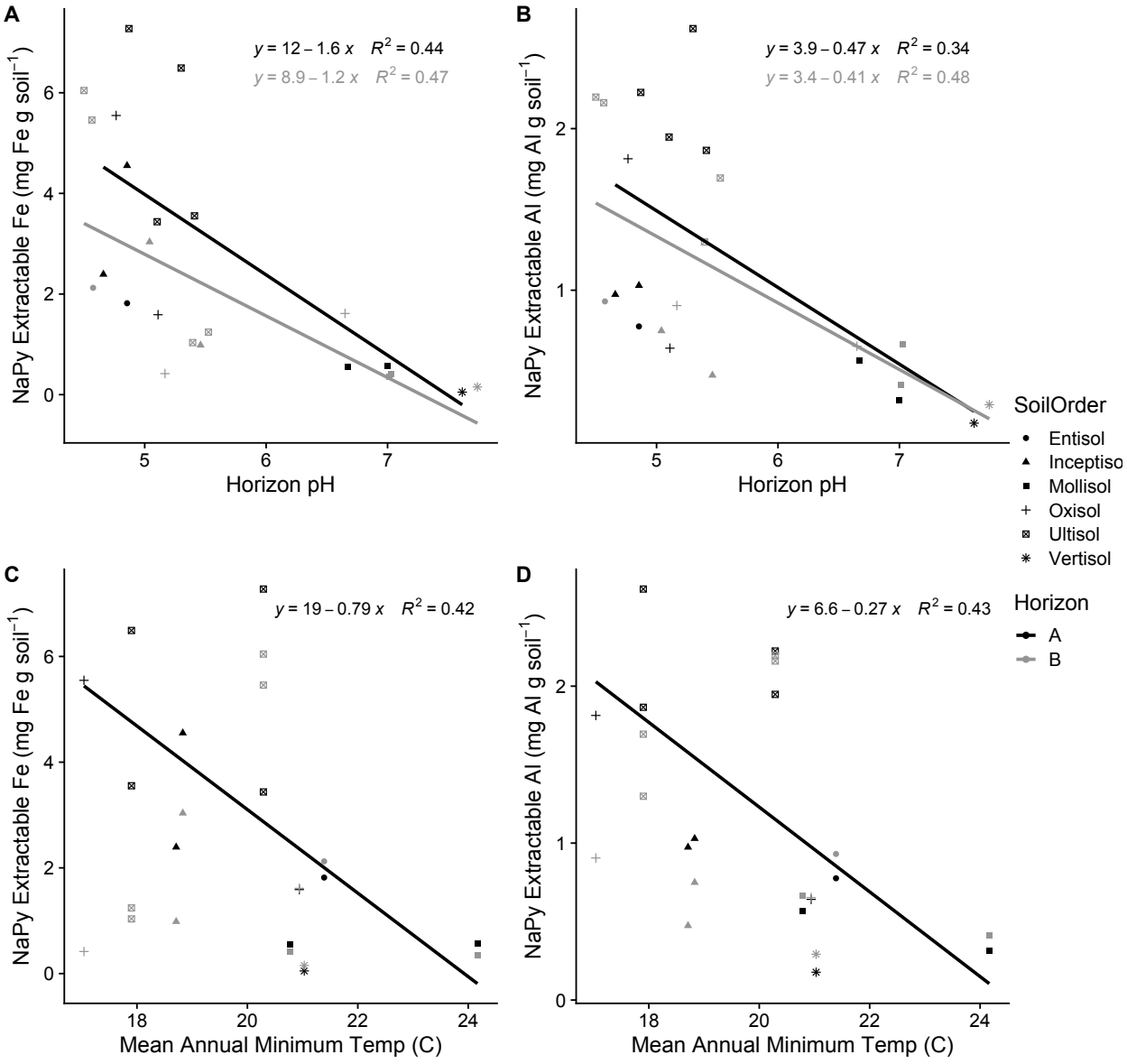

Figure 10. Relationships between environmental site variables and extractable Fe and Al concentrations. Regression lines are shown for horizons where the relationship was significant ($p < 0.05$)

Literature Cited

Beare, M. H., S. J. McNeill, D. Curtin, R. L. Parfitt, H. S. Jones, M. B. Dodd, and J. Sharp. 2014. Estimating the organic carbon stabilisation capacity and saturation deficit of soils: a New Zealand case study. Biogeochemistry 120:71–87.

Beinroth, F., M. Vázquez, V. Snyder, P. Reich, and L. Pérez Alegria. 1996. Factors controlling carbon sequestration in tropical soils: a case study of Puerto Rico. University of Puerto Rico-Mayagüez, USDA National Resources Conservation Service.

Bruun, T. B., B. Elberling, and B. T. Christensen. 2010. Lability of soil organic carbon in tropical soils with different clay minerals. Soil Biology and Biochemistry 42:888–895.

Coleman, K., and D. S. Jenkinson. 1996. RothC-26.3 - A Model for the turnover of carbon in soil. Pages 237–246 *in* D. S. Powlson, P. Smith, and J. U. Smith, editors. Evaluation of Soil Organic Matter Models. Springer Berlin Heidelberg, Berlin, Heidelberg.

Coward, E. K., A. T. Thompson, and A. F. Plante. 2017. Iron-mediated mineralogical control of organic matter accumulation in tropical soils. Geoderma 306:206–216.

Don, A., T. Scholten, and E.-D. Schulze. 2009. Conversion of cropland into grassland: Implications for soil organic-carbon stocks in two soils with different texture. Journal of Plant Nutrition and Soil Science 172:53–62.

Fisher, M., I. Rao, M. Ayarza, C. Lascano, J. Sanz, R. Thomas, and R. Vera. 1994. Carbon storage by introduced deep-rooted grasses in the South American savannas. Nature 371:236–238.

Garrido, E., and F. Matus. 2012. Are organo-mineral complexes and allophane content determinant factors for the carbon level in Chilean volcanic soils? CATENA 92:106–112.

Hall, S. J., G. McNicol, T. Natake, and W. L. Silver. 2015. Large fluxes and rapid turnover of mineral-associated carbon across topographic gradients in a humid tropical forest: insights from paired 14C analysis. Biogeosciences 12:2471–2487.

Hall, S. J., and W. L. Silver. 2015. Reducing conditions, reactive metals, and their interactions can explain spatial patterns of surface soil carbon in a humid tropical forest. Biogeochemistry 125:149–165.

Heckman, K., C. R. Lawrence, and J. W. Harden. 2018. A sequential selective dissolution method to quantify storage and stability of organic carbon associated with Al and Fe hydroxide phases. Geoderma 312:24–35.

Hua, Q., M. Barbetti, and A. Z. Rakowski. 2013. Atmospheric Radiocarbon for the Period 1950–2010. Radiocarbon 55:2059–2072.

Kaiser, K., and G. Guggenberger. 2000. The role of DOM sorption to mineral surfaces in the preservation of organic matter in soils. Organic Geochemistry 31:711–725.

Kaiser, K., and G. Guggenberger. 2003. Mineral surfaces and soil organic matter. European Journal of Soil Science 54:219–236.

Khomo, L., S. Trumbore, C. R. Bern, and O. A. Chadwick. 2017. Timescales of carbon turnover in soils with mixed crystalline mineralogies. SOIL 3:17–30.

Li, D., S. Niu, and Y. Luo. 2012. Global patterns of the dynamics of soil carbon and nitrogen stocks following afforestation: a meta-analysis. New Phytologist 195:172–181.

López-Ulloa, M., E. Veldkamp, and G. H. J. de Koning. 2005. Soil carbon stabilization in converted tropical pastures and forests depends on soil type. Soil Science Society of America Journal 69:1110.

Loveland, P. J., and P. Digby. 1984. The extraction of Fe and Al by 0.1 M pyrophosphate solutions: a comparison of some techniques. Journal of Soil Science 35:243–250.

Marín-Spiotta, E., W. L. Silver, C. W. Swanston, and R. Ostertag. 2009. Soil organic matter dynamics during 80 years of reforestation of tropical pastures. Global Change Biology 15:1584–1597.

Marín-Spiotta, E., C. W. Swanston, M. S. Torn, W. L. Silver, and S. D. Burton. 2008. Chemical and mineral control of soil carbon turnover in abandoned tropical pastures. Geoderma 143:49–62.

Masiello, C. A., O. A. Chadwick, J. Southon, M. S. Torn, and J. W. Harden. 2004. Weathering controls on mechanisms of carbon storage in grassland soils. Global Biogeochemical Cycles 18:n/a-n/a.

Mathieu, J. A., C. Hatté, J. Balesdent, and É. Parent. 2015. Deep soil carbon dynamics are driven more by soil type than by climate: a worldwide meta-analysis of radiocarbon profiles. Global Change Biology 21:4278–4292.

Mikutta, R., and K. Kaiser. 2011. Organic matter bound to mineral surfaces: Resistance to chemical and biological oxidation. Soil Biology and Biochemistry 43:1738–1741.

Mueller, C. W., and I. Koegel-Knabner. 2009. Soil organic carbon stocks, distribution, and composition affected by historic land use changes on adjacent sites. Biology and Fertility of Soils 45:347–359.

Neumann-Cosel, L., B. Zimmermann, J. S. Hall, M. van Breugel, and H. Elsenbeer. 2011. Soil carbon dynamics under young tropical secondary forests on former pastures—A case study from Panama. Forest Ecology and Management 261:1625–1633.

Parton, W. J., J. W. B. Stewart, and C. V. Cole. 1988. Dynamics of C, N, P and S in grassland soils: a model. Biogeochemistry 5:109–131.

Powers, J. S., M. D. Corre, T. E. Twine, and E. Veldkamp. 2011. Geographic bias of field observations of soil carbon stocks with tropical land-use changes precludes spatial extrapolation. Proceedings of the National Academy of Sciences 108:6318–6322.

R Core Team. 2019. R: A language and environment for statistical computing. R Foundation for Statistical Computing.

Rabbi, S. M. F., M. Tighe, A. Cowie, B. R. Wilson, G. Schwenke, M. Mcleod, W. Badgery, and J. Baldock. 2014. The relationships between land uses, soil management practices, and soil carbon fractions in South Eastern Australia. Agriculture, Ecosystems & Environment 197:41–52.

Rasmussen, C., K. Heckman, W. R. Wieder, M. Keiluweit, C. R. Lawrence, A. A. Berhe, J. C. Blankinship, S. E. Crow, J. L. Druhan, C. E. Hicks Pries, E. Marín-Spiotta, A. F. Plante, C. Schädel, J. P. Schimel, C. A. Sierra, A. Thompson, and R. Wagai. 2018. Beyond clay: towards an improved set of variables for predicting soil organic matter content. Biogeochemistry 137:297–306.

Riedel, T., D. Zak, H. Biester, and T. Dittmar. 2013. Iron traps terrestrially derived dissolved organic matter at redox interfaces. Proceedings of the National Academy of Sciences 110:10101–10105.

Rowley, M. C., S. Grand, and É. P. Verrecchia. 2018. Calcium-mediated stabilisation of soil organic carbon. Biogeochemistry 137:27–49.

Rumpel, C., and I. Kögel-Knabner. 2011. Deep soil organic matter—a key but poorly understood component of terrestrial C cycle. Plant and Soil 338:143–158.

Saidy, A. R., R. J. Smernik, J. A. Baldock, K. Kaiser, and J. Sanderman. 2013. The sorption of organic carbon onto differing clay minerals in the presence and absence of hydrous iron oxide. Geoderma 209–210:15–21.

Saidy, A. R., R. J. Smernik, J. A. Baldock, K. Kaiser, J. Sanderman, and L. M. Macdonald. 2012. Effects of clay mineralogy and hydrous iron oxides on labile organic carbon stabilisation. Geoderma 173–174:104–110.

Schmidt, M. W. I., M. S. Torn, S. Abiven, T. Dittmar, G. Guggenberger, I. A. Janssens, M. Kleber, I. Kögel-Knabner, J. Lehmann, D. A. C. Manning, P. Nannipieri, D. P. Rasse, S. Weiner, and S. E. Trumbore. 2011. Persistence of soil organic matter as an ecosystem property. Nature 478:49–56.

Schneider, M. P. W., T. Scheel, R. Mikutta, P. van Hees, K. Kaiser, and K. Kalbitz. 2010. Sorptive stabilization of organic matter by amorphous Al hydroxide. Geochimica et Cosmochimica Acta 74:1606–1619.

Schrumpf, M., and K. Kaiser. 2015. Large differences in estimates of soil organic carbon turnover in density fractions by using single and repeated radiocarbon inventories. Geoderma 239–240:168–178.

Sierra, C. A. 2018. Forecasting atmospheric radiocarbon decline to pre-bomb values. Radiocarbon 60:1055–1066.

Sierra, C. A., M. Müller, H. Metzler, S. Manzoni, and S. E. Trumbore. 2017. The muddle of ages, turnover, transit, and residence times in the carbon cycle. Global Change Biology 23:1763–1773.

Sierra, C. A., S. E. Trumbore, E. A. Davidson, S. D. Frey, K. E. Savage, and F. M. Hopkins. 2012. Predicting decadal trends and transient responses of radiocarbon storage and fluxes in a temperate forest soil. Biogeosciences 9:3013–3028.

Six, J., H. Bossuyt, S. Degryze, and K. Denef. 2004. A history of research on the link between (micro)aggregates, soil biota, and soil organic matter dynamics. Soil and Tillage Research 79:7–31.

Six, J., E. T. Elliott, and K. Paustian. 2000. Soil macroaggregate turnover and microaggregate formation: a mechanism for C sequestration under no-tillage agriculture. Soil Biology and Biochemistry 32:2099–2103.

Six, J., and K. Paustian. 2014. Aggregate-associated soil organic matter as an ecosystem property and a measurement tool. Soil Biology and Biochemistry 68:A4–A9.

Sollins, P., C. Swanston, M. Kleber, T. Filley, M. Kramer, S. Crow, B. A. Caldwell, K. Lajtha, and R. Bowden. 2006. Organic C and N stabilization in a forest soil: Evidence from sequential density fractionation. Soil Biology and Biochemistry 38:3313–3324.

Spielvogel, S., J. Prietzel, and I. Kogel-Knabner. 2008. Soil organic matter stabilization in acidic forest soils is preferential and soil type-specific. European Journal of Soil Science 59:674–692.

Stuiver, M., and H. A. Polach. 1977. Reporting of 14C Data. Radiocarbon 19:355–363.

Swanston, C. W., M. S. Torn, P. J. Hanson, J. R. Southon, C. T. Garten, E. M. Hanlon, and L. Ganio. 2005. Initial characterization of processes of soil carbon stabilization using forest stand-level radiocarbon enrichment. Geoderma 128:52–62.

Torn, M. S., A. G. Lapenis, A. Timofeev, M. L. Fischer, B. V. Babikov, and J. W. Harden. 2002. Organic carbon and carbon isotopes in modern and 100-year-old-soil archives of the Russian steppe. Global Change Biology 8:941–953.

Torn, M. S., S. E. Trumbore, O. A. Chadwick, P. M. Vitousek, and D. M. Hendricks. 1997. Mineral control of soil organic carbon storage and turnover. Nature 389:170–173.

Trumbore, S. E. 1993. Comparison of carbon dynamics in tropical and temperate soils using radiocarbon measurements. Global Biogeochemical Cycles 7:275–290.

Trumbore, S. E., E. A. Davidson, P. Barbosa de Camargo, D. C. Nepstad, and L. A. Martinelli. 1995. Belowground cycling of carbon in forests and pastures of eastern Amazonia. Global Biogeochemical Cycles 9:515–528.

Vaughan, E., M. Matos, S. Ríos, C. Santiago, and E. Marín-Spiotta. 2019. Clay and climate are poor predictors of regional-scale soil carbon storage in the US Caribbean. Geoderma 354:113841.

Wiesmeier, M., L. Urbanski, E. Hobley, B. Lang, M. von Lützow, E. Marín-Spiotta, B. van Wesemael, E. Rabot, M. Ließ, N. Garcia-Franco, U. Wollschläger, H.-J. Vogel, and I. Kögel-Knabner. 2019. Soil organic carbon storage as a key function of soils - A review of drivers and indicators at various scales. Geoderma 333:149–162.

CHAPTER 3

Soil carbon dynamics following forest succession along a weathering gradient in a tropical karst area

Co-authors: Erika Marín-Spiotta[1]

[1]Department of Geography, University of Wisconsin-Madison

Abstract

Land use change can influence soil carbon (C) storage, although the direction and magnitude of change is inconsistent, particularly for transitions between pastures and secondary forests. This inconsistency may be driven in part by different soil properties which can mediate soil C stability and accumulation under changing vegetation and land use. This work uses a chronosequence of forest succession along a soil-weathering gradient in the karst region of Puerto Rico to address the role of soil properties in determining soil C change. Samples were collected from secondary forests from two age classes as well as active pastures on Mollisols and Alfisols derived from the same limestone parent material. Soil organic C (SOC), total C (TC) and nitrogen (N) stocks were measured along with soil pH to assess the relative importance of land cover and soil properties on controlling soil C. Alfisols contained greater SOC stocks to 1 m, primarily due to having deeper profiles on average, indicating a positive relationship between the degree of weathering and SOC stocks. Mollisols contained greater TC stocks than Alfisols, reflecting the contribution of parent material inorganic carbon in more shallow horizons. Despite expected increases in aboveground biomass with forest growth on pastures, there was no difference in SOC or N stocks among pasture soils or forest successional stage at any depth. Soil pH was positively correlated with TC stocks, indicating the role of calcium carbonate in contributing to inorganic C stocks. Karst-derived soils are important but relatively understudied in the tropics, and this study provides additional understanding of soil C dynamics in these soils.

Introduction

Changes in land cover and land use are currently an important contribution to total anthropogenic C emissions (Houghton and Nassikas 2017), while also representing a potential source of C sequestration, depending on land management (Griscom et al. 2017). It is well-known that secondary forest succession can enhance aboveground C accumulation and storage (Poorter et al. 2016, Chazdon et al. 2016, Powers and Marín-Spiotta 2017). As one of the largest terrestrial C reservoirs, soils play an important role in ecosystem responses to land-cover and land-use change (hereafter land change). However, responses of soil C are not consistent, especially for transitions from pasture to forest, where studies in the tropics have found SOC stocks to increase (Fisher et al. 1994, de Koning et al. 2003, Desjardins et al. 2004, Eclesia et al. 2012), decreases (Desjardins et al. 1994, Don et al. 2011), or show no change (Marín-Spiotta et al. 2009). Global metanalyses also come to different conclusions on the magnitude and direction of SOC change following reforestation of pastures (Post and Kwon 2000, Li et al. 2012). Managed grazing lands represent 25% of the global land surface area (Asner et al. 2004), and understanding the changes that occur in soils following conversion to or from pasture are important to understanding global C cycling.

One possible explanation for inconsistent soil C responses to land cover change is the importance of environmental conditions and soil properties in mediating SOM persistence following land change (López-Ulloa et al. 2005, Wiesmeier et al. 2015). For example, soil texture can affect the accumulation and decomposition of SOM due to its effect on soil moisture retention and its role in aggregate formation (Six et al. 1998, 2000) and mineral-organic associations (MOAs). MOAs

often contain the majority of OM in soils and are associated with longer soil C turnover times (von Lützow et al. 2006, Trumbore 2009, Kleber et al. 2015). Clay-sized particles exhibit large surface area and can contribute to high ion exchange capacity. Soils with fine textures are expected to store more C in MOAs than soils with lower clay content or coarser textures. Numerous studies have reported positive correlations between the amount of clay in a soil and its C content (Feller and Beare 1997, Post and Kwon 2000, López-Ulloa et al. 2005), and prominent biogeochemical models include clay content as a main predictor of soil C (Parton et al. 1993). However, given the wide range in mineralogy among clay-sized particles and subsequent reactivities, clay content can be a poor predictor of soil C storage (Vaughan et al. 2019) while additional physicochemical properties like clay mineralogy (Torn et al. 1997, Six et al. 2002), exchangeable calcium, and iron- and aluminum-oxyhydroxides may be more important (Ch. 2, Rowley et al. 2018, Rasmussen et al. 2018) but are not included in most biogeochemical models. In one tropical study, the change in SOC following pasture reforestation differed between Inceptisols and Andisols due to their differing mineralogy and resultant mechanisms of C stabilization (López-Ulloa et al. 2005).

Puerto Rico offers a compelling place to study interactions between soil properties and land change, given the great diversity of soil environments and extensive history of land change. The island contains 10 of the 12 USDA soil orders, given the diversity of climate, parent material, and relief found on the island. There is also a well-documented land change transition that has occurred across most of the island. Up to 94 % of forest cover was lost by the 1940s as land was converted to agriculture and pasture use (Franco et al. 1997). Driven by socioeconomic and demographic changes in the middle of the 20th century, widespread abandonment of agricultural

land resulted in mostly unassisted secondary forest succession across the island (Helmer et al. 2002, Parés-Ramos et al. 2008). Current estimates place island forest cover around 55 % (Marcano-Vega 2017). Regular aerial photography since the 1940s allows study of these land change transitions on a scale and detail not possible in much of the tropics.

Karst landforms, overlying calcareous bedrock, comprise about 27 % of Puerto Rico's land area (Lugo et al. 2001) and up to 15 % of the earth's surface (Goldscheider et al. 2020). The soils that form in these landscapes are unique, and understanding soil C dynamics in calcareous soils has important implications for regional soil C budgets. However, geographic biases in soil studies of soil C response to land change means that these soils are understudied relative to more highly weathered soils in the tropics (Powers et al. 2011).

To determine how soil properties affect response of SOC to land-use change, we studied changes in soil C as forests regrow on former pastures along a toposequence that represents a weathering gradient. Specifically, we compared chronosequences of secondary forest age on Mollisols and on Alfisols in a karst region of northern Puerto Rico. The two soils have developed on the same limestone parent material under forests, but have undergone different weathering intensities due to differences in relief and landscape position. The Mollisols are found on steeper slopes and are relatively less weathered. The Alfisols are found in flatter areas and toe slopes and are more weathered. The specific research questions we asked were:

1. How does soil C vary with forest succession on two soils along a weathering gradient?
2. How do soil properties, including pH, influence soil C storage?

We hypothesized that SOC would increase with forest age in both soil orders. We hypothesized and that Mollisols would contain greater SOC stocks in surface soils, but lesser SOC stocks to 1 m due to having shallower profiles. We also hypothesized that soils with higher pH would contain greater SOC stocks, due to the presence of exchangeable calcium in higher pH soils.

Methods

Site Selection and Field Sampling

All field sites were located in the karst region of north central Puerto Rico (Fig. 1). Climate in the region is classified as subtropical moist forest in the Holdridge life zone (Ewel and Whitmore 1974). Mean annual precipitation in the region is approximately 2000 mm per year, with a mean annual maximum temperature of 29.6 ºC and a mean annual minimum temperature of 17.8 ºC (Daly et al. 2003). Bedrock in the region is primarily Lares (upper Oligocene) limestone and Montebello (Tertiary) limestone (USGS; https://mrdata.usgs.gov/geology/pr/). The majority of the region followed a land change trajectory similar to that documented throughout the island as described earlier (Helmer et al. 2002). Current land cover is primarily a mix of secondary forest and pasture.

Soils in the region are highly heterogeneous due to the karst topography, with generally less-weathered soils at the top of mogotes (steep karst hills) and more highly-weathered soils in valleys. Progressing down hillsides, a predictable catena is often found along a topographic weathering gradient, from Inceptisols, to Mollisols, to Alfisols, to Ultisols. Because the parent

material and climate are similar throughout this region, topography is the primary soil forming factor that differs along this catena. Soil moisture and soil stability in Puerto Rican karst areas varies based on slope and aspect, leading to differences in weathering rates. Hilltops tend to be xeric, northern slopes tend to gentler relief and moist, while southwest slopes tend to be steeper and wetter (Ewel and Whitmore 1974).

We sampled from Mollisols and Alfisols along this catena selecting sites along a chronosequence of forest succession. Mollisols came primarily from the Soller series, which are clayey, mixed, active, isohyperthermic, shallow Typic Haprendolls (NRCS Official Series Description). Some Mollisols were classified as being in the Colinas or Naranjo series, both Haprendolls, or the San German series, which are Haplustolls. Stabilization of SOM due to association with exchangeable calcium and fine particles likely leads to a buildup of SOC in these Mollisols, some of which are known as rendzinas in other classification schemes (Duchaufour 1976). Alfisols were primarily from the Tanama series, which are clayey, mixed, active, isohyperthermic Lithic Hapludalfs. See Figure 2 for a visual representation of soil properties for each soil type. Within each soil order, we sampled four pasture sites, four young secondary forests (< 30 years old) and four older secondary forests (> 40 years old), except we sampled five young secondary forest Alfisol sites, for a total of 25 sites.

Sites were selected based on USDA Natural Resource Conservation Service (NRCS) soil maps, aerial photographs and conversations with local conservation organizations (Para La Naturaleza), UPR Extension agents, and local landowners. Forest age was determined to the nearest ten years by using aerial photographs that have been taken every 10 years as well as interviews with

landowners. To the best of our knowledge, the most recent previous land use for all secondary forest sites was pasture, although it is possible that some sites had other agricultural uses in the past.

At each site, a pit was dug and described to make sure that the soil was in the appropriate order, and then two additional pits were dug 30 m away on either side following the topographic relief. From each pit, soils were sampled down to 100 cm, or bedrock, whichever came first, following the protocol used in the NRCS Rapid Carbon Assessment (RaCA) (Soil Survey Staff 2016, Vaughan et al. 2019). In short, within each pit soils were sampled from 0-5 cm using a 10 cm x 10 cm x 5 cm scoop to measure bulk density. Below that to 50 cm, soils were sampled by horizon using a 7-cm diameter core to measure bulk density. Below 50 cm, soils were sampled by horizon using a bucket auger. Soils were air-dried in Puerto Rico and then shipped back to UW-Madison for analysis.

Laboratory Analysis

Air-dried soils were sieved to 2 mm. Bulk density was measured for all samples with and upper depth less than 50 cm. Soil bulk density values were calculated after subtracting the mass and volume of rocks and roots from the total sample mass and volume. Soil pH was measured using a glass probe in a 1:1 slurry of soil to deionized water after a 30-minute equilibration period. Two pH measurements were taken about five minutes apart and repeated until measurements were within 0.1 unit. pH values reported are the analytical mean.

A subsample of each soil was ground in a SpexMill 8000D for analysis of total C (TC) and total nitrogen (TN). The presence of inorganic carbon was tested by watching for effervescence after adding 4 M HCl to ground soil. Soils that contained inorganic C were fumigated overnight using concentrated HCl (Harris et al. 2001). All samples were analyzed on a Flash 2000 Elemental Analyzer (Thermo Scientific) in duplicate with a replicate error < 10% and aspartic acid and soil reference material as a standard and both aspartic acid and soil reference material as check standards. For soils that were fumigated, the difference in C between the fumigated sample and the un-fumigated sample was taken to represent inorganic C. SOC, TC and TN stocks were calculated using OC, TC, and TN concentrations corrected for oven-dried moisture content, bulk density, and horizon thickness. This dissertation presents laboratory data for at least two of the three pits from each site.

Because soils were sampled by horizon, comparisons between sites were complicated by different horizon depths and depth to bedrock. To assist in comparing stocks across standardized depths for the whole dataset, we also divided and aggregated profiles into a “shallow” 0-30 cm portion and a “deep” 30-100 cm portion. This was done using the ‘slice’ and ‘slab’ functions in the *aqp* package version 1.19 in R (Baudette et al. 2013). Horizons were divided into 1 cm slices, and then aggregated. Soil profiles that were shallower than 100 cm were aggregated as above, but only to their actual depth. Soil properties within the aggregated depths were weighted by the relative horizon contributions to each depth.

There were significant differences in A horizon bulk density by forest age class, with pastures having greater bulk densities than forest sites (Supplemental Fig. S1), so we also calculated SOC

stocks for the 0 to 30 cm depth increment using a minimum equivalent soil mass (ESM_{min}) approach (Lee et al. 2009). However, this approach did not substantively change our interpretation, so we present the uncorrected SOC stocks in the main body of the text and show the ESM_{min} corrected stocks as a supplemental figure (Fig. S2).

Statistical Analyses

All statistical analyses were conducted using R version 3.6 (R Core Team 2019). We conducted two-way ANOVA tests to assess differences in SOC, TC, and TN stocks across soil order and forest age class groupings for 0-100 cm, 0-30 cm, and 30-100 cm. Tukey's HSD tests were used to compare means following a significant effect in an ANOVA. We also tested the relationship between horizon level pH measurements and C and N horizon C densities (g C cm^{-3}) and percent C and N. All models were assessed to meet assumptions of normality of residuals and homogeneity of variance and data were transformed if needed. In all cases, TC values were log-transformed for statistical analysis, but are shown in figures without transformation.

We assessed the importance of various soil and site properties (soil order, forest age class, pH, and site depth) in predicting OC stocks using an exhaustive search model selection approach to maximize parsimony and explanatory power. Bayesian information criterion (BIC) was used as the criterion and the model selection was done using the *leaps* package in R (Lumley 2020).

Results

The two soil orders differed in soil physical properties, reflecting differences in position on the landscape and in soil weathering rates. Mollisols averaged 54 ± 6 cm depth to bedrock and Alfisols averaged 86 ± 7 cm depth to bedrock. Mollisols had an average A horizon thickness of 12.9 ± 1.2 cm compared to 8.1 ± 0.5 cm for Alfisols. Mollisols had an average pH of 7.58 ± 0.1 while Alfisols had an average pH of 6.85 ± 0.18. Bulk density of the A horizon differed between soil orders and forest age classes. Bulk density was greater in Mollisols (0.91 g cm^{-3}) than Alfisols (0.75 g cm^{-3}) and decreased from pastures through the medium-age successional forests on both soil orders (Fig. S1).

In Mollisols, Mean SOC stocks to 100 cm were 117 ± 9.7 Mg C ha^{-1} for Mollisols and 163 ± 8.3 Mg C ha^{-1} for Alfisols (Fig. 3). TC stocks to 100 cm averaged 346 ± 79.9 Mg C ha^{-1} for Mollisols and 185.8 ± 21.7 Mg C ha^{-1} for Alfisols. Mean TN stocks were 14.4 ± 1.4 Mg C ha^{-1} for Mollisols and 19.5 ± 1.2 Mg C ha^{-1} for Alfisols. Soil OC, TC, or N stocks did not differ with forest succession on former pastures within Alfisols or Mollisols for any of the depth increments studied (Fig. 3). There was no difference between pastures and forests or among forests of different ages within a soil order.

Horizon SOC density and N density (g cm^{-3}) were weakly negatively correlated with horizon pH in A horizon samples ($p = 0.03$, $R^2 = 0.06$), with no relationship in B horizon samples (Fig. 4). Horizon TC density was positively and non-linearly related with horizon pH for both A and B horizon samples. Soil pH explained 45 % of the variability in TC density for A horizon samples, and 26 % of the variability for B horizon samples (both using log-transformed TC values). Soil

pH did not explain a significant amount of variation in N density for either horizon. Similar trends were observed for horizon C and N concentration (%) as with horizon C and N density.

Model selection indicated that the best predictor of site SOC stocks was average site soil profile depth (Table 1, Fig. 5). The most parsimonious model predicting SOC stocks contained just soil depth, although soil order and soil pH were both marginally significant predictors in the full model as well. The full model with all predictor variables explained 69% of the variability in SOC stocks, while mean site soil depth described 54% of the variability by itself.

Discussion

No difference in soil carbon or nitrogen with forest succession in a karst landscape

Across a karst mogote landscape, soil carbon and nitrogen content did not vary with secondary forest succession on either Mollisols or Alfisols. Soil C trajectories with reforestation of tropical pastures in the literature are highly variable (Post and Kwon 2000, Powers et al. 2011, Li et al. 2012). In Puerto Rico, studies have found either a positive relationship between secondary forest age and soil C (Brown and Lugo 1990, Beinroth et al. 1996, Vaughan et al. 2019) or no relationship, especially in highly-weathered Oxisols (Marín-Spiotta et al. 2009). Forest cover can contribute to increased soil C stocks due to increased C inputs of aboveground litter. Forests can also experience lower decomposition rates than pastures due to less soil disturbance caused by intensive grazing or mechanization in some pastures (Asner et al. 2004). Alternatively, changes in SOC with land cover could be mediated by soil type, with different successional trajectories

influenced by soil properties rather than vegetation or land cover type (Tan et al. 2004, López-Ulloa et al. 2005, Laganiére et al. 2010).

Other studies in karst landscapes, primarily from China, tend to show that secondary forest succession increases SOC stocks relative to both agricultural fields and grasslands with recovery of C stocks to levels similar to primary forests within 40 years (Han et al. 2015, Yang et al. 2016, Ye et al. 2020). These differences have been linked to loss of C in aggregates due to disruption by tillage or other land conversion and subsequent recovery under growing forests (Liu et al. 2020, Ye et al. 2020). It is possible that grazing intensity at our sites is relatively low compared to these other locations although there was variation in grazing intensity at our pasture sites, ranging from a few animals per hectare to commercial dairy operations with many more animals, and visual differences in pasture condition. Tropical pastures can have high belowground inputs from roots, especially at depth which can explain similar or increased below ground OC or N stocks compared to forests (Fisher et al. 1994, Stahl et al. 2017).

Greater weathering and depth of Alfisols contributes to increased SOC storage

As hypothesized, Alfisols contained greater SOC and N stocks to 1 m than Mollisols, primarily due to greater average soil depth. Counter to what we expected, there was no difference in SOC or N stocks by soil order for the 0 to 30 cm depth. Mollisols by definition have organic-rich surface horizons and Mollisols in this study had thicker A horizons, so the lack of difference between these two soil orders indicates that the Alfisols also have great C concentrations. Mollisols had greater TC stocks than Alfisols, especially for the 0 to 30 cm depth fraction that

better controlled for the shallower average depth of Mollisols. Mollisols in this study are less weathered than Alfisols, and thus contain a greater amount of inorganic C derived from the limestone parent material. Inorganic C comprised up to 90% of total soil C in some Mollisol sites. The degree of weathering can be seen in part by shallower average profile depth of Mollisols, as well as higher pH reflective of greater persistence of bedrock-derived calcium carbonate. The greater degree of weathering and the associated greater average soil depth in Alfisols contributed positively to overall SOC storage in this landscape.

Tropical Mollisols are both regionally and globally important, making up 15 % of Puerto Rican soils (González et al. 2019), over 60 % of US Virgin Island soils (USDA NRCS) as well as significant portions of Central America and Southeast Asia (Winbourne et al. 2017). Alfisols are less abundant, comprising 5% of Puerto Rico (González et al. 2019), but combined, these soil orders represent a substantial contribution to overall C stocks, especially considering their substantial inorganic C stocks. While inorganic C is likely less susceptible to human activity, it contributes to soil C budgets and should not be overlooked. Tropical Mollisols and Alfisols are particularly different from the highly-weathered Oxisols and Ultisols that are often associated with the tropics and are the most-studied (Powers et al. 2011). This makes it important to understand the factors important to controlling soil C dynamics within them as they are likely to be quite different (Winbourne et al. 2017).

Soil pH relates to TC and SOC concentrations and may indicate different organic matter stabilization mechanisms

At our sites, TC stocks increased strongly and non-linearly with soil pH. Soil pH is closely related to the parent material mineralogy and degree of weathering of soils, and also independently controls many important soil processes relating to the persistence of soil C and N and can serve as a useful indicator of SOM stabilization mechanisms (Rasmussen et al. 2018). Somewhat counter to our hypotheses, we found only a weak, and negative relationship between pH and SOC content in A horizon soils, and no relationship for deeper B horizons. Organic matter can decrease soil pH, so a negative relationship, especially in OM-rich surface soils can be explained, although the weak trend is likely due to the buffering provided by calcium carbonates present in many of our soils. When included in site-level models and controlling for other covarying explanatory variables, soil pH did show a positive relationship with SOC stocks, similar to what we expected, and possibly indicating the importance of pH-influenced SOM stabilization mechanisms.

Soil pH is especially important in determining soil microbial communities (Fierer and Jackson 2006), but also plays a role in MOA formation and plant growth (Kleber et al. 2015). In these soils, the influence of pH on SOC is likely due primarily to the relationship between pH and exchangeable calcium. A study from a Chinese karst region found SOC stocks to correlate most strongly with exchangeable calcium and magnesium, both of which would be expected to correlate positively with soil pH (Yang et al. 2016). Exchangeable calcium in soil can stabilize SOM through several mechanisms. Exchangeable calcium can form cation bridges between OM and minerals, stabilizing OM in MOAs due to reduced effectiveness or accessibility of enzymes (Oades 1988, von Lützow et al. 2006, Rowley et al. 2018, Rasmussen et al. 2018). Additionally, calcium can contribute to aggregate formation, which physically protects SOM by excluding

microbial decomposers and enzymes and contributes to microenvironmental conditions that can slow decomposition (e.g., low oxygen, moisture, or nutrients) (Six et al. 2004, von Lützow et al. 2006). Although both soils in this study are formed from similar limestone parent material and are expected to contain large amounts of exchangeable calcium, the Mollisols are less weathered and should have greater calcium concentrations, which would be expected to lead to greater SOC concentrations. It is also worth noting that given the average difference in pH between the two soil orders, (7.58 for Mollisols and 6.85 for Alfisols), there is likely a significant presence of carbonate minerals in many of the Mollisols while they are likely minimal in Alfisols, with implications for exchangeable calcium and SOM stabilization (Rowley et al. 2018).

General mineralogy between the two soil types is likely to be similar given the similarity in parent material (Norrish and Rogers 1956), but it is possible that the more highly-weathered Alfisols have greater abundances of advanced weathering clay minerals such as kaolinite (Zagórski 2010) as well as iron and aluminum (Rowley et al. 2020), both of which could influence soil C and N dynamics. Changes in soil color with depth (Fig. 2) suggest differences in mineralogy and organic matter content between the two soil orders further highlighting the importance of relating weathering histories to different mechanisms of SOC stabilization.

Conclusion

We found little effect of forest succession on soil C and N storage across two limestone-derived soils along a weathering gradient. There was a stronger effect of soil properties on soil OC, TC and N, including soil order, soil depth, and soil pH. Studying similar land use trajectories across

two closely related soils provides a valuable and unique approach to elucidate the interactive effects of soil properties and land change on soil C and N dynamics. This study shows the important role that topographically-influenced differences in weathering play in SOC accumulation and storage. Tropical karst regions are both regionally and globally important, but generally understudied, so this information will help improve our understanding of soil dynamics in these systems.

Tables

Table 1. Multiple regression model results for site OC stocks with all predictor variables used. Site depth is the mean depth to bedrock or 100 cm among pits at a site. Site pH is the mean of the weighted pit pH values at a site. The number of sites is 25.

Variable	df	F-value	*p*
Site Depth	1	13.2	0.002
Soil Order	1	4.3	0.053
Site pH	1	3.36	0.084
Forest Age Class	2	1.9	0.17
Soil Order *x* Age Class	2	0.3	0.74

Figures

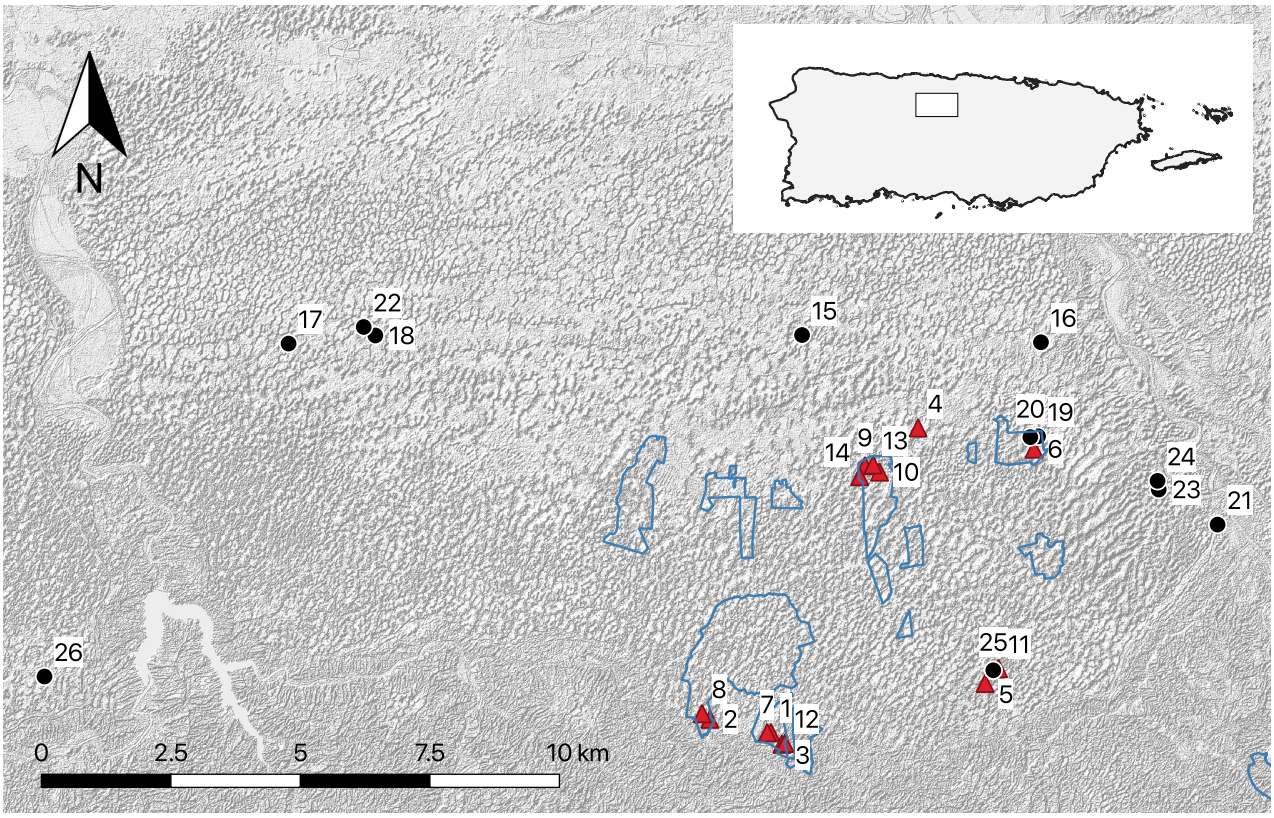

Figure 1. Map of sampling sites showing karst mogote topography. Black circles are Mollisol sites, and red triangles are Alfisols. Outlined areas on the inset map indicate protected areas managed by Para la Naturaleza.

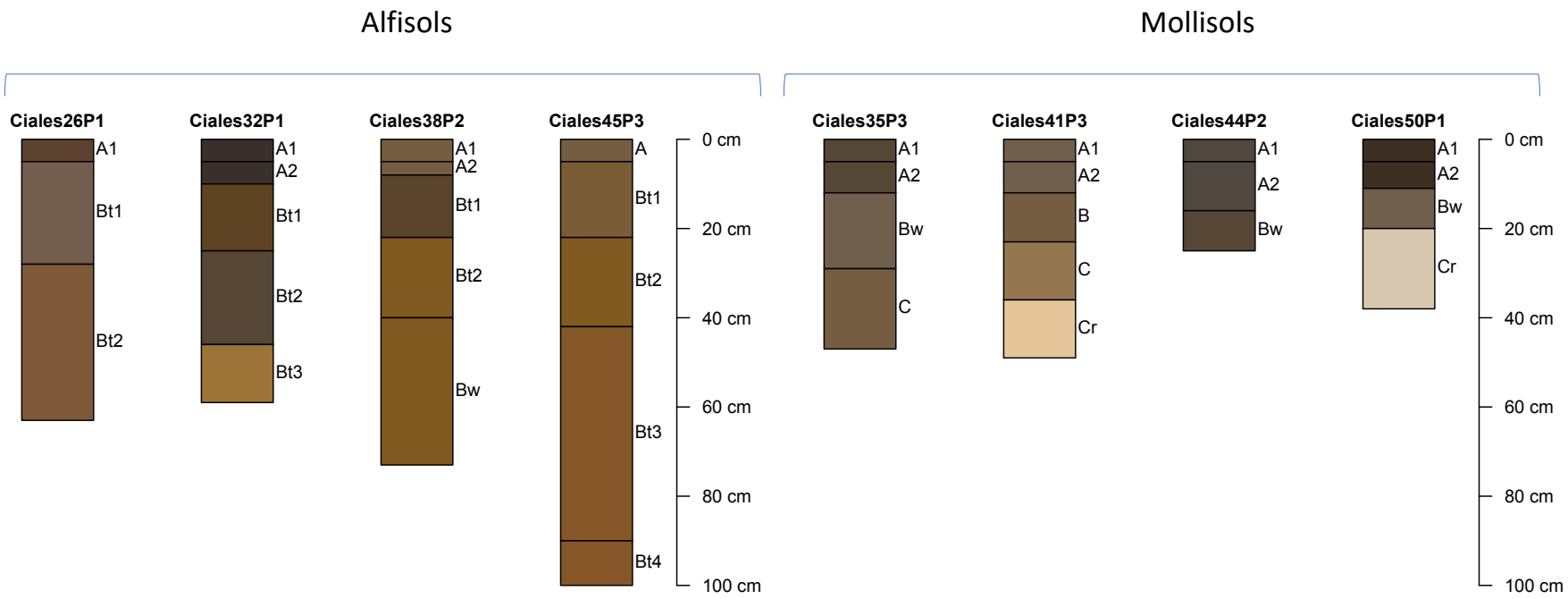

Figure 2. Selected soil profiles with horizon designations and moist soil color approximated from Munsell colors using the *aqp* package (Baudette et al. 2013).

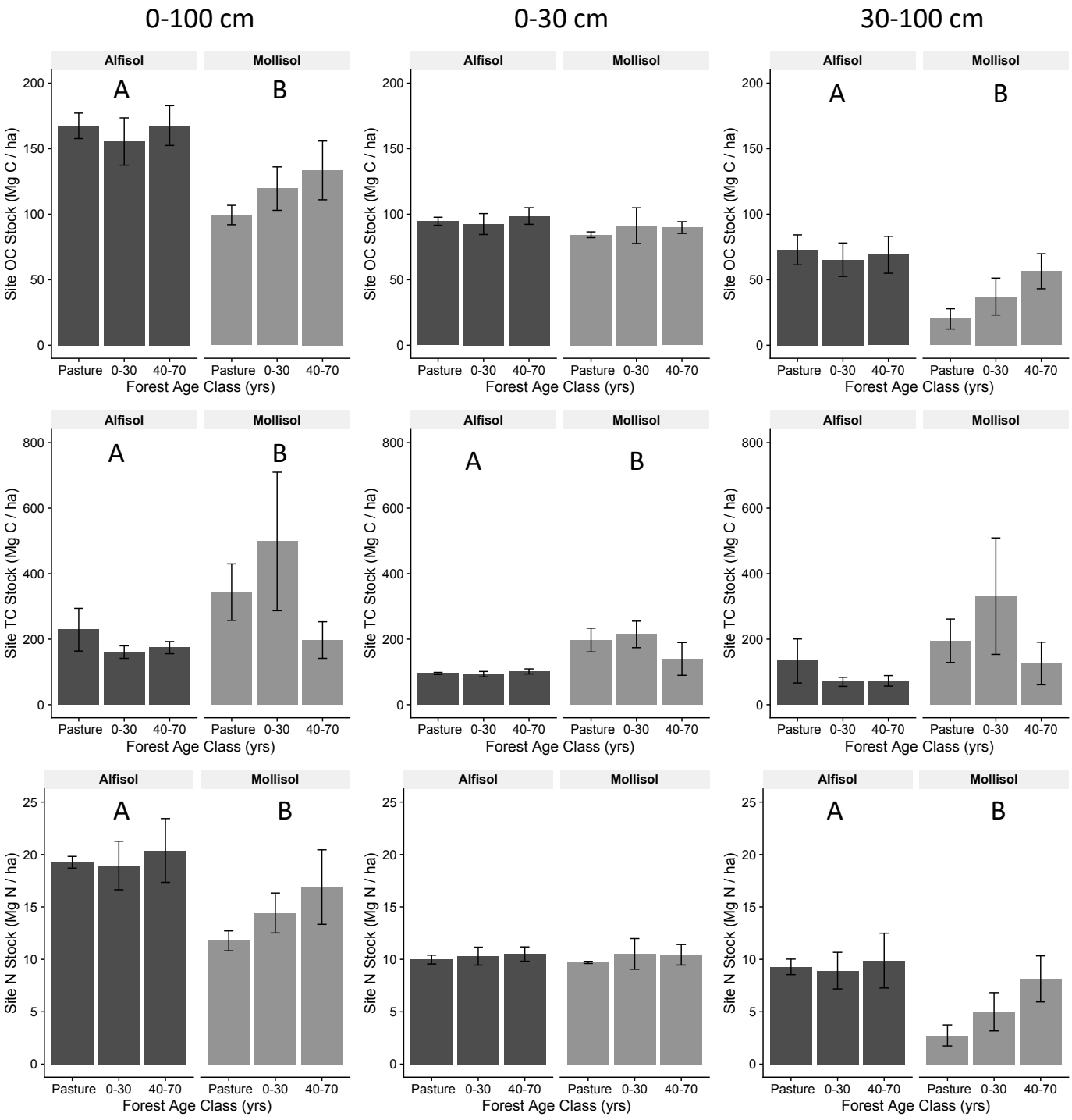

Figure 3. Organic soil carbon (OC) (top row), total carbon (TC) (middle row) and total nitrogen (TN) (bottom row) for three depth increments (0-100, 0-30, 30-100 cm) in Alfisols (dark gray) and Mollisols (light gray) in a karst landscape in Puerto Rico. Note the different scale for the OC, TC and TN. Different letters represent significant differences between soil orders within a given depth increment ($p < 0.05$).

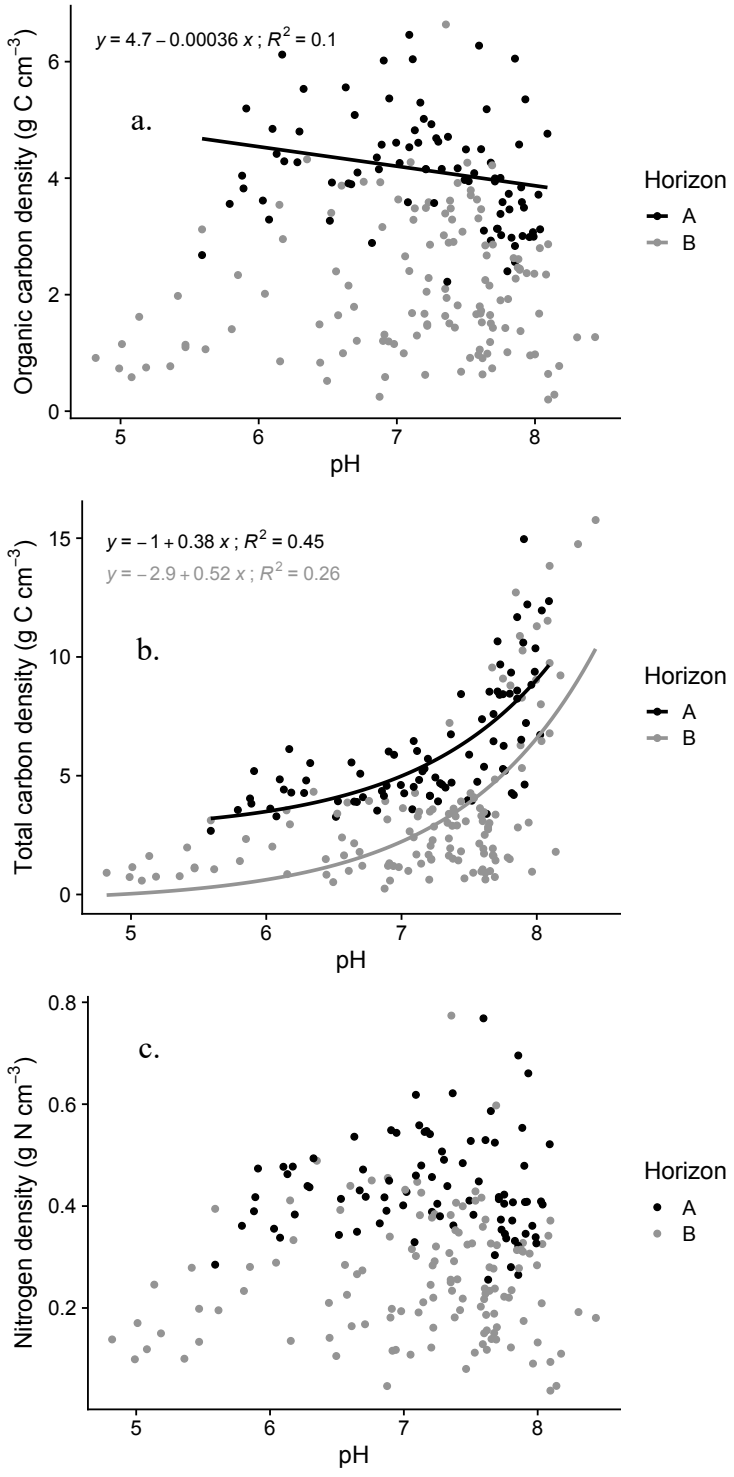

Figure 4. Soil organic carbon (a), total carbon (b) and nitrogen (c) as a function of horizon pH. Regression lines for a horizon indicate a significant relationship ($p < 0.05$). Note, the regression equations and statistics presented for the TC data are for log-transformed TC values, while the data and trend lines are shown here un-transformed.

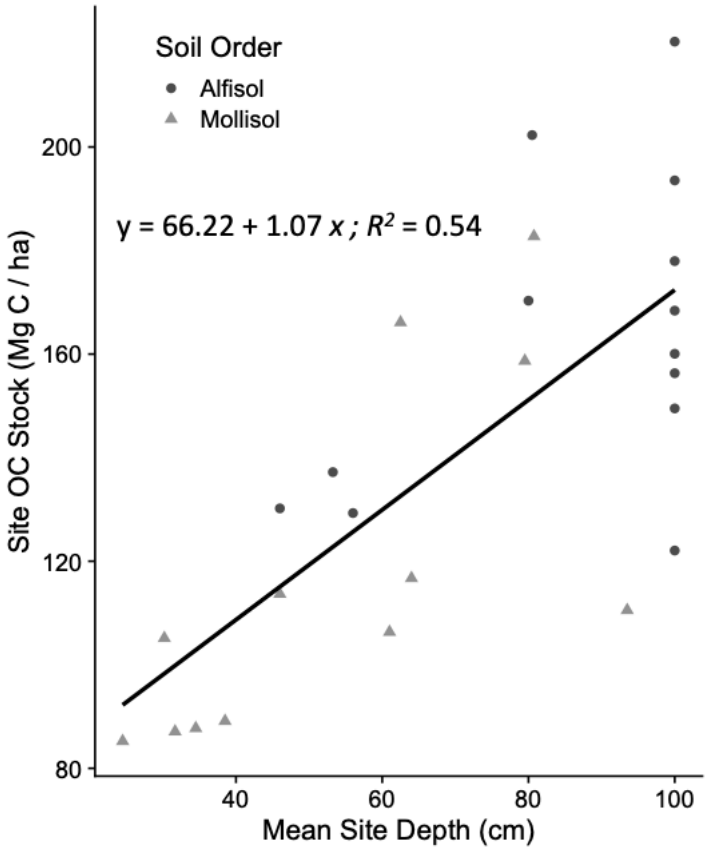

Figure 5. Relationship between mean site soil depth and site OC stocks.

Literature Cited

Asner, G. P., A. J. Elmore, L. P. Olander, R. E. Martin, and A. T. Harris. 2004. Grazing systems, ecosystem responses, and global change. Annual Reviews of Environmental Resources 29:261–299.

Baudette, D. E., P. Roudier, and A. T. O'Geen. 2013. Algorithms for Quantitative Pedology: A Toolkit for Soil Scientists. Computers and Geosciences 52:258–268.

Beinroth, F., M. Vázquez, V. Snyder, P. Reich, and L. Pérez Alegria. 1996. Factors controlling carbon sequestration in tropical soils: a case study of Puerto Rico. University of Puerto Rico-Mayagüez, USDA National Resources Conservation Service.

Brown, S., and A. E. Lugo. 1990. Effects of forest clearing and succession on the carbon and nitrogen content of soils in Puerto Rico and US Virgin Islands. Plant and Soil 124:53–64.

Chazdon, R. L., E. N. Broadbent, D. M. A. Rozendaal, F. Bongers, A. M. A. Zambrano, T. M. Aide, P. Balvanera, J. M. Becknell, V. Boukili, P. H. S. Brancalion, D. Craven, J. S. Almeida-Cortez, G. A. L. Cabral, B. de Jong, J. S. Denslow, D. H. Dent, S. J. DeWalt, J. M. Dupuy, S. M. Durán, M. M. Espírito-Santo, M. C. Fandino, R. G. César, J. S. Hall, J. L. Hernández-Stefanoni, C. C. Jakovac, A. B. Junqueira, D. Kennard, S. G. Letcher, M. Lohbeck, M. Martínez-Ramos, P. Massoca, J. A. Meave, R. Mesquita, F. Mora, R. Muñoz, R. Muscarella, Y. R. F. Nunes, S. Ochoa-Gaona, E. Orihuela-Belmonte, M. Peña-Claros, E. A. Pérez-García, D. Piotto, J. S. Powers, J. Rodríguez-Velazquez, I. E. Romero-Pérez, J. Ruíz, J. G. Saldarriaga, A. Sanchez-Azofeifa, N. B. Schwartz, M. K. Steininger, N. G. Swenson, M. Uriarte, M. van Breugel, H. van der Wal, M. D. M. Veloso, H. Vester, I. C. G. Vieira, T. V. Bentos, G. B. Williamson, and L. Poorter. 2016. Carbon sequestration potential of second-growth forest regeneration in the Latin American tropics. Science Advances 2:e1501639.

Daly, C., E. H. Helmer, and M. Quiñones. 2003. Mapping the climate of Puerto Rico, Vieques and Culebra. International Journal of Climatology 23:1359–1381.

Desjardins, T., F. Andreux, B. Volkoff, and C. C. Cerri. 1994. Organic carbon and 13C contents in soils and soil size-fractions, and their changes due to deforestation and pasture installation in eastern Amazonia. Geoderma 61:103–118.

Desjardins, T., E. Barros, M. Sarrazin, C. Girardin, and A. Mariotti. 2004. Effects of forest conversion to pasture on soil carbon content and dynamics in Brazilian Amazonia. Agriculture, Ecosystems & Environment 103:365–373.

Don, A., J. Schumacher, and A. Freibauer. 2011. Impact of tropical land-use change on soil organic carbon stocks - a meta-analysis. Global Change Biology 17:1658–1670.

Duchaufour, P. 1976. Dynamics of organic matter in soils of temperate regions: Its action on pedogenesis. Geoderma 15:31–40.

Eclesia, R. P., E. G. Jobbagy, R. B. Jackson, F. Biganzoli, and G. Piñeiro. 2012. Shifts in soil organic carbon for plantation and pasture establishment in native forests and grasslands of South America. Global Change Biology 18:3237–3251.

Ewel, J. J., and J. L. Whitmore. 1974. The ecological life zones of Puerto Rico and the U.S.Virgin Islands. US Forest Service.

Feller, C., and M. H. Beare. 1997. Physical control of soil organic matter dynamics in the tropics. Geoderma 79:69–116.

Fierer, N., and R. B. Jackson. 2006. The diversity and biogeography of soil bacterial communities. Proceedings of the National Academy of Sciences 103:626–631.

Fisher, M., I. Rao, M. Ayarza, C. Lascano, J. Sanz, R. Thomas, and R. Vera. 1994. Carbon storage by introduced deep-rooted grasses in the South American savannas. Nature 371:236–238.

Franco, P. A., P. L. Weaver, and S. Eggen-McIntosh. 1997. Forest Resources of Puerto Rico, 1990. Page 54. USDA Forest Service - Southern Research Station.

Goldscheider, N., Z. Chen, A. S. Auler, M. Bakalowicz, S. Broda, D. Drew, J. Hartmann, G. Jiang, N. Moosdorf, Z. Stevanovic, and G. Veni. 2020. Global distribution of carbonate rocks and karst water resources. Hydrogeology Journal.

González, G., E. Marín-Spiotta, and M. Matos. 2019. Appendix: Soil Assessment for the U.S. Caribbean. (in National Soils Assessment).

Griscom, B. W., J. Adams, P. W. Ellis, R. A. Houghton, G. Lomax, D. A. Miteva, W. H. Schlesinger, D. Shoch, J. V. Siikamäki, P. Smith, P. Woodbury, C. Zganjar, A. Blackman, J. Campari, R. T. Conant, C. Delgado, P. Elias, T. Gopalakrishna, M. R. Hamsik, M. Herrero, J. Kiesecker, E. Landis, L. Laestadius, S. M. Leavitt, S. Minnemeyer, S. Polasky, P. Potapov, F. E. Putz, J. Sanderman, M. Silvius, E. Wollenberg, and J. Fargione. 2017. Natural climate solutions. Proceedings of the National Academy of Sciences 114:11645–11650.

Han, G., F. Li, and Y. Tang. 2015. Variations in soil organic carbon contents and isotopic compositions under different land uses in a typical karst area in Southwest China. Geochemical Journal 49:63–71.

Harris, D., W. R. Horwáth, and C. van Kessel. 2001. Acid fumigation of soils to remove carbonates prior to total organic carbon or carbon-13 isotopic analysis. Soil Science Society of America Journal 65:1853.

Helmer, E. H., O. Ramos, T. del M. López, and M. Quiñones. 2002. Mapping the forest type and land cover of Puerto Rico, a component of the Caribbean biodiversity hotspot. Caribbean Journal of Science 38:165–183.

Houghton, R. A., and A. A. Nassikas. 2017. Global and regional fluxes of carbon from land use and land cover change 1850-2015: Carbon Emissions From Land Use. Global Biogeochemical Cycles 31:456–472.

Kleber, M., K. Eusterhues, M. Keiluweit, C. Mikutta, R. Mikutta, and P. S. Nico. 2015. Mineral–organic associations: formation, properties, and relevance in soil environments. Pages 1–140 Advances in Agronomy. Elsevier.

de Koning, G. H. J., E. Veldkamp, and M. López-Ulloa. 2003. Quantification of carbon sequestration in soils following pasture to forest conversion in northwestern Ecuador. Global Biogeochemical Cycles 17:n/a-n/a.

Laganiére, J., D. A. Angers, and D. Paré. 2010. Carbon accumulation in agricultural soils after afforestation: a meta-analysis. Global Change Biology 16:439–453.

Lee, J., J. W. Hopmans, D. E. Rolston, S. G. Baer, and J. Six. 2009. Determining soil carbon stock changes: Simple bulk density corrections fail. Agriculture, Ecosystems & Environment 134:251–256.

Li, D., S. Niu, and Y. Luo. 2012. Global patterns of the dynamics of soil carbon and nitrogen stocks following afforestation: a meta-analysis. New Phytologist 195:172–181.

Liu, M., G. Han, and Q. Zhang. 2020. Effects of agricultural abandonment on soil aggregation, soil organic carbon storage and stabilization: Results from observation in a small karst catchment, Southwest China. Agriculture, Ecosystems & Environment 288:106719.

López-Ulloa, M., E. Veldkamp, and G. H. J. de Koning. 2005. Soil carbon stabilization in converted tropical pastures and forests depends on soil type. Soil Science Society of America Journal 69:1110.

Lugo, A. E., L. M. Castro, A. Vale, E. H. Prieto, Martinó Andrés García, A. R. P. Rolón, A. G. Tossas, D. A. McFarlane, T. Miller, A. Rodríguez, J. Lundberg, J. Thomlinson, J. Colón, J. Schellekens, O. Ramos, and E. H. Helmer. 2001. Puerto Rican Karst - A Vital Resource. United States Department of Agriculture Forest Service.

Lumley, T. (based on code by A. M. 2020. Leaps Regression Subset Selection. R.

von Lützow, M., I. Kogel-Knabner, K. Ekschmitt, E. Matzner, G. Guggenberger, B. Marschner, and H. Flessa. 2006. Stabilization of organic matter in temperate soils: mechanisms and their relevance under different soil conditions - a review. European Journal of Soil Science 57:426–445.

Marcano-Vega, H. 2017. Forest of Puerto Rico, 2014. Page 4. U.S. Department of Agriculture, Forest Service, Southern Forest Experiment Station, Asheville, NC.

Marín-Spiotta, E., W. L. Silver, C. W. Swanston, and R. Ostertag. 2009. Soil organic matter dynamics during 80 years of reforestation of tropical pastures. Global Change Biology 15:1584–1597.

Norrish, K., and L. E. R. Rogers. 1956. The mineralogy of some terra rossas and rendzinas of south Australia. Journal of Soil Science 7:294–301.

Oades, J. M. 1988. The retention of organic matter in soils. Biogeochemistry 5:35–70.

Parés-Ramos, I. K., W. A. Gould, and T. M. Aide. 2008. Agricultural Abandonment, Suburban Growth, and Forest Expansion in Puerto Rico between 1991 and 2000. Ecology and Society 13.

Parton, W. J., J. M. O. Scurlock, D. S. Ojima, T. G. Gilmanov, R. J. Scholes, D. S. Schimel, T. Kirchner, J.-C. Menaut, T. Seastedt, E. Garcia Moya, A. Kamnalrut, and J. I. Kinyamario. 1993. Observations and modeling of biomass and soil organic matter dynamics for the grassland biome worldwide. Global Biogeochemical Cycles 7:785–809.

Poorter, L., F. Bongers, T. M. Aide, A. M. Almeyda Zambrano, P. Balvanera, J. M. Becknell, V. Boukili, P. H. S. Brancalion, E. N. Broadbent, R. L. Chazdon, D. Craven, J. S. de Almeida-Cortez, G. A. L. Cabral, B. H. J. de Jong, J. S. Denslow, D. H. Dent, S. J. DeWalt, J. M. Dupuy, S. M. Durán, M. M. Espírito-Santo, M. C. Fandino, R. G. César, J. S. Hall, J. L. Hernandez-Stefanoni, C. C. Jakovac, A. B. Junqueira, D. Kennard, S. G. Letcher, J.-C. Licona, M. Lohbeck, E. Marín-Spiotta, M. Martínez-Ramos, P. Massoca, J. A. Meave, R. Mesquita, F. Mora, R. Muñoz, R. Muscarella, Y. R. F. Nunes, S. Ochoa-Gaona, A. A. de Oliveira, E. Orihuela-Belmonte, M. Peña-Claros, E. A. Pérez-García, D. Piotto, J. S. Powers, J. Rodríguez-Velázquez, I. E. Romero-Pérez, J. Ruíz, J. G. Saldarriaga, A. Sanchez-Azofeifa, N. B. Schwartz, M. K. Steininger, N. G. Swenson, M. Toledo, M. Uriarte, M. van Breugel, H. van der Wal, M. D. M. Veloso, H. F. M. Vester, A. Vicentini, I. C. G. Vieira, T. V. Bentos, G. B. Williamson, and D. M. A. Rozendaal. 2016. Biomass resilience of Neotropical secondary forests. Nature 530:211–214.

Post, W. M., and K. C. Kwon. 2000. Soil carbon sequestration and land-use change: processes and potential. Global Change Biology 6:317–327.

Powers, J. S., M. D. Corre, T. E. Twine, and E. Veldkamp. 2011. Geographic bias of field observations of soil carbon stocks with tropical land-use changes precludes spatial extrapolation. Proceedings of the National Academy of Sciences 108:6318–6322.

Powers, J. S., and E. Marín-Spiotta. 2017. Ecosystem processes and biogeochemical cycles in secondary tropical forest succession. Annual Review of Ecology, Evolution, and Systematics 48:497–519.

R Core Team. 2019. R: A language and environment for statistical computing. R Foundation for Statistical Computing.

Rasmussen, C., K. Heckman, W. R. Wieder, M. Keiluweit, C. R. Lawrence, A. A. Berhe, J. C. Blankinship, S. E. Crow, J. L. Druhan, C. E. Hicks Pries, E. Marín-Spiotta, A. F. Plante,

C. Schädel, J. P. Schimel, C. A. Sierra, A. Thompson, and R. Wagai. 2018. Beyond clay: towards an improved set of variables for predicting soil organic matter content. Biogeochemistry 137:297–306.

Rowley, M. C., S. Grand, T. Adatte, and E. P. Verrecchia. 2020. A cascading influence of calcium carbonate on the biogeochemistry and pedogenic trajectories of subalpine soils, Switzerland. Geoderma 361:114065.

Rowley, M. C., S. Grand, and É. P. Verrecchia. 2018. Calcium-mediated stabilisation of soil organic carbon. Biogeochemistry 137:27–49.

Six, J., H. Bossuyt, S. Degryze, and K. Denef. 2004. A history of research on the link between (micro)aggregates, soil biota, and soil organic matter dynamics. Soil and Tillage Research 79:7–31.

Six, J., R. T. Conant, E. A. Paul, and K. Paustian. 2002. Stabilization mechanisms of soil organic matter: Implications for C-saturation of soils.

Six, J., E. T. Elliott, and K. Paustian. 2000. Soil macroaggregate turnover and microaggregate formation: a mechanism for C sequestration under no-tillage agriculture. Soil Biology and Biochemistry 32:2099–2103.

Six, J., E. T. Elliott, K. Paustian, and J. W. Doran. 1998. Aggregation and Soil Organic Matter Accumulation in Cultivated and Native Grassland Soils. Soil Science Society of America Journal 62:1367.

Soil Survey Staff. 2016. Rapid carbon assessment: Methodology, sampling, and summary. USDA, Natural Resources Conservation Service.

Stahl, C., S. Fontaine, K. Klumpp, C. Picon-Cochard, M. M. Grise, C. Dezécache, L. Ponchant, V. Freycon, L. Blanc, D. Bonal, B. Burban, J.-F. Soussana, and V. Blanfort. 2017. Continuous soil carbon storage of old permanent pastures in Amazonia. Global Change Biology 23:3382–3392.

Tan, Z. X., R. Lal, N. E. Smeck, and F. G. Calhoun. 2004. Relationships between surface soil organic carbon pool and site variables. Geoderma 121:187–195.

Torn, M. S., S. E. Trumbore, O. A. Chadwick, P. M. Vitousek, and D. M. Hendricks. 1997. Mineral control of soil organic carbon storage and turnover. Nature 389:170–173.

Trumbore, S. 2009. Radiocarbon and soil carbon dynamics. Annual Review of Earth and Planetary Sciences 37:47–66.

Vaughan, E., M. Matos, S. Ríos, C. Santiago, and E. Marín-Spiotta. 2019. Clay and climate are poor predictors of regional-scale soil carbon storage in the US Caribbean. Geoderma 354:113841.

Wiesmeier, M., M. von Lützow, P. Spörlein, U. Geuß, E. Hangen, A. Reischl, B. Schilling, and I. Kögel-Knabner. 2015. Land use effects on organic carbon storage in soils of Bavaria: The importance of soil types. Soil and Tillage Research 146:296–302.

Winbourne, J. B., S. W. Brewer, and B. Z. Houlton. 2017. Iron controls over di-nitrogen fixation in karst tropical forest. Ecology 98:773–781.

Yang, L., P. Luo, L. Wen, and D. Li. 2016. Soil organic carbon accumulation during post-agricultural succession in a karst area, southwest China. Scientific Reports 6.

Ye, Y., S. Xiao, S. Liu, W. Zhang, J. Zhao, H. Chen, G. Guggenberger, and K. Wang. 2020. Tillage induces rapid loss of organic carbon in large macroaggregates of calcareous soils. Soil and Tillage Research 199:104549.

Zagórski, Z. 2010. Clay minerals as indicators of the soil substrate origin of Rendzinas (Rendzic Leptosols) from the Małopolska Upland (S Poland). Brisbane, Australia.

Supplemental Figures

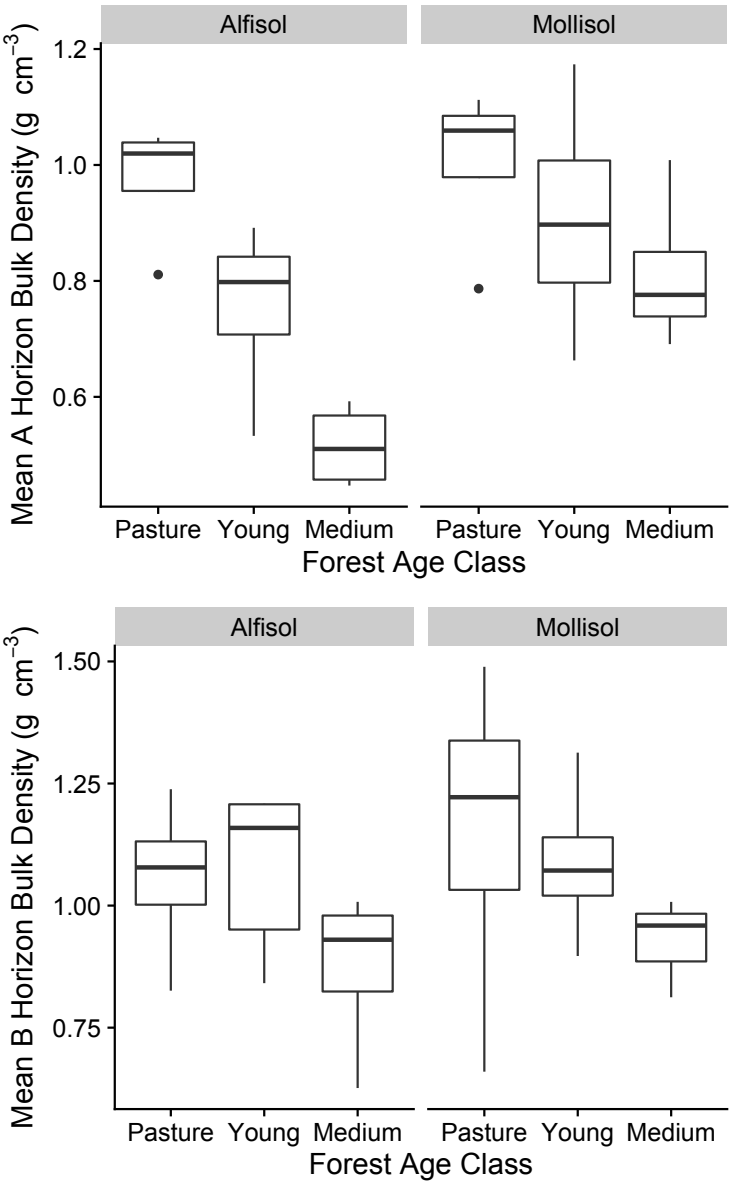

Supplemental Figure S1. Mean bulk density by forest age class and soil order for A horizon samples (a) and B horizon samples (b). For A horizon samples, there is a significant difference by soil order ($p = 0.01$) and forest age class ($p < 0.001$).

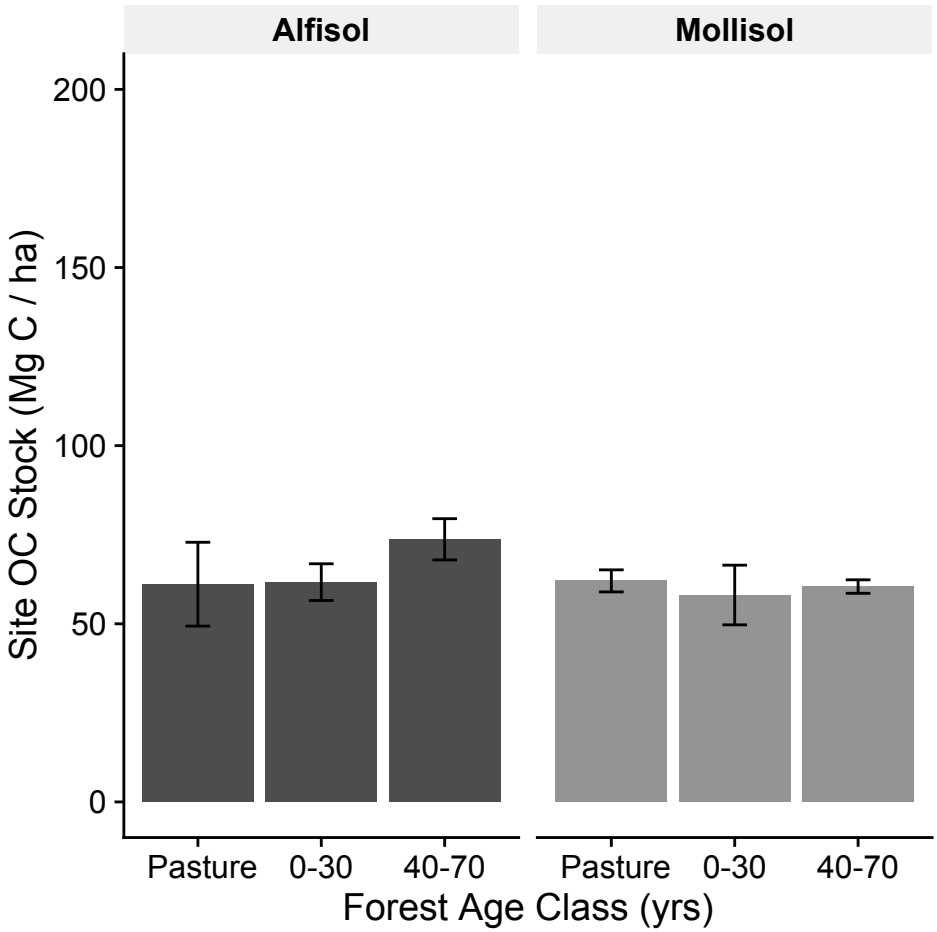

Supplemental Figure S2. Site OC stocks to 30 cm, corrected for differences in bulk density by forest age class using the minimum equivalent soil mass approach.

CHAPTER 4

Micro-scale patterns of organic matter decomposition and storage within a buried paleosol

Co-authors: Erika Marín-Spiotta[1] and Carsten W. Mueller[2]

[1]Department of Geography, University of Wisconsin-Madison

[2]Department of Geosciences and Natural Resource Management, University of Copenhagen

Abstract

Buried soils represent a potentially substantial and often overlooked component of soil carbon (C) budgets. Although deep soil C is usually thought to be stable and resistant to disturbances, changes at the surface as well as landscape-level changes can expose ancient organic matter (OM) to enhanced decomposition. The Brady soil is a buried paleosol found in Nebraska, which in places is being exposed to the surface through erosion of the overlying soil. To explore the effects of exposure on organic matter composition and decomposition of fresh plant litter, we collected samples collected along a gradient of degree of exposure, ranging from 20 cm below the current soil surface to 450 cm below the current surface. ^{13}C nuclear magnetic resonance (NMR) spectroscopy was used along with a molecular mixing model to compare OM composition between the modern surface soil and the Brady soil at different depths. The modern surface soil contained greater proportions of carbohydrate and protein, while the Brady soil at all depths had greater proportions of pyrogenic C (char). OM in the shallower Brady soils was less decomposed than OM in deeper Brady soils, indicating inputs of modern OM and/or enhanced decomposition of ancient OM. Nano-scale Secondary Ion Mass Spectrometry (NanoSIMS) imaging was used to observe spatial patterns of OM decomposition and OM storage following a 30-day laboratory incubation of the Brady soil with ^{13}C-enriched root litter. We observed decomposition and incorporation of enriched litter by microbes at all depths, although primarily by bacteria, while fungi or actinomycetes appeared to incorporate less of the enriched OM. This work provides insights into mechanisms and patterns of OM decomposition in a changing soil environment on the molecular scale and will be used to corroborate additional work done in these sites.

Introduction

Soils represent one of the largest terrestrial carbon (C) stocks. Soil C is sensitive to disturbance, whether due to human land use, climate change, or landscape evolution. Historically, studies of soil C stocks and susceptibility to disturbance have generally focused on surface soils, in part due to the assumptions of lower C concentrations in deep soils and that deep soil C is less reactive than shallower soil C (Rumpel and Kögel-Knabner 2011). Growing evidence suggests that deep soil C may represent a significant proportion of global C stocks and may also be susceptible to changes at the surface (Fisher et al. 1994, Jobbagy and Jackson 2000, Harrison et al. 2011, Rumpel and Kögel-Knabner 2011, Harper and Tibbett 2013).

Among deep soils, buried soils in particular represent a potentially overlooked component of deep soil C and one that may contain substantial C stocks in some areas (Chaopricha and Marín-Spiotta 2014, Marín-Spiotta et al. 2014, Ferguson et al. 2020). Buried soils differ from many other deep soils due to greater C concentrations than would be expected at depth. Soils can be buried through a number of different mechanisms, including landslides, erosional deposits, fluvial deposition and aeolian deposition (Jacobs and Mason 2005, Berhe et al. 2007, Chaopricha and Marín-Spiotta 2014). In all cases, soil burial leads to different conditions than those in which the soils were formed, and probable differences in organic matter (OM) inputs and OM decomposition rates. OM composition and C cycling dynamics have been shown to differ between modern surface soils and buried paleosols (Jacobs and Mason 2005, Marín-Spiotta et al. 2014), although less is known about what happens as buried soils become exposed to the modern surface through landscape evolution.

Long-term climate change, as well as changes to other drivers of rates of erosion and deposition can expose soils that have been disconnected from the surface for millennia. Exposure of buried soils could enhance decomposition of ancient OM, through priming effects due to input of modern OM (Fontaine et al. 2007), as well as changing edaphic conditions such as moisture and temperature. The response of millennial-aged C currently stored in buried soils to exposure could have implications for atmospheric C and climate change.

The use of modern techniques can improve our understanding of SOM dynamics at the micro-scale where decomposition occurs. Solid-state cross-polarization magic angle spinning ^{13}C nuclear magnetic resonance (NMR) spectroscopy gives valuable information on SOM chemical structure (Kögel-Knabner 1997) and when combined with molecular mixing models (Nelson and Baldock 2005) can give estimates of the contribution of different C compounds to the SOM pool. Nano-scale secondary ion mass spectrometry (NanoSIMS) provides the ability to image elemental distributions in soils at high resolution (30 μm x 30 μm) and with sufficient specificity to distinguish between elemental isotopes (Mueller et al. 2012). This allows for understanding of spatial patterns of OM distribution within soil biota, aggregates, and particles, especially when paired with studies using isotopically-enriched tracers.

We used these techniques on samples from the Nebraska loess-tablelands, as a case study of what happens as buried soils become exposed. Climate change over the last 15,000 years has led to the formation, burial, and subsequent exposure of the Brady soil, a late-Pleistocene paleosol buried by loess deposits starting around 10,500 to 9000 years ago (Johnson and Willey 2000, Mason et al. 2008). Depending on differences in landscape position, erosional processes over the last several hundred years have removed the overlying loess in places, differentially exposing the

Brady soil to the modern atmosphere and soil surface conditions. This study uses this gradient in Brady soil exposure to ask the following questions:

1) Does organic matter composition differ with exposure of the Brady soil to the surface?
2) How does decomposition of fresh plant litter differ with exposure of the Brady soil to the surface?

We hypothesized that organic matter composition would differ between the Brady soil and the modern surface soil, and that the difference would be greatest where the Brady soil was still most deeply buried. Further, we predicted that OM in the deepest Brady soils would show a higher degree of decomposition as determined using alkyl:O/N-alkyl ratios. We predicted that there would be incorporation of fresh plant litter by microbes within all Brady soil depths.

Methods

Site description and sampling design

The study site is located in southwestern Nebraska, USA (40.50º N, 101.42º W; Fig. 1). Current vegetation is primarily shortgrass prairie, with mean annual temperature of 10.3 ° C and mean annual precipitation of 487 mm (climate data are from the Wauneta weather station, High Plains Regional Climate Center; climod.unl.edu) The modern surface soils are primarily Mollisols.

The Brady soil is a paleosol that formed in Peoria loess deposits during the Pleistocene-Holocene transition (Johnson and Willey 2000). The Brady soil was subsequently buried by the deposition of Bignell loess following the last deglaciation in North America starting between 10.5 cal ka

and 9 cal ka (Mason et al. 2008). The thickness of the overlying Bignell loess ranged across the landscape from < 0.5 to at least 6 m. Subsequent erosion has removed this overlying loess in some locations, with the degree of erosion varying by landscape position (Jacobs and Mason 2005). Transects were sampled across a gradient of both original burial depth and erosional exposure. This study reports results from samples collected along three erosional transects, representing locations where the Brady soil was originally buried under approximately 4.5 m of loess. Brady soil was sampled along each transect at approximately 4.5 to 6 m deep, 1.2 m deep, 0.4 m deep, and 0.2 m deep (Fig. 1). Modern surface soil was also collected from each location along the transect. The 4.5 m and 1.2 m Brady soils were collected using a hydraulic drilling rig and Giddings soil probe, while the shallower soils were collected from hand-dug pits.

Nuclear Magnetic Resonance (NMR) analysis

Soils were prepared for NMR analysis by air-drying and then separated using a modified electrostatic fractionation approach (Kaiser et al. 2009). This approach yielded a particulate organic matter (POM) fraction, a <53 μm silt and clay fraction, and a >53 μm sand and aggregate fraction.

We used solid-state cross-polarization magic angle spinning ^{13}C nuclear magnetic resonance (NMR) spectroscopy to characterize the relative abundance of C functional groups in POM and < 53 μm fractions isolated from samples collected from different depths along the erosional transect. The analysis was done with a Bruker DSX 400 spectrometer at the Lehrstuhl für Bodenkunden at the Technical University of München. Samples were loaded into zirconium dioxide rotors and spun in a MAS probe at a speed of 6.8 kHz. We used a delay time of 1.0 seconds for POM samples and of 0.4 seconds for the <53 μm samples. NMR spectra were

integrated in the following chemical shift (ppm) regions: -10 to 45 (alkyl C), 45 to 60 (n-alkyl C), 60 to 90 (O-alkyl C), 90 to 110 (di-O-alkyl C), 110 to 140 (aromatic C), 140 to 160 (O-aryl C) and 160 to 220 ppm (carboxyl and carbonyl C). We also calculated alkyl:O/N-alkyl ratios, which were defined as the alkyl C integral (-10 to 45 ppm) divided by the summed integral from 45 to 110 ppm (n-alkyl + O-alkyl + di-O-alkyl).

These integrals were used to calculate the contribution of six different C compounds (carbohydrates, carbonyl, lipids, protein, char, to bulk SOM using a molecular mixing model (Nelson and Baldock 2005) with the measured C:N used to constrain the results.

NanoSIMS analysis

We used Nano-scale Secondary Ion Mass Spectrometry (NanoSIMS) to determine the fate of fresh isotopically-labeled organic matter in buried soils following a laboratory incubation. For the incubation, soils were taken from the three shallowest Brady positions along each transect (1.2 m, 0.4 m, and 0.2 m). Eighty grams of Brady soil was combined with 42 mg of ^{13}C-enriched *Avena root* litter and brought to 60% water holding capacity using Academic deionized water. The ^{13}C-enriched litter was enriched to 92 atom% ^{13}C as in de Graaff et al. (2010). Soils were incubated at room temperature and maintained at constant moisture. Following 30 days, a subsample of soil was removed from each jar, and divided. Half of the subsample was immediately placed in 99% ethanol and stored in a -20 ˚C freezer in order to fix microbial cell structure, and the remainder of the subsample was air-dried.

Samples were prepared for NanoSIMS imaging depending on how they had been stored in part to test a new method of fixing microbial cells for imaging. A subsample of the air-dried soil was

placed in deionized water at a ratio of 1 g L^{-1} and placed in a sonic bath to disperse and suspend the soil. A drop of the resulting suspension was pipetted onto a silica wafer and air-dried in a desiccator (Mueller et al. 2012). Samples stored in ethanol were prepared two ways to compare the preservation of microbial cell structure. One set of samples was dispersed in the original ethanol using sonication and pipetted onto a silica wafer prepared as described earlier. Although this method preserved microbial cell structure, we observed elevated levels of ^{13}C dispersed across the entire sample, indicating possible dissolution of the labeled OM (Fig. 3). To address this, we took the samples in ethanol and rinsed them five times using clean ethanol by mixing gently before centrifuging and decanting the supernatant. This method appeared successful at both preserving cell structure and removing the background contamination (Fig. 3).

A scanning electron microscope (SEM) was used to identify specific coordinates for NanoSIMS imaging. First, samples were coated with a thin layer of gold under an argon atmosphere (Mueller et al. 2012). Using the SEM (Jeol JSM 5900), individual and representative microaggregates were identified, along with clearly identifiable microbial cells and hyphae. A minimum of five separate regions from each sample were selected for imaging on a NanoSIMS 50L (Cameca, Gannelliers, France). We used a cesium primary ion beam with 16 kV impact energy for analyses after sputtering away surface impurities with a higher energy beam first. We simultaneously recorded ion distributions for $^{12}C^{-}_{2}$, $^{12}C^{-13}C^{-}$, $^{12}C^{14}N^{-}$, $^{56}Fe^{16}O^{-}$, $^{27}Al^{16}O^{-}$, and ^{32}S. We calculated the ratios of $^{12}C^{14}N$:$^{12}C_2$ and $^{12}C^{13}C$: $^{12}C_2$.

NanoSIMS images were corrected and analyzed using the OpenMIMS plugin for ImageJ (Gormanns et al. 2012). Regions of interest (ROI) were identified and drawn by hand using the distribution for $^{12}C^{13}C$, which overlapped very closely the distribution of $^{12}C^{14}N$, and corresponds to OM (Mueller et al. 2012). ROIs were visually identified based on whether they

were fungal hyphae (or possibly actinomycetes), single-celled microbes (assumed to be bacteria, and called bacteria hereafter), plant-derived particulate OM, or OM associated with aggregate surfaces or small, clay-sized minerals. ROIs that were not positively identified are discussed as 'unknown' in the text. Due to the limited number of intact bacterial cells we found, we used the ROIs from the samples with background contamination in our analyses. To address the contamination, we calculated a background contamination value as the mean $^{12}C^{13}C$: $^{12}C_2$ of the background aggregate matrix. This value was then subtracted from all ROIs within those samples.

We also calculated natural abundance $^{12}C^{13}C$: $^{12}C_2$ on a reference field sample from the <53 μm fraction of the 1.2 m deep Brady soil. Similar to other samples used for NanoSIMS imaging, we selected 5 representative areas, and then identified a total of 32 ROIs from these areas. The mean natural abundance $^{12}C^{13}C$: $^{12}C_2$ for all reference ROIs was 216, and the maximum was 233. We take any value above 233 to be suggestive of enrichment due to the labeled material.

Statistics

Differences in OM chemical composition from the mixing model were determined using two-way ANOVAs with depth and fraction as independent variables and with each chemical compound as the dependent variable. Following significant test results ($p < 0.05$), Tukey's HSD post hoc tests were used to determine pairwise differences. A Kruskall-Wallace test was used to determine differences in ^{13}C enrichment for classified NanoSIMS ROIs, given the non-normally distributed data. Dunn's post hoc test was used to determine differences between groups. To test similarities between different classification groups of ROIs, principal components analysis (PCA) was performed using the six elements and element ratios described above. All statistics

were conducted using R version 3.6 (R Core Team 2019) with the *FSA* package used for the Dunn's test (Ogle et al. 2020).

Results

NMR results

NMR spectroscopy revealed significant differences in OM chemical composition between the modern surface soil and the Brady soil at all depths for both fractions reported here. Specifically, the modern surface soil <53 μm fraction exhibited increased peak intensity in the carbonyl-C and O-alkyl-C regions relative to the Brady soils, while the Brady soils <53 μm fraction exhibited relatively more aryl-C (Table 1, Fig. 4). The modern surface POM fraction had relatively greater O-alkyl-C compared to the Brady soil POM (Fig. 4). The alky:O/N-alkyl ratio, an indicator of the degree of OM decomposition (Baldock et al. 1997), increased with depth in the POM fraction but showed no consistent trend with depth in the <53 μm fraction (Fig. 5).

Molecular mixing model results also indicated differences in the overall contribution from various types of OM compounds between the two fractions, and between the Brady soil at different depths and the modern surface soil. Char made up between 8 and 11 % of OM in the Brady soil < 53μm fraction, with the greatest contribution from char in the deepest Brady soil (Fig. 6). Char constituted 1 % of the modern surface <53 μm fraction, and less than 1 % in all POM samples. The contribution of carbonyl-C was lower in the modern surface POM compared to the 120 cm-deep Brady soil ($p = 0.06$). The contribution from lipids did not differ between soil types and depths within fractions but was greater in the POM fraction compared to the <53 μm fraction ($p = 0.06$). The contribution from lignin was greater in the POM fraction compared to

the <53 μm fraction ($p < 0.0001$) but did not differ by depth within each fraction. The contribution from protein was greater in the <53 μm fraction than in the POM fraction ($p < 0.0001$) and differed significantly within the <53 μm fraction by depth. The modern surface soil had a greater contribution from protein than the three deepest Brady soils, but was not different from the shallowest Brady soil. There was a greater contribution from carbohydrates in the POM fraction compared to the <53 μm fraction ($p < 0.0001$). Within the POM fraction, the carbohydrate contribution was similar between the shallowest Brady soil and the modern surface soil, but both were greater than the deeper Brady soils. Within the <53 μm fraction, there was a greater contribution from carbohydrates in the modern surface soil compared to all of the Brady soil depths.

NanoSIMS Imaging Results

NanoSIMS imaging showed evidence of incorporation of enriched plant root litter by microbes. Specifically, significant isotopic enrichment was observed in unicellular microorganisms (bacteria), and only slight enrichment was observed in fungal hyphae (Figs. 3, 7, 8). $^{12}C^{13}C:^{12}C_2$ values differed between the reference sample and all ROI groups from the incubated samples (Table 2). There was also a significant difference in the $^{12}C^{13}C:^{12}C_2$ values between bacterial cells and all classification groups except for aggregate surfaces. There was no difference in $^{12}C^{13}C:^{12}C_2$ between hyphae, small minerals, and aggregate surfaces. Ordination techniques did not show distinct separation between organic matter associated with different aggregate and mineral surfaces using the elements measured in this analysis (Fig. 9).

Discussion

Bacteria we found were heavily enriched

The incubation experiment followed by NanoSIMS imaging showed that there was active incorporation and processing of fresh plant litter within the Brady soil across all depths of the exposure sequence. In particular, we observed that within 30 days, decomposition of fresh plant material seemed to be driven by bacteria or other single-celled microbes. Although the sample size was limited, all intact bacteria observed were greatly enriched with the ^{13}C label. ROIs identified as fungal hyphae or actinomycetes on the other hand were only slightly enriched, whereas OM associated with small minerals and aggregate surfaces was variable, but mostly showed low levels of enrichment similar to hyphae. This suggests that either fungi were not important decomposers of fresh plant litter under the conditions of the laboratory incubation, or that there was not sufficient time since the start of the incubation for fungi to incorporate the fresh plant litter. Other studies using similar incubation approaches have observed fungal responses to C amendments on timescales similar to this incubation (de Graaff et al. 2010) although the C in our study was plant litter as opposed to labile exudate C. Field studies have also shown positive responses in growth, abundance and incorporation of C amendments by fungi (Chigineva et al. 2009, Hopkins et al. 2014). We did not quantify actual fungal abundances or biomass in this project, so we cannot speak to the overall response of fungi during the incubation.

We did not find enough bacteria through our imaging approach to determine if there were differences in bacterial decomposition dynamics between the different Brady soil depths. We did observe evidence of processed enriched litter at all three of the soil depths used for the incubation (20 cm, 40 cm, and 120 cm) as enriched OM that was associated both with aggregate structures and smaller mineral surfaces. Microbial processing facilitates the preservation of OM

on mineral surfaces and in aggregates (Rumpel and Kögel-Knabner 2011, Schmidt et al. 2011, Cotrufo et al. 2013). We were not able to observe different elemental composition between OM associated with mineral and aggregate surfaces. Ongoing work will better determine the specific identities and dynamics within the microbial communities of the different Brady soil depths.

Additional work should also elucidate whether there is any priming of old OM following inputs of labile, modern plant inputs (Kuzyakov 2010). Other work has shown that modern OM inputs can enhance decomposition of ancient OM (Fontaine et al. 2007, Gurwick et al. 2008), which suggests that one possible explanation for the lack of enrichment of fungal hyphae is that they are accessing older OM. However, this will need to be corroborated using additional methods.

This work also highlights a potentially novel approach to fixing microbial cells for high-resolution imaging including scanning electron microscopy and NanoSIMS. The use of ethanol with subsequent air-drying was effective at stabilizing and preserving intact microbial cells (Fig. 3). Additional washing with clean ethanol was needed to remove background contamination of the label although evidence of microbial enrichment is still evident even without an additional rinsing. It is possible that this process also destroyed some intact cells, contributing to the relative scarcity in our images.

OM composition differs between surface soil and Brady soil, and with degree of Brady exposure

Our study shows consistent differences in OM composition between the modern surface soil and the Brady soil at all depths. OM in the Brady soil was characterized as being more decomposed than the modern surface soil, as evidenced by the alkyl:O/N-alkyl ratio (Baldock et al. 1997). This could indicate two possible and non-mutually exclusive explanations. First, this likely

indicates the lack of modern plant inputs at depth, leading to the dominance of older and more processed OM. It is also possible that as the Brady soil is exposed to surface conditions, the older OM is decomposed, and replaced with fresher inputs. Indeed, there was no difference in alkyl:O/N-alkyl ratio between the shallowest Brady soil samples (~ 20 cm) and the modern surface soil. Additional evidence for more decomposed OM with depth is seen in the decreasing prevalence of carbohydrates in both the POM and < 53 μm fractions with depth. This is similar to what was reported for a Brady soil at 6m depth (Marín-Spiotta et al. 2014). Carbohydrates are expected to be relatively susceptible to decomposition, and indicative of more recent plant inputs. However, it is worth noting that even in the deepest Brady samples, carbohydrates composed over 10% of OM. As these soils have presumably been mostly isolated from surface inputs for thousands of years, this indicates the importance of additional stabilization mechanisms and that chemical recalcitrance may not be the primary control on long-term OM persistence (Schmidt et al. 2011).

Another important difference between the Brady soil and modern soil was the presence of char, or pyrogenic OM (PyOM) in the Brady <53 μm fraction. The mixing model reported between 8 and 10 percent PyOM contribution to total OM in all Brady soil samples, with less than 1 percent for the modern surface soil. PyOM was not a significant contribution to the POM fraction of any samples. This finding corroborates previous work on the Brady soil that found significant PyOM contribution within the Brady soil (Marín-Spiotta et al. 2014) although that study reported up to 30% of total OM in some fractions. It is likely that the use of different OM fractionation methods contributed to this discrepancy and that the PyOM contributions we report were diluted by other compounds relative to that study. The abundance of PyOM is probable evidence of significant burning during the formation of the Brady soil, and provides a possible mechanism for long-term stability of OM, as PyOM is thought to be more resistant to decomposition than other forms of C

(Schmidt et al. 2011). An alternative and non-mutually exclusive explanation for the relative enrichment of PyOM in the Brady soil could be due to selective loss of other C compounds through time, and not necessarily increased rates of fire. In any case, pyrogenic OM is capable of being decomposed on short timescales (days to years) by bacteria and fungi under certain conditions (Hockaday et al. 2006, de la Rosa and Knicker 2011), so it may be susceptible to decomposition with exposure of the Brady soil.

In general, differences in OM composition were greatest between the modern surface soil and all the Brady soil samples regardless of depth. However, the most exposed Brady soil at 20 cm depth shared a number of common features with the modern surface soil, including the previously mentioned alkyl:O-N alkyl ratio and the amount of carbohydrate in both the POM and <53μm fractions. This suggests that exposure of the Brady soil to the surface does lead to changes in OM composition, whether by transformation of ancient OM or incorporation of modern OM. However, changes are slow, and differences, including the persistence of pyrogenic OM, persist even when the Brady soil gets within 20 cm of the surface. Ongoing work will determine what implications if any exposure has for bulk C storage as well as any influence on OM fractions.

Conclusion

This study contributes to our understanding of C dynamics within a buried soil that is being exposed to surface conditions. We found evidence of increased inputs of fresh plant material to the more exposed buried soils, as well as the prevalence of older, more decomposed OM in the deeper buried soil. We also observed evidence of decomposition and incorporation of fresh plant material in all the Brady soil samples during a laboratory incubation, primarily by bacteria or

other single-celled microbes. Fungi were only slightly enriched, indicating small amounts of active decomposition of fresh material. This work will be especially useful as it can corroborate other more quantitative approaches from both the field and laboratory incubations.

Figures and Tables

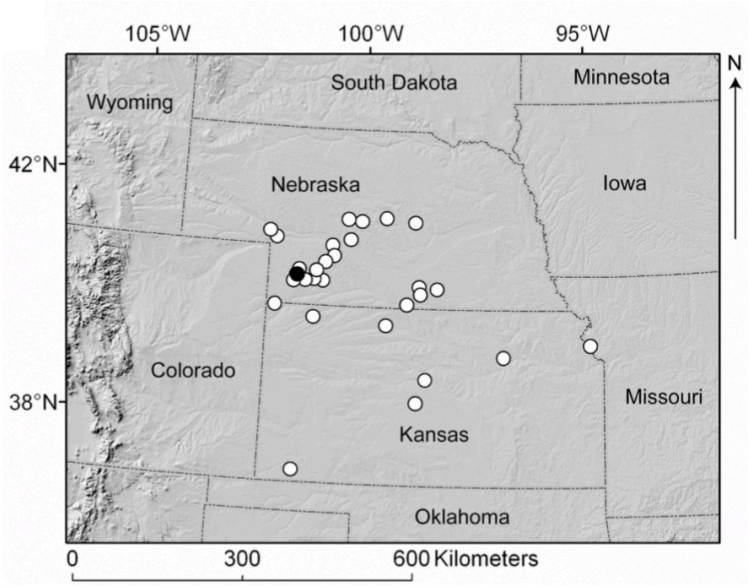

Figure 1. Map of Brady soil extent (open circles) and the study site (closed circle). From Marín-Spiotta et al. (2014).

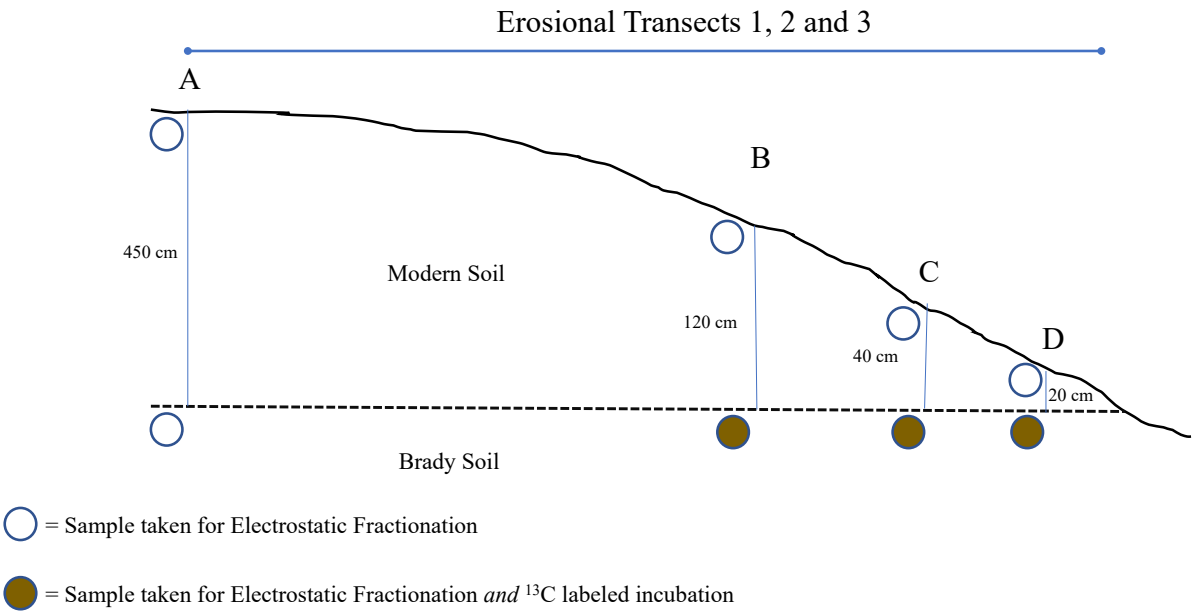

Figure 2. Sampling design along erosional transect with differing degrees of exposure of the Brady soil. Samples were collected at points A, B, C, and D, corresponding to approximate Brady soil depths of 450 cm, 120 cm, 40 cm, and 20 cm. Figure is not to scale.

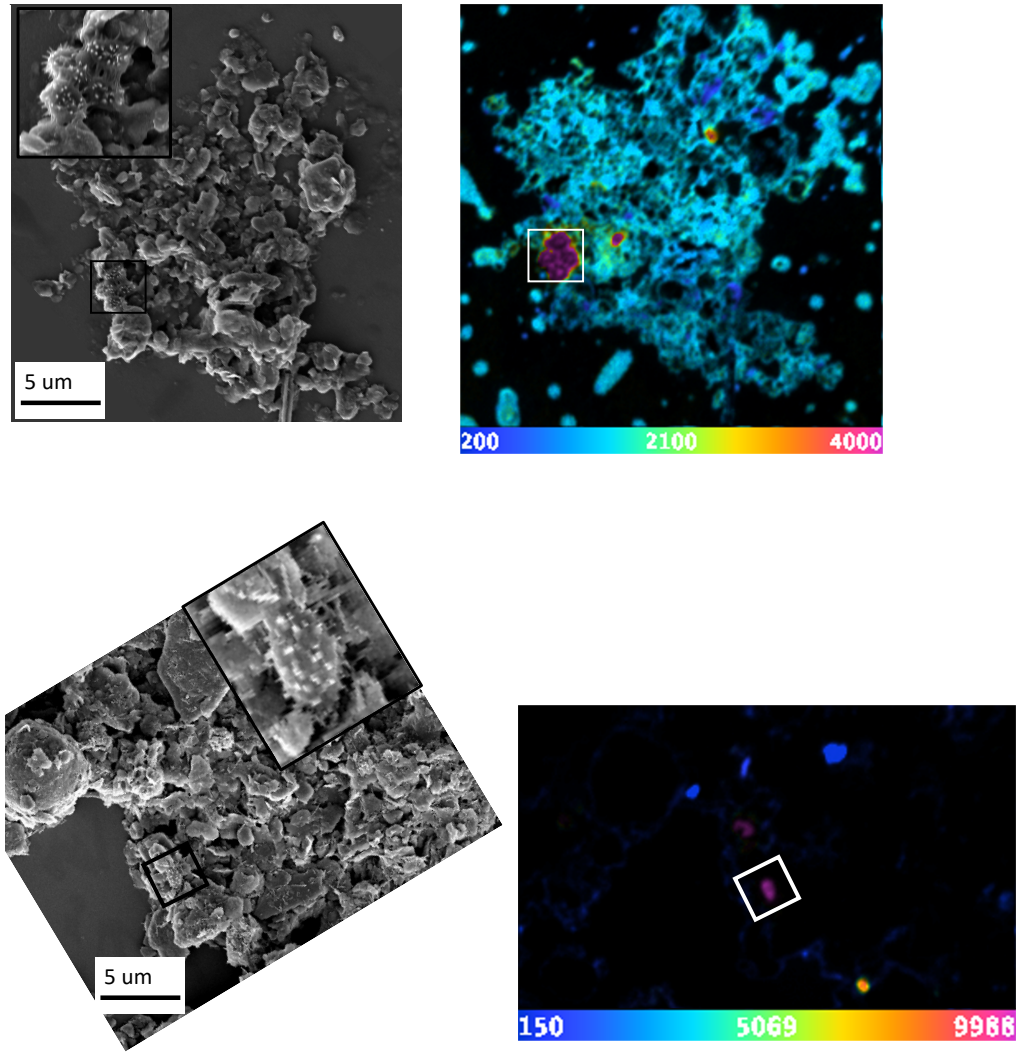

Figure 3. Scanning electron microscope (left column) and NanoSIMS (right column) imaging of putative bacterial cells for two regions. Insets on the SEM image show the bacterial cells. The color scale on the right shows the ratio of $^{12}C^{13}C$:$^{12}C_2$ where warmer colors indicate relative enrichment in ^{13}C. Both samples were fixed in ethanol as described in the methods section, but the sample in the top row was not rinsed in pure ethanol, while the sample in the bottom row was rinsed with pure ethanol.

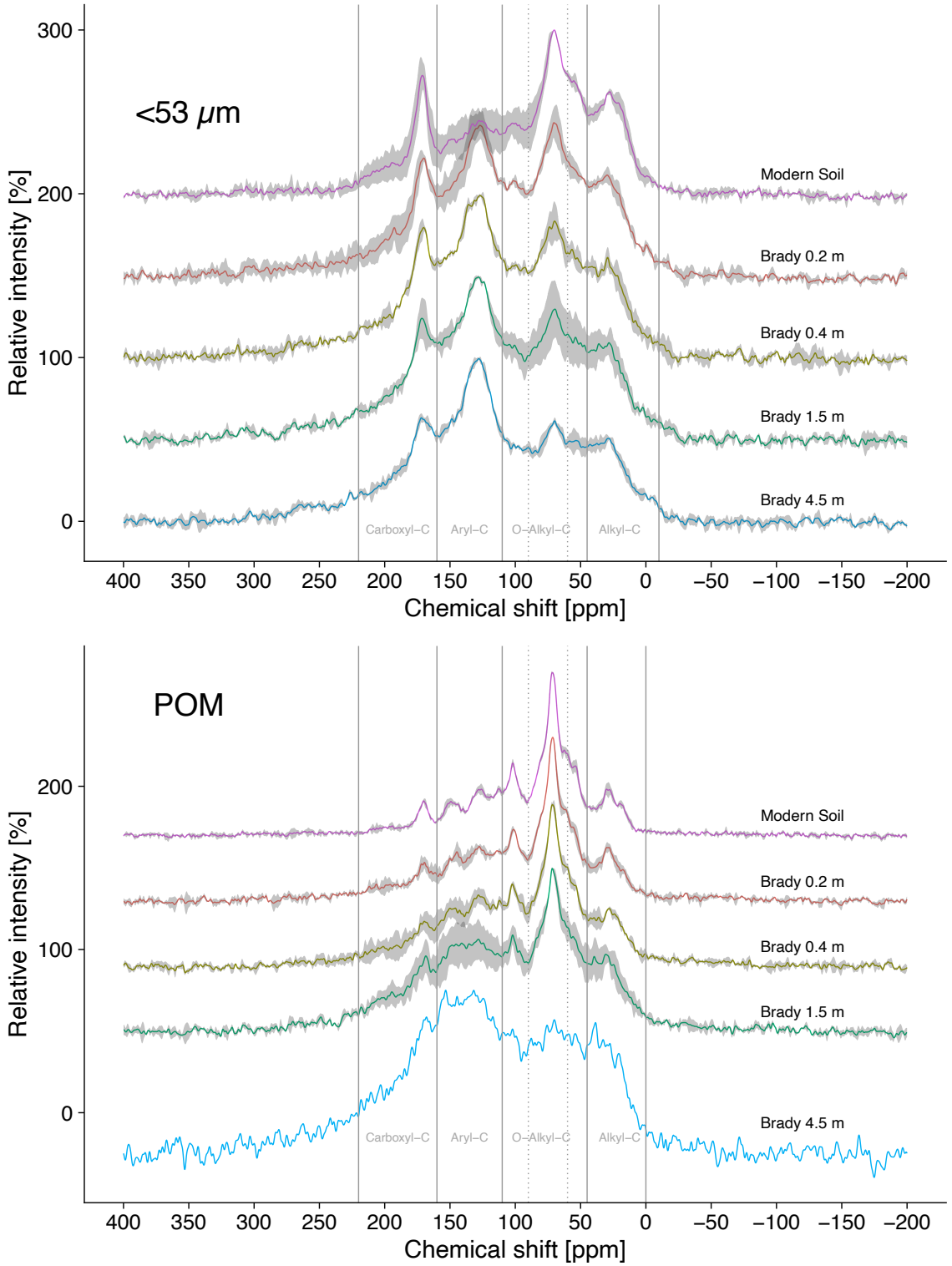

Figure 4. Mean of three NMR spectra for two soil organic matter fractions; < 53 µm (top) and particulate organic matter (bottom). The shaded gray area represents one standard error. Note that there was only one spectra for the Brady 4.5 m POM samples due to low sample mass. The dotted lines within the O-alkyl region denote the further subdivisions used for the molecular mixing model (see methods).

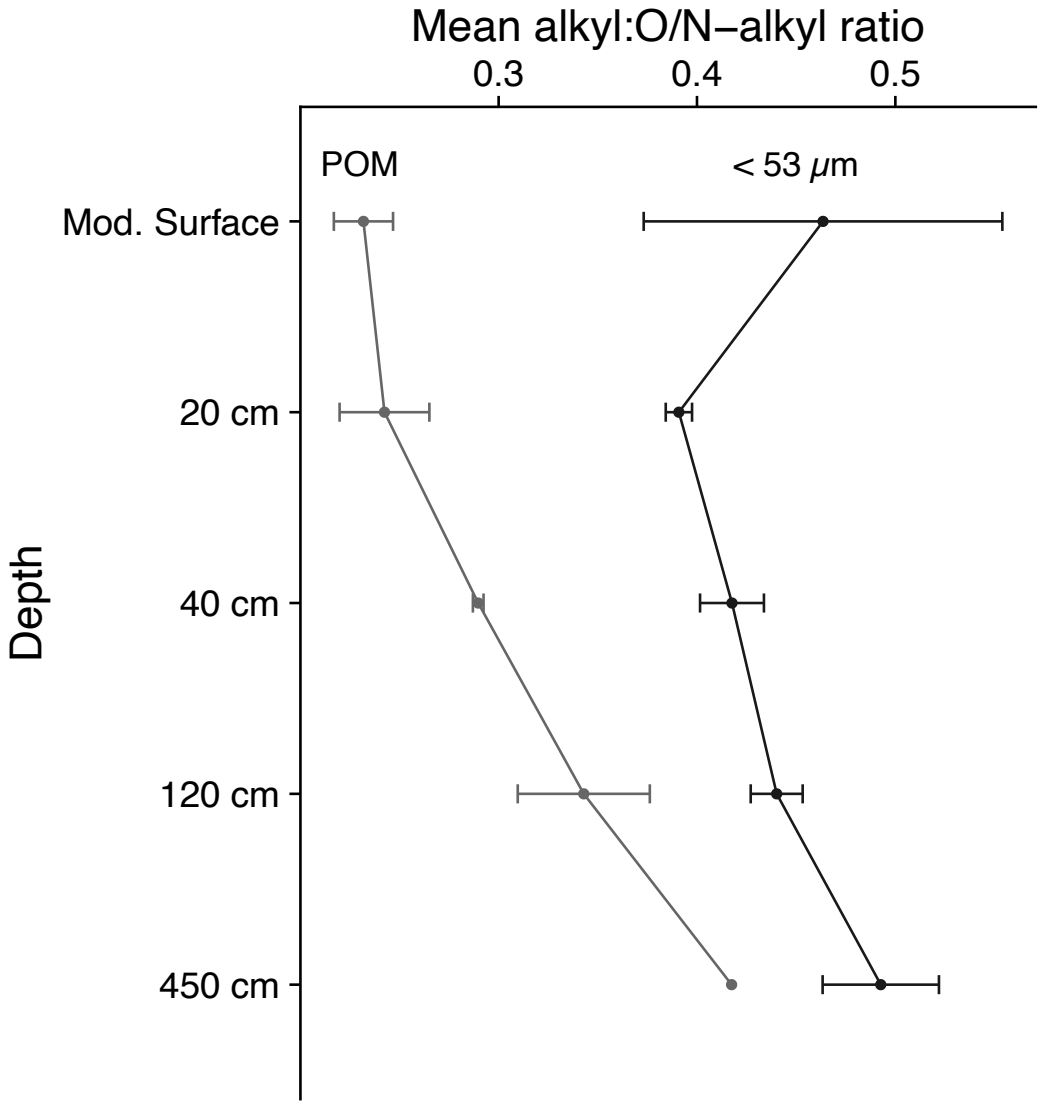

Figure 5. Alkyl:O/N-alkyl ratio for two organic matter fractions by depth. The error bars represent one standard error in either direction. Note, the point for the POM 450 cm sample just had one replicate due to low sample mass, and was likely contaminated with <53 μm fraction.

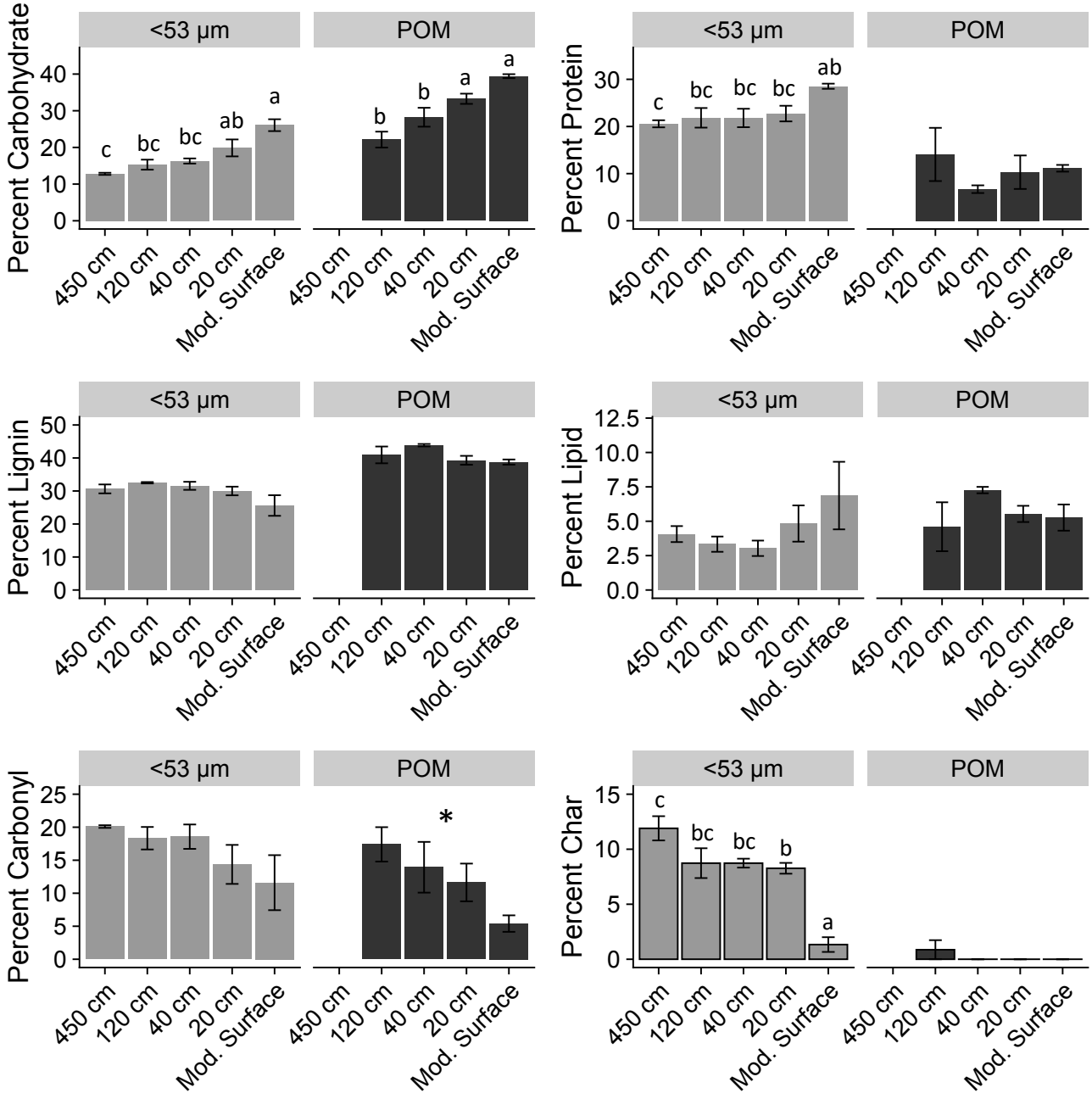

Figure 6: Proportion contribution of different C compounds to overall OM composition. Contributions were determined using a six-component molecular mixing model. The Brady 4.5 m POM results are not shown because the NMR results were not reliable due to low sample mass and likely contamination. Error bars represent one standard error. Bars sharing a letter within a fraction are not significantly different at $p < 0.05$. The lack of letters for a fraction indicates no significant difference by depth within that fraction. An asterisk means that there was a marginally significant ($p < 0.1$) effect of depth within a fraction.

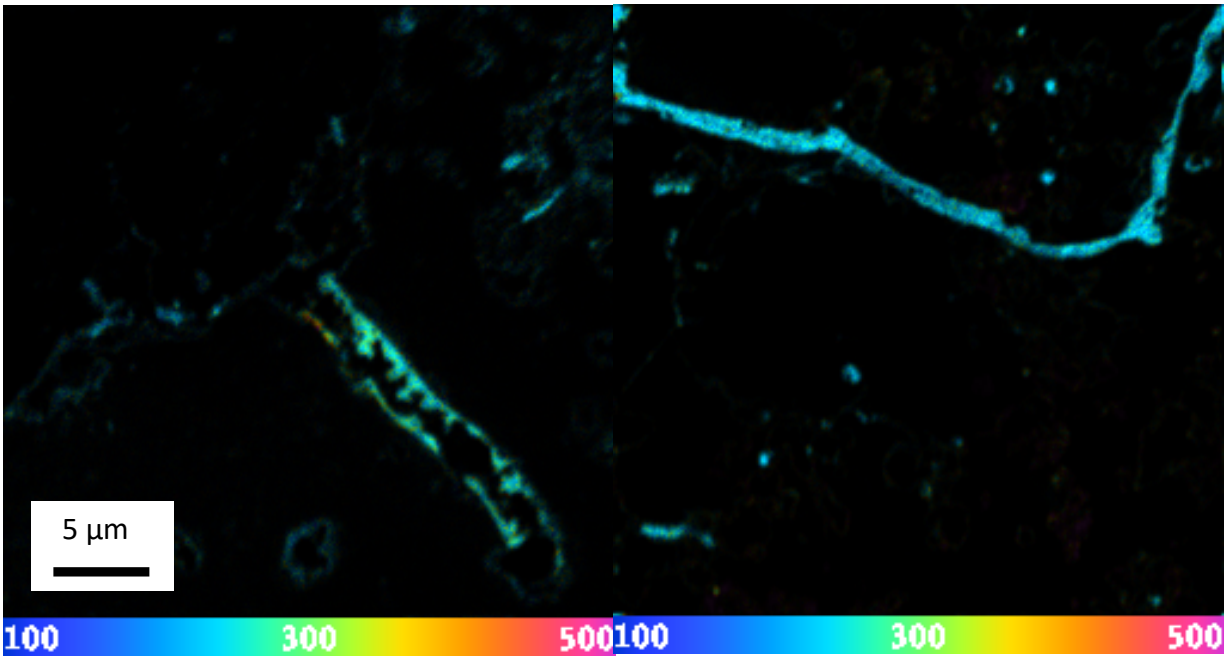

Figure 7. NanoSIMS imaging of two fungal hyphae or actinomycetes showing the ratio of $^{12}C^{13}C:^{12}C_2$. Note that the maximum color scale differs from the earlier NanoSIMS images.

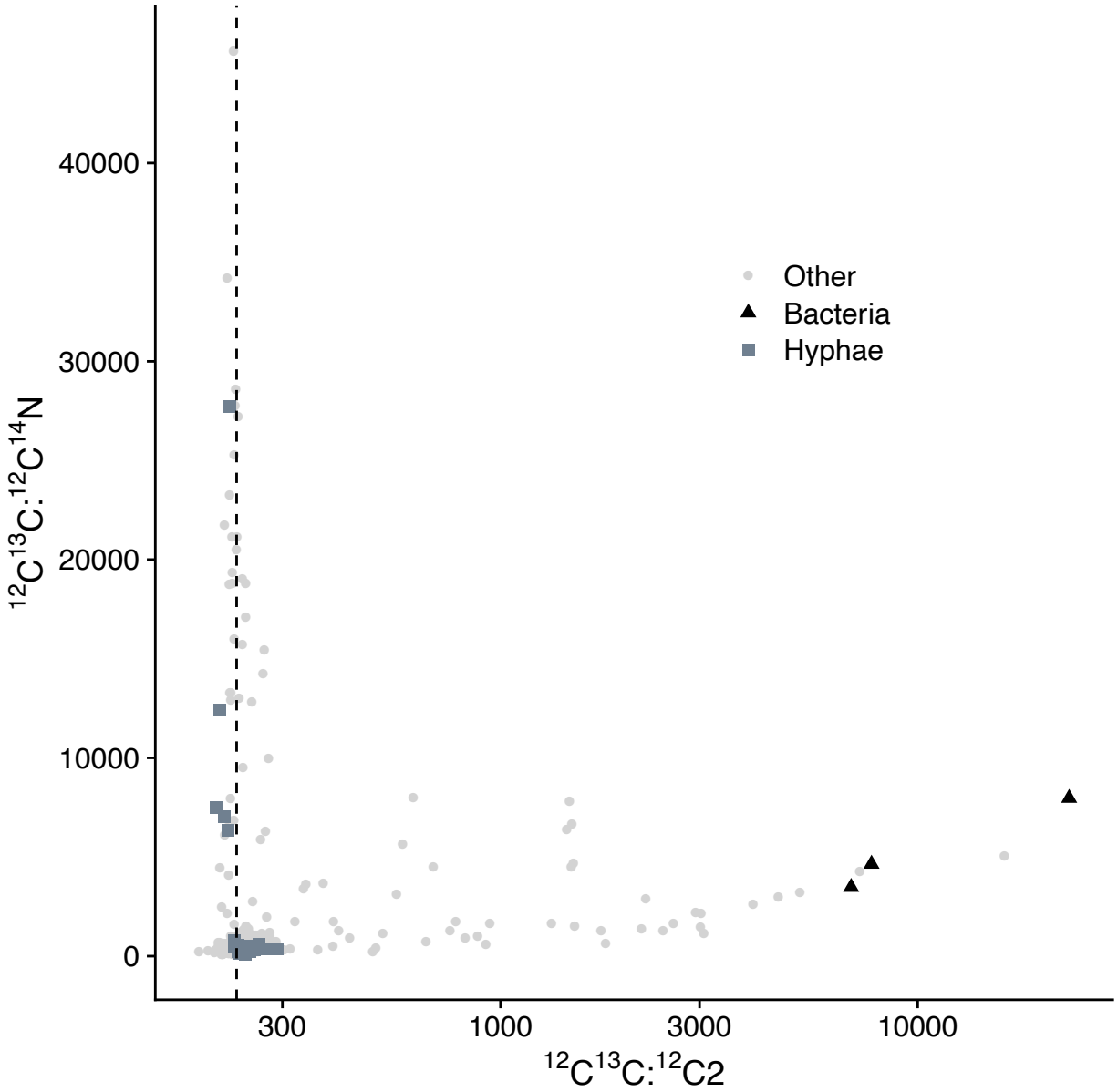

Figure 8. Plot of elemental isotope ratios from NanoSIMS regions of interest (ROI). The vertical dashed line represents the maximum measured natural abundance $^{12}C^{13}C:^{12}C_2$. Samples to the right of this line can be assumed to be enriched in ^{13}C. Note the log scale of the x axis. The category 'Other' includes identifiable POM, as well as all ROIs associated with small mineral or aggregate surfaces.

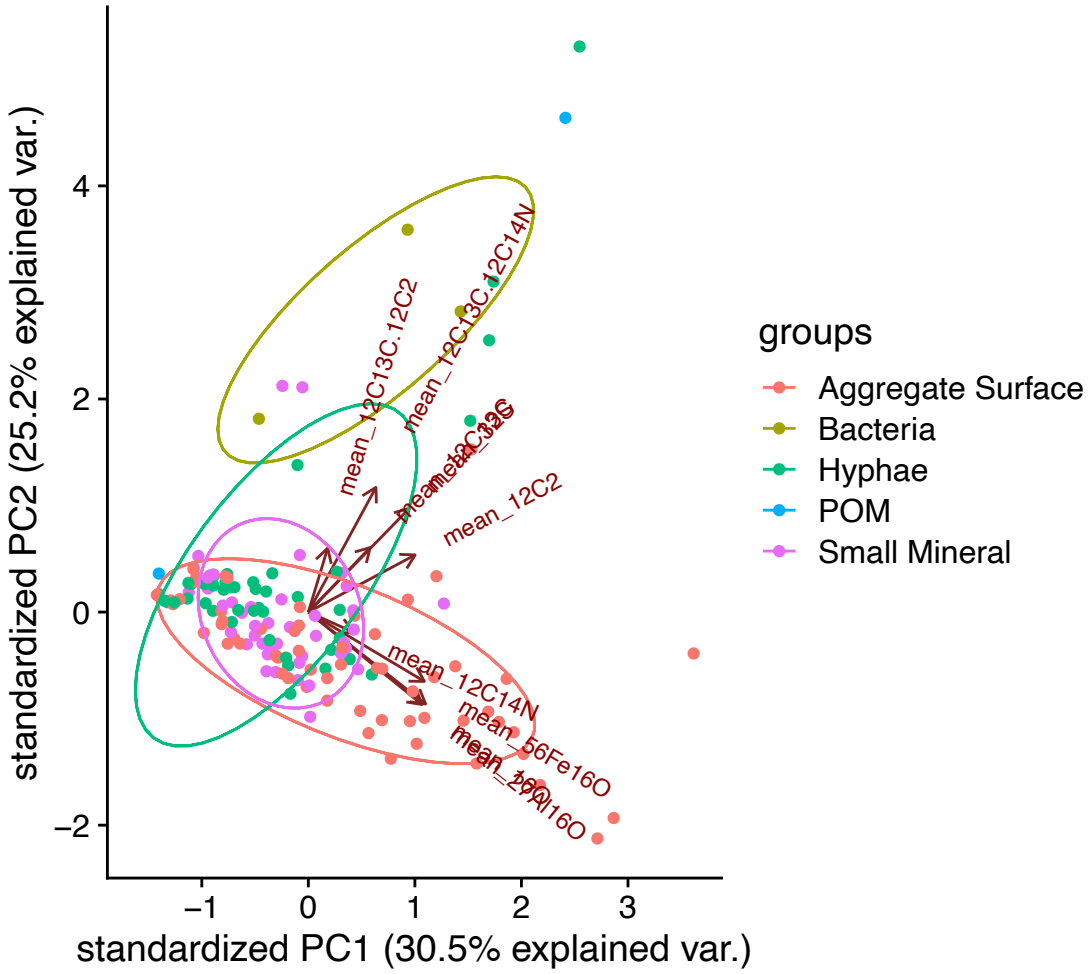

Figure 9. PCA ordination of NanoSIMS regions of interest (ROI) based on 5 elemental isotope counts, and two elemental ratios (see Methods for more details). Ellipses represent the 95% normal probability contour for each group.

Table 1. Mean integral values from three spectra for NMR regions used in molecular mixing model.

Fraction	Depth	Alkyl C (-10 – 45 ppm)	n-alkyl C (45 – 60)	O-alkyl C (60 - 90)	di-O-alkyl C (90 - 110)	Aromatic C (110 - 140)	O-aryl C (140 - 160)	Carboxyl/carbonyl C (160 - 220)	Sum
< 53 µm	Mod. Surface	21.0	10.0	22.7	8.4	12.4	6.3	16.8	97.5
	120 cm	15.4	6.9	15.1	8.4	19.7	10.1	17.9	93.5
	20 cm	16.9	7.7	18.1	8.9	18.7	8.8	16.2	95.5
	40 cm	15.1	6.9	15.8	8.5	19.5	9.8	18.1	93.7
	450 cm	15.6	6.3	13.3	8.2	21.8	10.6	18.7	94.4
POM	Mod. Surface	13.5	10.0	32.8	11.8	13.7	6.3	8.1	96.3
	120 cm	14.7	7.8	21.3	9.8	15.3	9.6	15.3	93.7
	20 cm	13.7	8.9	29.1	10.8	14.0	7.3	11.2	95.0
	40 cm	14.6	8.8	26.2	10.8	15.3	8.5	11.6	95.6
	450 cm	15.0	6.4	13.6	8.7	16.8	11.6	19.3	91.4

Table 2. Summary statistics for identified NanoSIMS regions of interest (ROI) for $^{12}C^{13}C:^{12}C_2$. ROI groups not sharing a letter indicates a statistical difference ($p < 0.05$) in $^{12}C^{13}C:^{12}C_2$ values.

Group		Mean $^{12}C^{13}C:^{12}C_2$	Median $^{12}C^{13}C:^{12}C_2$	SD $^{12}C^{13}C:^{12}C_2$	Maximum $^{12}C^{13}C:^{12}C_2$	Minimum $^{12}C^{13}C:^{12}C_2$	n
Natural Abundance	*A*	216	217	8	233	189	32
Hyphae	*B*	243	240	16	291	208	43
Small Mineral	*B*	692	241	2442	16153	216	43
Aggregate Surface	*BC*	496	248	706	4029	217	60
Bacteria	*C*	12135	6927	9481	23078	6399	3

Literature Cited

Baldock, J. A., J. M. Oades, P. N. Nelson, T. M. Skene, A. Golchin, and P. Clarke. 1997. Assessing the extent of decomposition of natural organic materials using solid-state 13C NMR spectroscopy. Soil Research 35:1061–1084.

Berhe, A. A., J. Harte, J. W. Harden, and M. S. Torn. 2007. The significance of the erosion-induced terrestrial carbon sink. BioScience 57:337–346.

Chaopricha, N. T., and E. Marín-Spiotta. 2014. Soil burial contributes to deep soil organic carbon storage. Soil Biology and Biochemistry 69:251–264.

Chigineva, N. I., A. V. Aleksandrova, and A. V. Tiunov. 2009. The addition of labile carbon alters litter fungal communities and decreases litter decomposition rates. Applied Soil Ecology 42:264–270.

Cotrufo, M. F., M. D. Wallenstein, C. M. Boot, K. Denef, and E. Paul. 2013. The Microbial Efficiency-Matrix Stabilization (MEMS) framework integrates plant litter decomposition with soil organic matter stabilization: do labile plant inputs form stable soil organic matter? Global Change Biology 19:988–995.

Ferguson, B., W. E. Lukens, B. El Masri, and G. E. Stinchcomb. 2020. Alluvial landform and the occurrence of paleosols in a humid-subtropical climate have an effect on long-term soil organic carbon storage. Geoderma 371:114388.

Fisher, M., I. Rao, M. Ayarza, C. Lascano, J. Sanz, R. Thomas, and R. Vera. 1994. Carbon storage by introduced deep-rooted grasses in the South American savannas. Nature 371:236–238.

Fontaine, S., S. Barot, P. Barré, N. Bdioui, B. Mary, and C. Rumpel. 2007. Stability of organic carbon in deep soil layers controlled by fresh carbon supply. Nature 450:277–280.

Gormanns, P., S. Reckow, J. C. Poczatek, C. W. Turck, and C. Lechene. 2012. Segmentation of multi-isotope imaging mass spectrometry data for semi-automatic detection of regions of interest. PLoS ONE 7:e30576.

de Graaff, M.-A., A. T. Classen, H. F. Castro, and C. W. Schadt. 2010. Labile soil carbon inputs mediate the soil microbial community composition and plant residue decomposition rates. New Phytologist 188:1055–1064.

Gurwick, N. P., D. M. McCorkle, P. M. Groffman, A. J. Gold, D. Q. Kellogg, and P. Seitz-Rundlett. 2008. Mineralization of ancient carbon in the subsurface of riparian forests. Journal of Geophysical Research: Biogeosciences 113:n/a-n/a.

Harper, R. J., and M. Tibbett. 2013. The hidden organic carbon in deep mineral soils. Plant and Soil 368:641–648.

Harrison, R. B., P. W. Footen, and B. D. Strahm. 2011. Deep soil horizons: contribution and importance to soil carbon pools and in assessing whole-ecosystem response to management and global change. Forest Science 57:67–76.

Hockaday, W. C., A. M. Grannas, S. Kim, and P. G. Hatcher. 2006. Direct molecular evidence for the degradation and mobility of black carbon in soils from ultrahigh-resolution mass spectral analysis of dissolved organic matter from a fire-impacted forest soil. Organic Geochemistry 37:501–510.

Hopkins, F. M., T. R. Filley, G. Gleixner, M. Lange, S. M. Top, and S. E. Trumbore. 2014. Increased belowground carbon inputs and warming promote loss of soil organic carbon through complementary microbial responses. Soil Biology and Biochemistry 76:57–69.

Jacobs, P. M., and J. A. Mason. 2005. Impact of Holocene dust aggradation on A horizon characteristics and carbon storage in loess-derived Mollisols of the Great Plains, USA. Geoderma 125:95–106.

Jobbagy, E., and R. Jackson. 2000. The vertical distribution of soil organic carbon and its relation to climate and vegetation. Ecological Applications 10:14.

Johnson, W. C., and K. L. Willey. 2000. Isotopic and rock magnetic expression of environmental change at the Pleistocene–Holocene transition in the central Great Plains. Quaternary International 67:89–106.

Kaiser, M., R. H. Ellerbrock, and M. Sommer. 2009. Separation of coarse organic particles from bulk surface soil samples by electrostatic attraction. Soil Science Society of America Journal 73:2118–2130.

Kögel-Knabner, I. 1997. 13C and 15N NMR spectroscopy as a tool in soil organic matter studies. Geoderma 80:243–270.

Kuzyakov, Y. 2010. Priming effects: Interactions between living and dead organic matter. Soil Biology and Biochemistry 42:1363–1371.

Marín-Spiotta, E., N. T. Chaopricha, A. F. Plante, A. F. Diefendorf, C. W. Mueller, A. S. Grandy, and J. A. Mason. 2014. Long-term stabilization of deep soil carbon by fire and burial during early Holocene climate change. Nature Geoscience 7:428–432.

Mason, J. A., X. Miao, P. R. Hanson, W. C. Johnson, P. M. Jacobs, and R. J. Goble. 2008. Loess record of the Pleistocene–Holocene transition on the northern and central Great Plains, USA. Quaternary Science Reviews 27:1772–1783.

Mueller, C. W., A. Kölbl, C. Hoeschen, F. Hillion, K. Heister, A. M. Herrmann, and I. Kögel-Knabner. 2012. Submicron scale imaging of soil organic matter dynamics using NanoSIMS – From single particles to intact aggregates. Organic Geochemistry 42:1476–1488.

Nelson, P. N., and J. A. Baldock. 2005. Estimating the molecular composition of a diverse range of natural organic materials from solid-state 13C NMR and elemental analyses. Biogeochemistry 72:1–34.

Ogle, D. H., P. Wheeler, and A. Dinno. 2020. FSA: Fisheries Stock Analysis.

R Core Team. 2019. R: A language and environment for statistical computing. R Foundation for Statistical Computing.

de la Rosa, J. M., and H. Knicker. 2011. Bioavailability of N released from N-rich pyrogenic organic matter: An incubation study. Soil Biology and Biochemistry 43:2368–2373.

Rumpel, C., and I. Kögel-Knabner. 2011. Deep soil organic matter—a key but poorly understood component of terrestrial C cycle. Plant and Soil 338:143–158.

Schmidt, M. W. I., M. S. Torn, S. Abiven, T. Dittmar, G. Guggenberger, I. A. Janssens, M. Kleber, I. Kögel-Knabner, J. Lehmann, D. A. C. Manning, P. Nannipieri, D. P. Rasse, S. Weiner, and S. E. Trumbore. 2011. Persistence of soil organic matter as an ecosystem property. Nature 478:49–56.

CONCLUSIONS

There is increased awareness of the need to better understand the mechanisms that control soil carbon (C) storage across the full range of pedological and environmental conditions, and at multiple scales. The factors are many, and the interactions among them can be complex and context dependent. This dissertation highlights both some of the challenges inherent in studying this topic, and provides additional understanding of both patterns and mechanisms, as well as future directions of study.

In general, my work showed that variations in soil properties were more important than the human activities under consideration. Nitrogen (N) enrichment increased soil C storage initially (Chapter 1), but those effects seem to have diminished following 15 years of continued fertilization and differed within two different forests. This is important because most anthropogenic sources of N are chronic, and this study perhaps provides more realistic understanding of the long-term ecosystem response. The value of long-term studies was also shown by the ability to use archived soils to improve models constrained by radiocarbon (^{14}C) dynamics. Future work in these sites could focus more on specific mechanisms controlling decomposition rates, including more detailed microbial community descriptions. The fate of additional N seems important, given that it does not appear to stay in the soil or vegetation and could have ecological and biogeochemical effects beyond the boundaries of the ecosystems being studied. Elevated atmospheric N deposition is predicted to continue in the tropics, and understanding the broader ecosystem effects of excess N in the soil and beyond would be worthwhile.

Land cover was generally found to be less important than soil properties in describing patterns in soil C storage (Chapters 2 and 3). Instead, soil properties related to soil order – including pH, iron and aluminum, and soil depth, which is related to soil weathering and topography, played a greater role across the diversity of soils studied here. Clearly human land use change and alterations to nutrient cycling can and do affect soil C dynamics. However, it seems that in these systems, landscape heterogeneity often masks the effects. An improved understanding of the spatial variation of these properties and others (e.g., calcium in karst soils) should allow for improved prediction of soil C stocks, as well as providing enough nuance to untangle the effects of human land use and management.

This dissertation also highlights the power of high-resolution imaging and organic matter (OM) chemical analysis in better understanding soil OM decomposition and persistence. Although NanoSIMS imaging is fairly qualitative, insights into the relative importance of bacteria and fungi in decomposition should allow for corroboration with other methods. Likewise, NMR analyses provide useful information on OM composition. The debate over the role of OM recalcitrance on long-term soil OM persistence continues (e.g., Schmidt et al. 2011), and this type of analysis shows that even ancient soil OM contains C assumed to be readily available to decomposers. Thus, other stabilization mechanisms are clearly important.

Above all, this work continues to show the importance of understanding the heterogeneity of soils, environmental conditions, and human activities. It is a reminder that soils of the tropics are diverse, and that drawing conclusions on biased observations is fraught (Powers et al. 2011). The

diversity of soils used in this research contributes to the representation of under-studied soil types in the tropics and can hopefully contribute to improving models that predict responses of soil C to future scenarios, with implications for climate change and the global C cycle.